Luminescent Metal-Ligand Complexes as Labels for Polarization Immunoassays and for Determination of Hydrogen Peroxide

Dissertation zur Erlangung des Doktorgrades der Naturwissenschaften

(Dr. rer. nat.)

der Fakultät Chemie und Pharmazie

der Universität Regensburg

vorgelegt von

Axel Dürkop

aus Drachselsried/Niederbayern

im März 2001

Das Promotionsgesuch wurde eingereicht am 21.03.2001

Diese Arbeit wurde angeleitet von Prof. Dr. O. Wolfbeis

Kolloquiumstermin: 27.04.2001

Prüfungsausschuß:

Vorsitzender:	Prof. Dr. A. Merz
Erstgutachter:	Prof. Dr. O. Wolfbeis
Zweitgutachter:	Prof. Dr. N. Korber
Drittprüfer:	Prof. Dr. M. Liefländer

Danksagung

Diese Arbeit entstand zwischen März 1998 und März 2001 am Institut für Analytische Chemie, Chemo- und Biosensorik an der Universität Regensburg

In erster Linie gilt mein Dank **Herrn Professor Dr. Otto S. Wolfbeis** für die Bereitstellung des interessanten Themas, für das durch viele interessante Diskussionen und Anregungen gekennzeichnete Arbeitsklima, sowie die hervorragenden Arbeitsbedingungen am Lehrstuhl.

Weiterhin gebührt **Herrn Dr. Frank Lehmann** und **Herrn Dr. Ewald Terpetschnig** mein besonderer Dank für die sehr gute persönliche Betreuung und viele Hilfen im Rahmen der täglichen Arbeit.

Ferner möchte ich mich bedanken bei **Herrn Dr. Maier** und seinem Team und **Herrn Dr. Hochmut** für die Aufnahme der Massenspektren,
Herrn Dr. K.-P. Rueß für die CA-Recherchen und **Herrn K.-H. Berghausen** für Hilfen und Tips zur Chromatographie,
meinen LaborkollegInnen **Michaela Arbter**, **Erika Simo** und **Mario Probst** und den KollegInnen **Christine Augustin**, **Dr. Bernhard Oswald** und **Bernhard Weidgans** für das angenehme Arbeitsklima und entspannende Teerunden,
der Kollegin **Katja Kastl** für die im Rahmen ihres Schwerpunktpraktikums geleistete Mitarbeit, sowie bei allen Mitarbeiterinnen und Mitarbeitern des Lehrstuhls, die zum Gelingen dieser Arbeit beigetragen haben.

Mein Dank geht auch an Frau Alder vom Lehrstuhl Prof. Dick und den Mitarbeitern von Prof. Grummt (Universität Jena) für die Hilfe bei den Messungen der Fundamentalpolarisation.

Vielen Dank der Deutschen Forschungsgemeinschaft für die finanzielle Unterstützung.

Schlußendlich gebührt der größte Dank meinen Eltern, die mir das Studium ermöglicht haben und immer zu mir standen, und meiner Freundin Sylvie Thaller.

Table of Contents

1. Introduction and Aim of Work 1

1.1 Ruthenium Metal-Ligand Complexes (MLCs) in Bioanalytical Applications and in Polarization Immunoassays 1

1.1.1 Spectral Characteristics of Ru MLCs 3

1.1.2 Applications for Determination of DNA and Membrane Dynamics 5

1.1.3 Sensing of pH, O_2 and CO_2 with Ru MLCs 6

1.1.4 Ruthenium, Rhenium and Osmium MLCs in Polarization Immunoassays 8

1.2 Europium Metal-Ligand Complexes in Analytical Biochemistry 11

1.2.1 Luminescence Properties of Eu^{3+} and Eu MLCs in Aqueous Solution 11

1.2.2 Applications of Eu^{3+} Complexes in Fluorescence Immmunoassays 12

1.3 Hydrogen Peroxide: Methods of Determination in Fluorescent Analysis 13

1.4 Aim of the Work 14

1.5 Literature 14

2. Background 18

2.1 Fluorescence Anisotropy or Polarization: Definitions and Theory 18

2.2 Measurement of Fluorescence Anisotropy 24

2.3 The Effect of Rotational Diffusion on Fluorescence Anisotropy as a Tool for Determination of Antigen Concentrations in Homogenous Immunoassays 27

2.4 Literature 29

3. Ruthenium Complexes as Labels for Polarization Immunoassays 31

3.1 Syntheses 31

3.1.1. Synthesis of the Pyrazine Ligands 31
3.1.2 Synthesis of the Bipyridine Ligands 33
3.1.3 Synthesis of the Ruthenium Metal Ligand Complexes 35
3.2 Spectral Characterization of the Complexes and Their Protein Conjugates 37
3.3 Homogenous Polarization Immunoassays with Labeled HSA and Myoglobin for the Determination of Antibody Concentrations 41
3.4 Competitive Polarization Immunoassays with HSA and Myoglobin for the Determination of Antigen Concentrations 43
3.5 Comparison of the Competitive Polarization Immunoassay for HSA with the AlbuminBlue 580 Test 45
3.6 Discussion 47
3.7 Literature 48

4. The Europium-Tetracycline Complex as a Molecular Sensor for Hydrogen Peroxide 50

4.1 Properties of the Europium-Tetracycline (EuTC) System 50
4.1.1 Introduction and Spectral Properties of the EuTC Complexes. 50
4.1.2 Effect of Eu^{3+}/TC Ratio on the Emission of the EuTC System 54
4.1.3 Effect of TC on the Absorption and Emission of the EuTC System 57
4.1.4 Effect of Eu^{3+} on the Absorption and Emission of the EuTC System 59
4.1.5 Effect of Oxygen in the Sample on the Emission of the Eu_3TC System 59
4.2 Effect of H_2O_2 on the Luminescence of other Ln^{3+} Tetracycline Complexes 60
4.2.1 Ln_3TC Complexes 60
4.2.2 LnTC Complexes and Ln_{10}TC complexes 63
4.3 Effect of H_2O_2 on the Luminescence of Cu^{2+} and Ni^{2+} Tetracycline Complexes 65

4.4 Effect of H_2O_2 on the Luminescence of Eu^{3+} Complexes with Other En-dione Ligands 66
4.5 Setup and Discussion of the New Sensing Scheme for H_2O_2 70
4.6 Determination of Glucose 74
4.6.1 Test of Applicability and Optimization of GOx Concentration 74
4.6.2 Determination of Glucose 77
4.7 Literature 79

5. Experimental Part 82

5.1 General Remarks 82
5.1.1 Chemicals, Solvents, Proteins 82
5.1.2 Buffer Solutions and pH Measurements 82
5.1.3 Thin Layer Chromatography and Gel Permeation Chromatography 82
5.1.4 Determination of Melting Points 83
5.1.5 Spectra 83
5.1.6 Determination of Molar Absorbance 84
5.2 Synthesis of the Bipyridine Ligands 84
5.2.1 General Procedure for the Coupling of Bromopyridines to the Respective Bipyridines 84
5.2.1.1 Preparation of 5-Methyl-2,2'-bipyridine 85
5.2.1.2 Preparation of 5,5'-Dimethyl-2,2'-bipyridine 85
5.2.2 General Procedure for the Oxidation of the Methylbipyridines to the Respective Carboxybipyridines 86
5.2.2.1 Preparation of 5-Carboxy-2,2'-bipyridine 86
5.2.2.2 Preparation of 5,5'-Dicarboxy-2,2'-bipyridine 87
5.3 Synthesis of the Activated Ruthenium Trisbipyridine Complexes 87
5.3.1 General Procedure for the Addition of a Third Bipyridine Ligand to $Ru(bipy)_2Cl_2$ 87
5.3.1.1 Preparation of [Ru(2,2'-bipyridine)$_2$(5-carboxy-2,2'-bipyridine)]$(PF_6)_2$ 88
5.3.1.2 Preparation of [Ru(2,2'-bipyridine)$_2$ (5,5'-dicarboxy-2,2'-bipyridine)]$(PF_6)_2$ 88

5.3.2 General Procedure for the Conversion of the Ruthenium Trisbipyridine Complexes to the Corresponding NHS-Esters 89
5.3.2.1 Preparation of [Ru(2,2'-bipyridine)$_2$(5-carboxy-(N-succimidyl)-2,2'-bipyridine)](PF$_6$)$_2$ 89
5.3.2.2 Preparation of [Ru(2,2'-bipyridine)$_2$(5,5'-dicarboxy-bis-(N-succimidyl)-2,2'-bipyridine)](PF$_6$)$_2$ 90
5.4 Labeling Procedures, Determination of Dye-to-Protein Ratios and Quantum Yields 90
5.4.1 General Protein Labeling Procedures 90
5.4.2 Determination of Dye-to-Protein Ratios 91
5.4.3 Determination of Quantum Yields 91
5.5 Immunoassays 92
5.5.1 Homogenous Immunoassay for the Determination of Antibody Concentrations 92
5.5.2 Competitive Immunoassay for Antigen Determination 92
5.5.3 Comparison of the Competitive Polarization Immunoassay for HSA with the AlbuminBlue 580 Test 92
5.6 Measurements with EuTC 93
5.6.1 Reagent Solutions and Analytical Procedure for the Determination of Hydrogen Peroxide 93
5.6.2 Reagent Solutions and Analytical Procedure for the Determination of Glucose 93
5.7 References 95

6. Abbreviations Used 97

7. Summary 99

7.1 In English 99
7.2 In German 100

8. Curriculum Vitae 102

9. List of Papers, Patents, Posters and Presentations 104

9.1 Papers 104

9.2 Patent 104

9.3 Poster 104

9.4 Oral Presentations 104

1. Introduction and Aim of Work

1.1 Ruthenium Metal-Ligand Complexes (MLCs) in Bioanalytical Applications and in Polarization Immunoassays

Fluorescence detection is in the process of replacing radiometric and spectrophotomeric methods for immunoassays. Apart from the detection of the emission intensity or the luminescence lifetime, the determination of fluorescence polarization offers a referenced method because a ratio of intensities is taken. The use of transition metal-ligand complexes in fluorescent analytical methods has grown rapidly during the latest fifteen years. Extensive work has been done on complexes of the heavier divalent cations of the sixth transition metal group, represented by Ru^{2+} and Os^{2+} [1-3]. Fluorescent complexes of rhenium(I), platinum(II) and iridium(III) for bioanalytical purposes have also been described [4-6].

Most of the compounds studied contained one diimine ligand. One of the earliest complexes was $[Ru(bipy)_3]^{2+}$, where bipy is 2,2'-bipyridine. The class of Ru-tris(bipyridine) complexes was originally developed for the conversion of solar energy into electricity. Upon absorption of a photon one of the bipy ligands is reduced and the metal ion is oxidized:

$$[Ru^{II}(bipy)_3]^{2+} \xrightarrow{hn} [Ru^{III}(bipy)_2(bipy)^{-}]^{2+}$$

Therefore $[Ru(bipy)_3]^{2+}$ becomes a metal-to-ligand charge transfer species with Ru(III) being a strong oxidant and bipy being a strong reductant. This CT-system was intended to be used to cleave water to hydrogen and oxygen.

Most of the MLCs used in fluorescent analysis have some unique properties compared to fluorescent organic labels such as fluoresceins or cyanines. The most important is their luminescence lifetime (some hundreds of nanoseconds to over 10 μs) compared to the organic fluorophores. This long lifetime enables measurements of slow biological processes like rotational motions of large proteins or of membrane bound proteins. MLCs with activated functional groups can be used as fluorescent markers for antigens and DNA in intensity-, lifetime- or polarization-based fluorescence immunoassays. The use of phosphorescence

(with lifetimes of sometimes over ten seconds) is disadvantageous for these applications because only few probes display phosphorescence at room temperature in solution, so that such measurements usually have to be carried out in complete absence of oxygen.

The origin of the long luminescence lifetime of ruthenium MLCs is a result of the particular arrangement of the electronic states which is in accordance with the crystal field theory. The combination of metal and ligand states results in the new metal-to-ligand charge transfer (MLCT) states. Electrons are promoted from the metal to the ligand into these MLCT states upon absorption of photons. This MLCT transition is the reason for the intense absorption maximum of Ru-tris(bipyridyl) complexes at around 450 nm. The absorption is followed by intersystem crossing to the triplet MLCT state within less than 300 fs in a high yield. From this state, radiative or nonradiative decay is possible. Another requirement for luminescence has to be fulfilled at this point. The *d-d* states have to be on a higher energy level than the triplet MLCT state due to a stronger crystal field. This is true for $[Ru(bipy)_3]^{2+}$ complexes but not for $[Fe(bipy)_3]^{2+}$ complexes. In the case of $[Fe(bipy)_3]^{2+}$ complexes, radiationless decay is preferred, because the *d-d* states are energetically lower than those of the Ru complexes (see Fig. 1). Therefore, iron MLCs are nonluminescent [7].

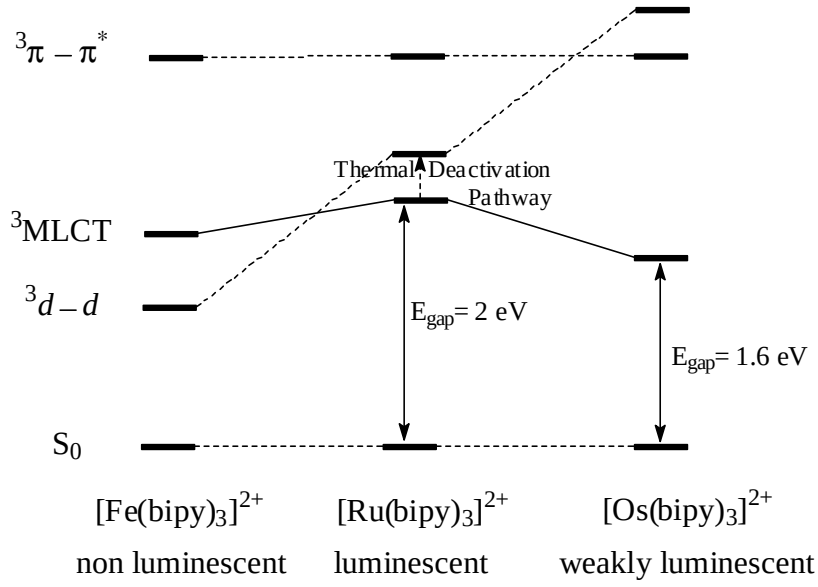

Fig. 1. Lowest-energy triplet states of the tris(bipyridyl) complexes of the 6th transition metal group (adapted and revised from Ref. 7).

The energy of the *d-d* levels of $[Os(bipy)_3]^{2+}$ is too high to be thermally accessible which is the reason for the high photostability of Os MLCs. In the case of the ruthenium complexes an increase of the temperature results in a higher population of the *d-d* states, followed by a rapid radiationless decay to the ground state.

Os MLCs are only weakly fluorescent in comparison to the Ru MLCs. This is a result of the energy-gap law. It implies that the rate of radiationless decay increases exponentially when the energy of the excited ^{3}MLCT state becomes closer to the ground state [8]. This is true for $[Os(bipy)_3]^{2+}$ as compared to $[Ru(bipy)_3]^{2+}$ (see Fig. 1).

1.1.1 Spectral Characteristics of Ru MLCs

Several electronic states are accessible upon light absorption. Ligand-centered (LC) absorption only will occur at wavelengths shorter than 300 nm. The major absorption band is around 450 nm due to metal-to-ligand charge transfer (MLCT) with molar absorbances (ε) between 10,000 and 30,000 L/(mol · cm) [8]. This band is not as sharp as in the case of an organic dye, and the ε values of the complex are lower but they are in the same order of magnitude and thus acceptable for most applications. The inexpensive blue LEDs with 450 nm output or the 488 nm emission line of argon ion lasers can be used as excitation sources because the absorption band at 450 nm is very broad. This is of particular interest for applications where modulated light is necessary, i.e. for frequency domain fluorescence lifetime measurements.

The emission maximum of Ru MLCs is at around 600-650 nm and is a result of an MLCT transition. In this work, data will be presented which show that wavelengths beyond 700 nm can be reached depending on the substitution pattern of the ligand. Besides a Stokes' shift of over 250 nm is possible for MLCs. This allows an easier separation of the emission from the excitation light compared to cyanines, fluoresceins or rhodamines whose Stokes' shift is about 20 nm. This separation can be achieved by glass cut-off filters using the Ru MLCs. Therefore, the use of simpler and less expensive instrumentation for fluorescence measurements is possible.

For measurements in blood, serum and through tissue an emission maximum of the dye at wavelengths of over 600 nm is desirable because biological materials display negligible

autofluorescence and the lowest absorption coefficients at these wavelengths (see Fig. 2). This means that the reabsorption of the emission light of the MLC is low.

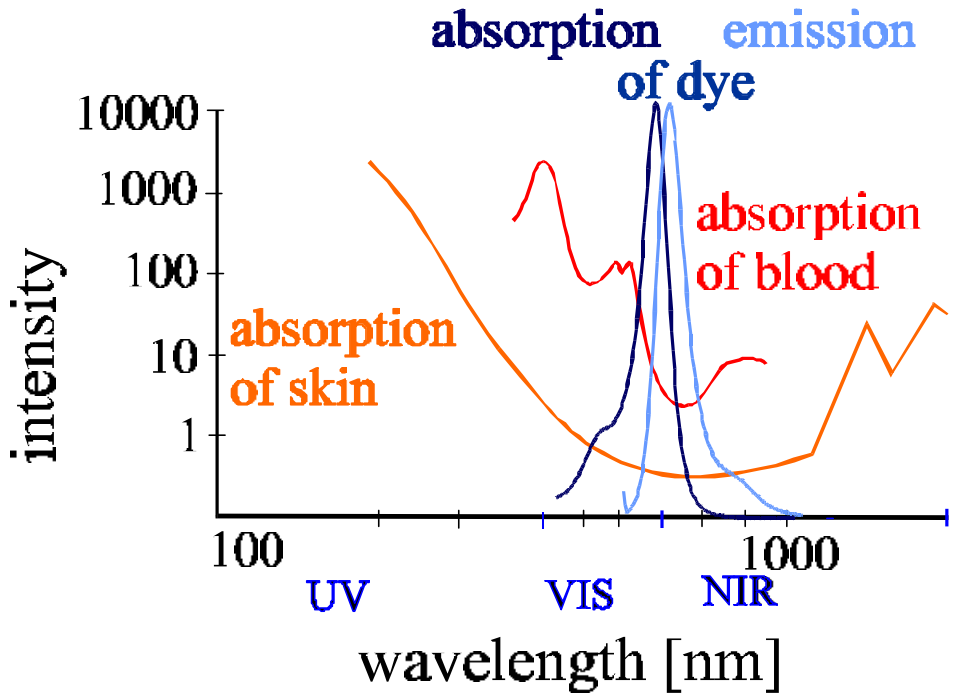

Fig. 2. Absorption characteristics of biological materials and a dye whose emission matches the optical window of these materials. Note that the y-axis is logarithmically.

Tyrosine and tryptophane fluorescence can exceed wavelengths of 400 nm [9] and thus disturb measurements with shorter-wavelength emitting fluorophores. The long lifetime of the MLC of over hundred ns compared to those of amino acids which are below 10 ns enables fluorescence measurements based on temporal discrimination. The lifetime of the MLC is detected after a delay time of a few ns during which the fluorescence of the natural fluorophores decays to zero. This is the so-called off-gated measurement of fluorescence lifetimes.

1.1.2 Applications for Determination of DNA and Membrane Dynamics

The dye most commonly used for the measurement of DNA rotational motions is ethidium bromide (EB). Apart from its very high toxicity [10] this compound has the disadvantage of a short lifetime of 30 ns. Only short time motions of the DNA can be detected by anisotropy changes of bound EB. The slower bending motions of the double helix can be detected with an intercalating probe which offers a longer fluorescence lifetime. This enables to examine the slow motions of DNA by their influence on fluorescence polarization.

The first MLC based probe published previously [11] contained a dipyrido-[3,2a:2',3'-c] phenazine (dppz) ligand (see Fig. 3).

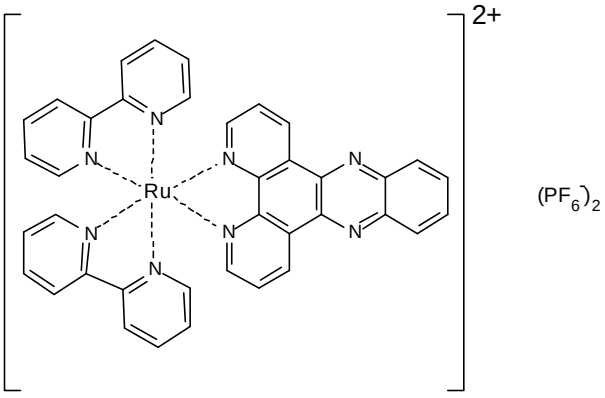

Fig. 3. Chemical structure of the DNA polarization probe $[Ru(bipy)_2(dppz)](PF_6)_2$.

The principle of increased luminescence upon intercalation of the complex into the double strand is the same compared to EB. The increase is caused by a shielding of the nitrogen atoms of the dppz ligand from solvent molecules by the DNA bases.

Long-lifetime MLC probes are of particular interest to study rotational motions in membranes or of vesicles. The MLCs employed herefore have to provide solubility in lipid-like solvents and have to display a sufficiently polarized emission for detection. Several of these probes have been discribed (see Fig. 4) [12-14]. They are advantageous over the commonly used DPH (1,6-diphenyl-1,3,5-hexatriene) due to their low toxicity, long-wavelength emission suitable for measurements in biological material and their comparably high anisotropy values.

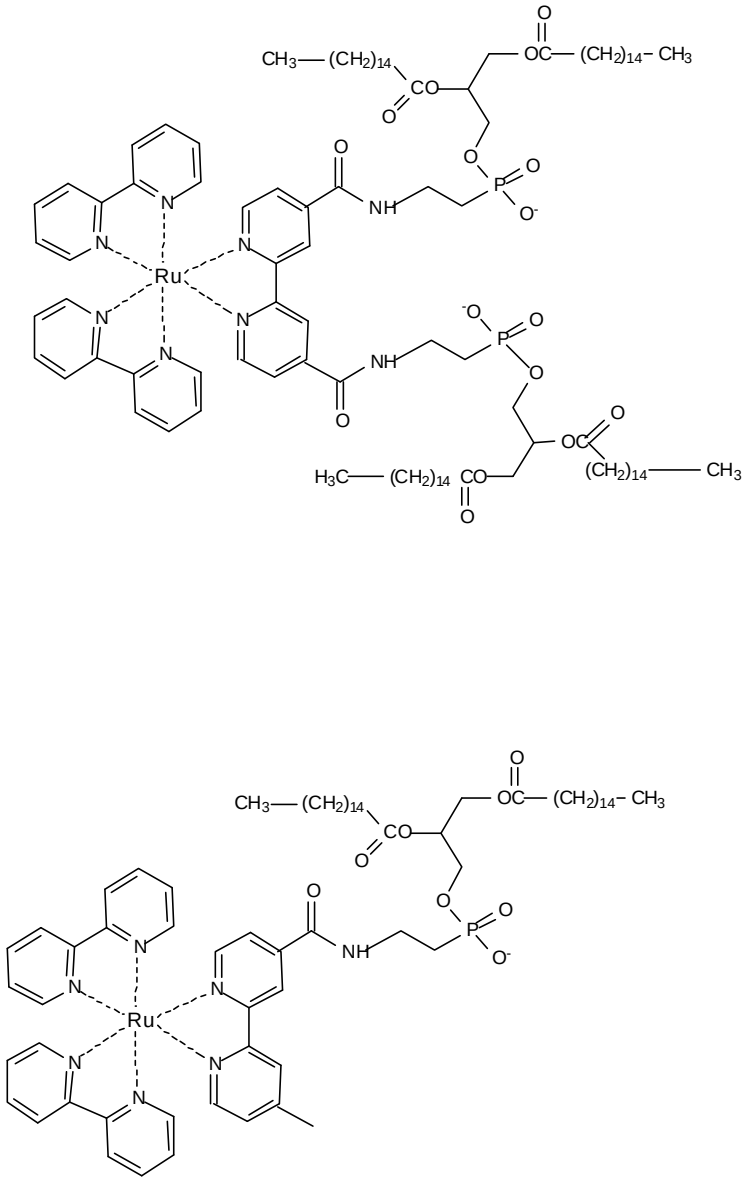

Fig. 4. MLC lipid membrane probes for anisotropy measurements.

1.1.3 Sensing of pH, O_2 and CO_2 with Ru MLCs

The equilibrium between the deprotonated and the protonated form of N,N'-diethylamino groups of a ligand was used for the design of a pH probe based on an MLC [15]. $[Ru(bipy)_2$ (4,4'-diethylaminomethyl-2,2'-bipyridine$](PF_6)_2$ (see Fig. 5, left) enables monitoring the pH between 2.5 and 11.5 due to a threefold increase of the emission intensity.

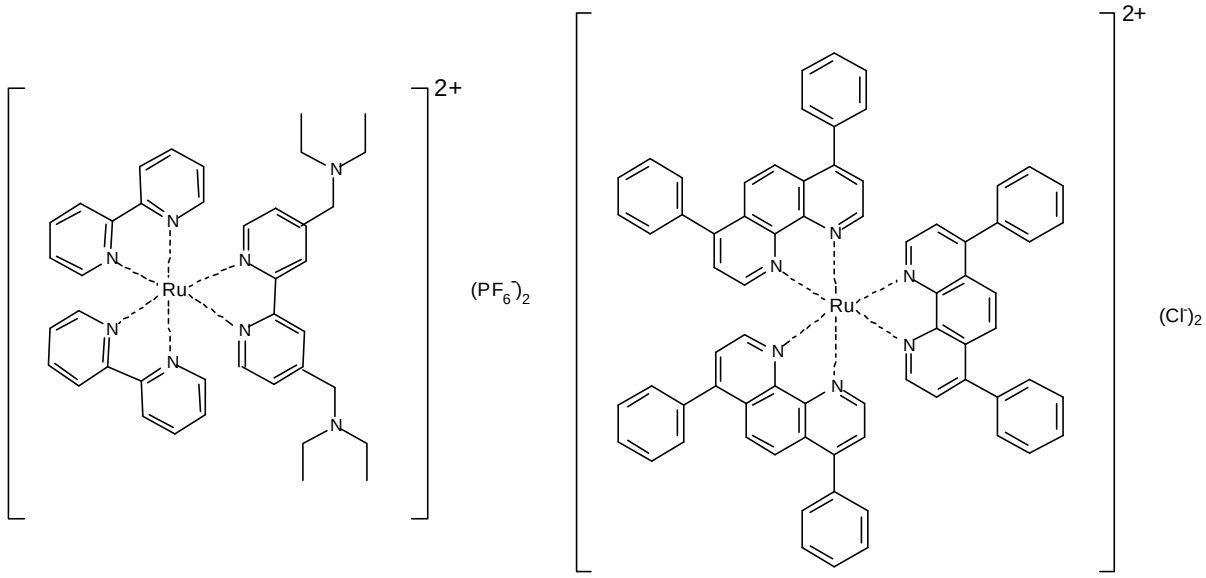

Fig. 5. Structure of the Ru complexes suitable for pH (left) and for O_2 and CO_2 (right) measurements.

The emission maximum shifts from 620 to 650 nm with increasing pH and thus a ratiometric determination of the pH is possible. This means that a ratio of the emission intensity is taken at two wavelengths. The advantages of ratiometric measurements are the elimination of disturbances due to photobleaching and due to fluctuations of the excitation source. Furthermore, the measurement is independent of the dye concentration. This principle is widely used for Ca^{2+} and $Mg^{2+}$with the Fura (two excitation wavelengths) and Indo (two emission wavelengths) dyes [16]. Ratiometric pH measurement was carried out using HPTS (1-hydroxypyrene-3,6,8-trisulfonate) [17], seminaphthofluoresceins (SNAFL) or seminaphthorhodamines (SNARF) [18]. The Ru MLC offers time domain or frequency domain measurements of the luminescence lifetime as a further detection principle of the pH value. An accuracy of ± 0.04 pH units can be achieved.

Another very important parameter to be measured in biological applications is the concentration of oxygen and carbon dioxide. The sensitivity of $[Ru(4,7\text{-diphenyl-}1,10\text{-phenanthroline})_3]^{2+}$ (see Fig. 5, right) to collisional quenching with oxygen is used as the detection method. This results in a decreased intensity and lifetime of the MLC, described by the Stern-Volmer Equation.

$$\frac{F_0}{F} = \frac{\tau_0}{\tau} = 1 + k_q \tau_0 [Q] = 1 + K[Q] \qquad (1.1)$$

Here F_0 and F are the emission intensities, τ_0 and τ the lifetimes in absence or presence of the quencher, K is the Stern-Volmer quenching constant and k_q is the bimolecular quenching constant.

The concentration of CO_2 is related to the pH of the solution via the hydrogencarbonate anion. Therefore a combination of a pH and an oxygen sensor can serve as a detection system for CO_2 [19, 20].

1.1.4 Ruthenium, Rhenium and Osmium MLCs in Polarization Immunoassays

The fact that asymmetric Ru MLCs with two identical ligands and one nonidentical ligand emit strongly polarized light has stimulated extensive research on such probes. Polarized emission combined with a lifetime in the microsecond range offer an opportunity to study slow processes like rotations of proteins or other macromolecules. This is a result of the dependence of the fluorescence polarization or fluorescence anisotropy (which both describe the same phenomenon, see chapter 2.1) of the fundamental anisotropy r_0 and the fluorescence lifetime τ, described by the Perrin equation

$$r = \frac{r_0}{1 + (\tau / \rho)} \qquad (1.2)$$

where θ is the rotational correlation time. Covalent attachment of a short-lifetime fluorophore like fluorescein to a small hapten (M ≈ 2,000 g/mol) with a correlation time of about 100 ps will display an anisotropy near zero. Upon formation of an antigen-antibody complex with a common IgG-type antibody (M = 160,000 g/mol) an r-value near r_0 will be measured because the θ-value enhances to 100 ns. This rotational correlation time is normally found for an antibody. Therefore short-lifetime fluorophores are valuable for monitoring concentrations of low molecular-weight drugs but not for the determination of high molecular-weight antigens in clinical applications.

However, antigens can display molecular masses of some ten thousands to million g/mol. Suppose fluorescein-labeled HSA (M = 66,000 g/mol, θ = 50 ns) has to be detected. Here the r-value will be near r_0 just in absence of antigen because the lifetime of fluorescein is only 4 ns but θ is more than ten times higher. Consequently, an anisotropy immunoassay with fluorescein as the label will display only a very small dynamic range for antigen detection. A variety of complexes capable to be attached covalently to macromolecules based on ruthenium have been described (see Fig. 6) [21-24].

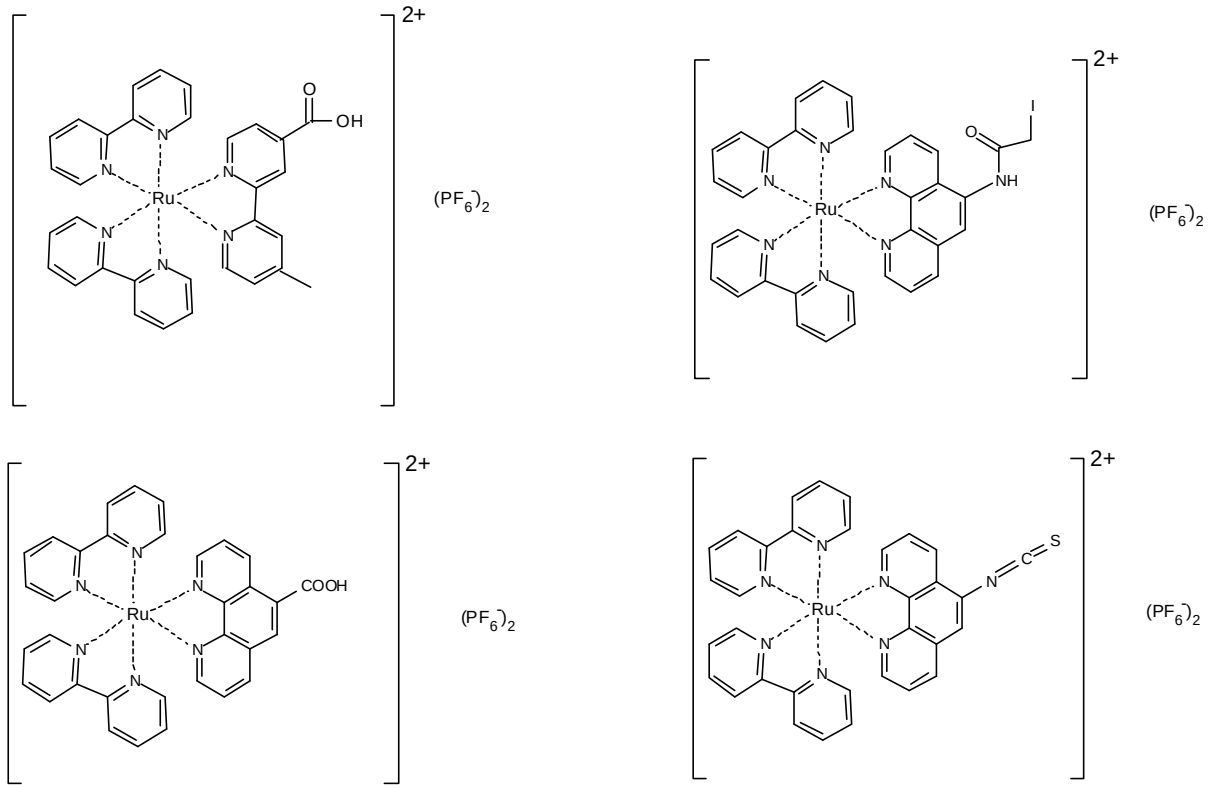

Fig. 6. Conjugatable Ru MLCs previously used for fluorescence anisotropy based immunoassays.

These MLCs offer lifetimes in the desired range of some hundreds of nanoseconds to about ten μs and large Stokes' shifts of up to 150 nm. This is advantageous to avoid disturbances due to excitation light or scattered light. Disadvantageous are the low quantum yields of less than 0.05 and an often difficult synthesis which involves the use of highly toxic chemicals like SeO_2. If only one of the 4-methyl groups at a 4,4'-dimethyl-2,2'-bipyridine ligand has to be activated to the corresponding acid the oxidation can be performed just within two steps. First the methyl

group is oxidized to the corresponding aldehyde with SeO_2. The further oxidation has to be continued using Ag_2O. Toxic phosgen gas has to be used for the preparation of a ligand containing isothiocyanate. For these Ru-MLCs no immunoassays in the most commonly competitive format have been described.

MLCs based on Re(I) to obtain higher anisotropies or MLCs based on Os(II) to enable diode-laser-wavelength excitation have been synthesized (see Fig. 7) [2,4]. The Re(I) complex displays high anisotropies (up to 0.3) and quantum yields of 0.2. This enabled the performance of a competitive immunoassay for HSA. The disadvantages are the much shorter excitation and emission wavelengths at 390 and 520 nm, respectively, compared to the Ru complexes [4]. A stronger damage of the biological material due to near-UV excitation is caused and the use of more expensive light sources like short-wavelength lasers or UV-LEDs is required. Furthermore, reabsorption of the emission by biological material is a serious problem at wavelengths below 600 nm (see Fig. 2).

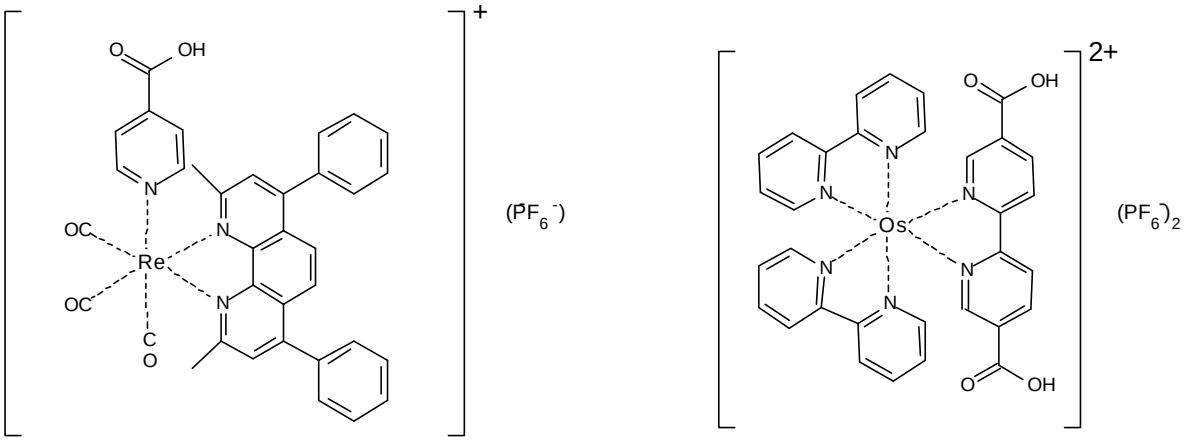

Fig. 7. Chemical structures of Re(I) and Os(II) MLCs used in polarization immunoassays.

The Os complex displays a long-wavelength absorption at 685 nm (close to the 690 nm laser diode) and an emission maximum at 760 nm. Unfortunately, the r_0 value is only around 0.15 [2]. The high toxicity of all osmium compounds also is disadvantageous.

1.2 Europium Metal-Ligand Complexes in Analytical Biochemistry

Europium metal-ligand complexes have become more and more important in biochemical applications in the past twenty years [25]. This is due to the fact, that europium and terbium ions and their complexes display luminescence above 77 K in aqueous buffer solutions suitable for biological applications. Eu^{3+} generally retains its luminescence when bound to a complex ligand system. Furthermore it exhibits multiple sharp emission lines due to electronic transitions whose relative intensities and line splitting patterns are sensitive to the ligand environment around the metal ion.

1.2.1 Luminescence Properties of Eu^{3+} and Eu MLCs in Aqueous Solution

The lowest-energy multiplets associated with the $4f^6$ electronic configuration of the Eu^{3+} ion is shown in Figure 8.

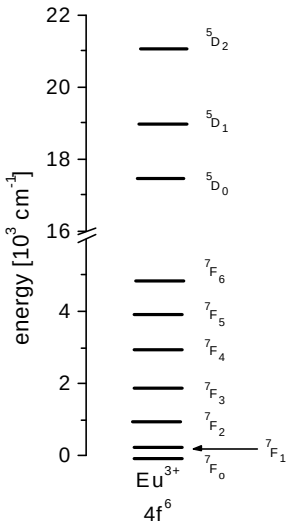

Fig. 8. Energy level diagram depicting the approximate locations of baricenters for the lowest-energy multiplet levels of Eu^{3+}. Each level is labeled according to its $^{2S+1}L_J$ Russell-Saunders component (adapted and revised from Ref. 25).

For all europium(III) complexes in aqueous solution, essentially all emission emanates from the nondegenerated $^5D_0$ level if the excitation is at wavelengths < 578 nm. The strongest

emissions are always observed in the $^5D_0 \rightarrow {}^7F_1$ and $^5D_0 \rightarrow {}^7F_2$ transition regions, and $^5D_0 \rightarrow {}^7F_4$ emission is frequently observed to have a moderately strong intensity. Emission intensities of the remaining $^5D_0 \rightarrow {}^7F_J$ transitions are generally either very weak or unobservable. The relative intensities of the $^5D_0 \rightarrow {}^7F_1$ (585-600 nm) and $^5D_0 \rightarrow {}^7F_2$ (610-620 nm) emissions are very sensitive to the detailed nature of the ligand environment. This phenomenon is called a hypersensitive band.

The luminescence lifetime of the $^5D_0$ emitting state of Eu^{3+} complexes in aqueous solution $\tau_{Eu}(^5D_0)$ is found in the 1 μs-1 ms range. This lifetime is quite sensitive to the nature of the ligand environment, and especially to the number of water molecules occupying inner coordination sites. The modulation of $\tau_{Eu}(^5D_0)$ by the ligand environment can be attributed to ligand dependent effects on both the radiative and the nonradiative $^5D_0 \rightarrow {}^7F_J$ transition probability [25].

1.2.2 Applications of Eu^{3+} Complexes in Fluorescence Immunoassays

A large variety of applications of fluorescent chelate labels have been described [26,27]. Two assay principles are commercially available at present. The DELFIA assay involves labeling of either antigen or antibody with a nonfluorescent rare earth complex. Hence, no energy can be transferred to the lanthanide ion. The ion is separated off the ligand into the solution after the immunoreaction, i.e. by the addition of acid. Then an “enhancement solution” of naphtoyl-trifluoroacetone and a detergent is added, followed by the determination of the enhanced fluorescence intensity [28].

The FIAGEN assay principle is based on the avidin-biotin system. Surface bound biotinylated antigen or antibody is reacted with BCPDA-labeled (4,7-bis(chlorosulfophenyl)-1,10-phenanthroline-2,9-dicarboxylic acid) avidin. An excess of europium solution is added after formation of the avidin-biotin adduct [29]. Finally a washing step is required. The fluorescence is measured after drying of the surface. The measurement of surface fluorescence, however, is optically more demanding, and sensitive fluorometry requires well dried surfaces [30].

1.3 Hydrogen Peroxide: Methods of Determination in Fluorescent Analysis

Peroxides appear in many enzymatic and atmospheric reactions. Oxidases convert their substrate under formation of hydrogen peroxide, and peroxidases use hydroperoxides and H_2O_2 as substrate for oxidation processes. In cellular processes released H_2O_2 is very toxic. Hence, the H_2O_2 degrading peroxidase is the enzyme with one of the highest turnaround numbers ever found. The turnaround rate to convert H_2O_2 to H_2O is diffusion controlled. In the atmosphere, peroxides play a role as reactive substances due to the formation of radicals by irradiation with sunlight. These radicals are suspected to be the reason for the degradation of the UV-protecting ozone layer in the atmosphere. Therefore, the determination of low concentrations of peroxides is an important objective in bioanalytics as well as in environmental analysis.

Many procedures applied for fluorimetric determination of peroxides use peroxidases to oxidize a fluorogenic substrate in presence of peroxides. Hydroxyphenylacetic acid and hydroxyphenylpropionic acid are well established reagents using this detection scheme. These substances are converted to their respective fluorescent biphenols by peroxidase catalysis. The emission is detected at 405 nm on excitation at 320 nm at pH 9.5. The disadvantage of this method is that it cannot discriminate between different peroxides due to the absence of a selectivity of the enzyme for some peroxides. The UV excitation light at 320 nm can cleave weak bonds in biomolecules and co-excite other organic fluorophores. This disturbs the measurement of the emission light of the biphenol. Furthermore not every biological material is stable at the highly alkaline pH of 9.5 [31].

A new method following the “enzyme amplified lanthanide luminescence” (EALL) concept was introduced recently [32]. Here the enzymatic reaction evolves a fluorophore which can undergo complexation with Tb(III)-EDTA. The fluorogenic substrates for horse radish peroxidase are 4-hydroxyphenylacetic acid or 4-hydroxyphenylpropanic acid. The enzyme converts H_2O_2 and the phenol to the respective biphenol at pH 9.5. This is followed by the complexation with Tb(III)-EDTA at pH 13 in presence of CsCl. An increased emission of the hypersensitive $^5D_4 \rightarrow {}^7F_4$ transition of Tb(III) is detected at 545 nm in presence of H_2O_2 but neither the problem of UV excitation nor the pH conditions were improved. Additionally, an assay for micro titer plates was presented [33]. Especially the pH has to be lowered to use this method for the determination of glucose oxidase (GOx)-generated H_2O_2 for indirect glucose

measurements. At pH 9.5 the turnaround number of this enzyme will be low because the pH optimum for GOx is at 5.1, in the more acidic pH range [34]. This would cause long detection times.

A spectrophotometric assay for H_2O_2 is available based on the decrease of the absorption of a Ti(IV)-porphyrine complex at 432 nm. The best results are obtained at the highly acidic pH of 0.3 [35] which is often impossible if biological material is employed.

1.4 Aim of the Work

The aim of the first part of this work was to characterize new ruthenium based MLCs which can be easily synthesized and covalently attached to a biomolecule to show changes of their fluorescence polarization in various formats of homogenous immunoassays.

In the second part a new method for the determination of hydrogen peroxide in aqueous solutions is introduced using the luminescence enhancement of the europium tetracycline complex upon binding of H_2O_2.

A further objective was to develop a glucose sensing method, based on the luminescence enhancement of a europium tetracycline complex due to enzymatically generated H_2O_2 at physiological glucose concentrations.

1.5 Literature

1. Demas, J. N., DeGraff, B. A., 1994, Design and Applications of Highly Luminescent Transition Metal Complexes, in *Topics in Fluorescence Spectroscopy, Vol. 4, Probe Design and Chemical Sensing*, J. R. Lakowicz (Ed.), Plenum Press, New York, 71-107.
2. Terpetschnig, E., Szmacinski, H., Malak, H., Lakowicz, J. R., 1996, Fluorescence polarization immunoassay of a high molecular weight antigen using a long wavelength absorbing and laser diode-excitable metal-ligand complex, *Anal. Biochem.*, **240**, 54-59.

3. Juris, A., Balzani, V., Barigelletti, F., Campagna, S., Belser, P., von Zelevsky, A., 1988, Ru(II) polypyridine complexes: Photophysics, photochemistry, electrochemistry and chemiluminescence, *Coord. Chem. Rev.*, **84**, 85-277.
4. Guo, X-Q., Castellano, F. N., Li, L., Lakowicz, J. R., 1998, Use of a long-lifetime Re(I) complex in fluorescence polarization immunoassays of high-molecular weight analytes, *Anal. Chem.*, **70**, 632-637.
5. Pang, Z., Gu, X., Yekta, A., Masuomi, Z., Foucher, D., Coll, J., Winnik, M. A., Manners, I., 1996, *Adv. Mater.*, **8**, 768.
6. Di Marco, G., Lanza, M., Mamo, A., Stefio, I., Di Pietro, C., Romeo, G., Campagna, S., 1998, Luminescent Mononuclear and Dinuclear Iridium(III) Cyclometalated Complexes Immobilized in a Polymeric Matrix as Solid State Oxygen Sensors, *Anal. Chem.*, **70**, 5019-5023.
7. Demas, J. N., DeGraff, B. A., 1991, Design and Applications of Highly Luminescent Transition Metal Complexes, *Anal. Chem.*, **63**, 829-837.
8. Lakowicz, J. R., 1999, *Principles of Fluorescence Spectroscopy*, 2nd Edition, Kluwer Academic/Plenum Publishers, New York, 577.
9. see Ref. 8, 446, 450.
10. Merck, 1996, *Reagenzien, Chemikalien, Diagnostica*, 608.
11. Friedman, A. E., Chambron, J.-C., Sauvage, J.-P., Turro, N. J., Barton, J.K., 1990, Molecular light switch for DNA: $Ru(bpy)_2dppz^{2+}$, *J. Am. Chem. Soc.*, **112**, 4960-4962.
12. Li, L., Szmacinski, H., Lakowicz, J. R., 1997, Long-lifetime lipid probe containing a luminescent metal-ligand complex, *Biospectroscopy*, **3**(2), 155-159.
13. Li, L., Szmacinski, H., Lakowicz, J. R., 1997, Synthesis and luminescence spectral characterization of long-lifetime lipid metal-ligand probes, *Anal. Biochem.*, **244**, 80-85.
14. Augustin, C., Lehmann, F., Wolfbeis, O. S., 2001, *Chem. Phys. Lipids.*, submitted.
15. Murtaza, Z., Chang, Q., Rao, G., Lin, H., Lakowicz, J., R., 1997, Long-lifetime metal-ligand pH probe, *Anal. Biochem.*, **247**, 216-222.
16. Grykiewicz, G., Poenie, M., Tsien, R. Y., 1985, A new generation of Ca^{2+} indicators with greatly improved fluorescence properties, *J. Biol. Chem.*, **264**, 19449-19457.
17. Wolfbeis, O. S., Fürlinger, E., Kroneis, H., Marsoner, H., 1983, Fluorimetric analysis. 1. A study on fluorescent indicators for measuring near neutral ("physiological") pH-values, *Fresenius' Z. Anal. Chem.*, **314**, 119-124.

18. Whitaker, J., E.,. Haugland, R., P., Prendergast, F., G., 1991, Spectral and photophysical studies of bezno[c]xanthene dyes. Dual emission pH sensors, *Anal. Biochem.*, **194**, 330-344.
19. Wolfbeis, O. S., 1991, Oxygen Sensors, in *Fiber Optic Chemical Sensors and Biosensors*, Vol. II, O. S. Wolfbeis (Ed.), CRC Press, Boca Raton, Florida, 19-53.
20. Lippitsch, M. E., Pusterhofer, J., Leiner, M. J. P., Wolfbeis, O. S., 1988, Fiber-optic oxygen sensor with the fluorescence decay time as the information carrier, *Anal. Chim. Acta*, **205**, 1-6.
21. Terpetschnig, E., Szmacinski, H., Malak, H., Lakowicz, J. R., 1995, Metal-ligand complexes as a new class of long lived fluorophores for protein hydrodynamics, *Biophys. J.*, **68**, 342-350.
22. Szmacinski, H., Terpetschnig, E., Lakowicz, J. R., 1995, Synthesis and evaluation of Ru-complexes as anisotropy probes for protein hydrodynamics and immunoassays of high-molecular weight antigens, *Biophys. Chem.*, **62**, 109-120.
23. Castellano, F., N., Dattelbaum, J. D., Lakowicz, J. R., 1998, Long-lifetime Ru(II) complexes as labeling reagents for sulfhydryl groups, *Anal. Biochem.*, **255**, 165-170.
24. Terpetschnig, E., Dattelbaum, J. D., Szmacinski, H., Lakowicz, J. R., 1997, Synthesis and spectral characterization of a thiol-reactive long-lifetime Ru(II) complex, *Anal. Biochem.*, **254**, 179-186.
25. Richardson, F. S., 1982, Terbium(III) and Europium(III) Ions as Luminescent Probes and Stains for Biomolecular Systems, *Chem. Rev.*, **82**, 541-552.
26. Wisser, H., 1985, L*abor Medizin*, **8**, 89.
27. Diamandis, E. P., Christopoulos, 1990, *Anal. Chem.*, **62**, 1149.
28. Hemmilä, I., 1995, *J. Alloys Comp.*, **225**, 480.
29. Evangelista, R. A., Pollak, A., Allore, B., Templeton, E.F., Morton, R. C., Diamandis, E. P., 1988, *Clin. Biochem.*, **21**, 173.
30. Hemmilä, I., 1993, *Fluorescence Spectroscopy, New Methods and Applications*, Wolfbeis O. S. (Ed.), Springer Verlag, Berlin/Heidelberg, 259-266.
31. Hellpointner, E., Gäb, S., 1989, *Nature*, **337**, 631-634.
32. Meyer, J., Karst, U., 1999, Zeitverzögerte Fluoreszenzspektroskopie mit Lanthanoid-komplexen - Prinzipien und Anwendungen, *NChTL.*, **47**, 1116-1119.
33. Meyer, J., Karst, U., 1998, Verfahren zur Bestimmung von Peroxiden, *DE 198 13 247.6.*

34. Sigma, *Biochemicals and Reagents*, 2000.
35. Matsubara, C., Kawamoto, N., Takamura, K., 1992, Oxo[5,10,15,20-tetra(4-pyridyl) porphyrinato]titanium(IV): An Ultra-high Sensitivity Spectrophotometric Reagent for Hydrogen Peroxide, *Analyst*, 117, 1781-1784.

2. Background

2.1 Fluorescence Anisotropy or Polarization: Definitions and Theory

There are two approaches both describing the same phenomenon from a different point of view to result in the definitions for anisotropy and polarization. They can easily be converted into each other.

Consider partially polarized light moving along the x-axis (see Fig. 9) and assume one measures the intensities of the light I_z and I_y which have been separated by a polarizer on the x-axis.

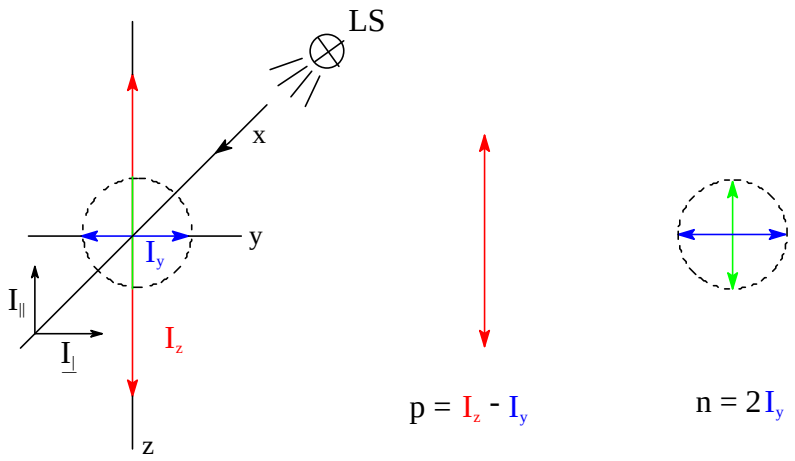

Fig. 9. Visualization of the polarized fraction of a ray of light.

The polarization P is then defined as the fraction of light that is linearly polarized or as the intensity of the polarized component p divided by the sum of the natural component n and p.

$$P = \frac{p}{p+n} \qquad (2.1)$$

As the intensity of $n = 2I_y$ the remaining intensity is the polarized component given by $p = I_z - I_y$. For vertically polarized excitation $I_z = I_{\parallel}$ and $I_y = I_{\perp}$ is valid. More figuratively, P is the ratio

of the excess intensity along the z-axis I_z - I_y divided by the total intensity I_z - I_y + $2I_y$. Substitution into Eq. (2.1) yields

$$P = \frac{I_{\parallel} - I_{\perp}}{I_{\parallel} + I_{\perp}} \tag{2.2}$$

which is the standard definition for polarization.

The anisotropy r of a light source is defined as the ratio of the intensity of the polarized component to the total intensity I_T.

$$r = \frac{I_z - I_y}{I_x + I_y + I_z} = \frac{I_z - I_y}{I_T} \tag{2.3}$$

Suppose the excitation is polarized along the z-axis, dipolar radiation from a fluorophore is also symmetric around the z-axis. Hence, $I_x = I_y$ and with $I_z = I_{\parallel}$ and $I_y = I_{\perp}$ Eq. (2.4) is obtained

$$r = \frac{I_{\parallel} - I_{\perp}}{I_{\parallel} + 2I_{\perp}} \tag{2.4}$$

which is the standard definition for anisotropy. Thus the anisotropy describes the ratio of the excess intensity parallel to the z-axis to the total intensity which is $I_{\parallel}$ + 2 $I_{\perp}$. Both polarization and anisotropy are dimensionless quantities. The values can be converted into each other using

$$P = \frac{3r}{2 + r} \tag{2.5}$$

$$r = \frac{2P}{3 - P} \tag{2.6}$$

The theory for fluorescence anisotropy is much easier to derive than that for polarization. Therfore, it is derived now for a single molecule of DPH. DPH displays nearly parallel

transition moments for the absorption and emission moments. Assume that the molecule is oriented with angles θ relative to the z-axis and with ϕ relative to the y-axis (see Fig. 10). The absence of rotational diffusion is supposed for simplification [1].

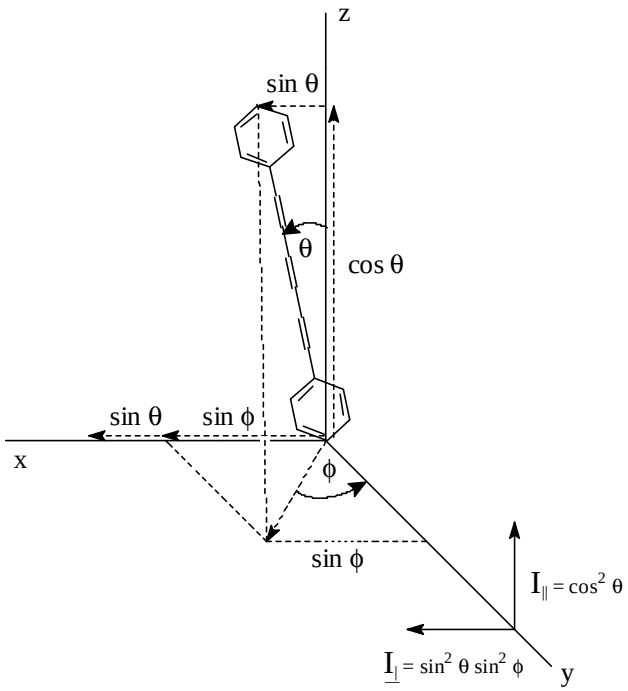

Fig. 10. Derivation of the emission intensities from the geometrical arrangement of a single fluorophore in a coordinate system (adapted and corrected from Ref. 1).

The intensity of the light radiated from such a dipole is proportional to the square of its vectors projected onto the axis of observation because fluorescing dipoles behave like radiating dipoles [2]. These projections are given by

$$I_{\parallel}(\theta,\phi) = \cos^2 \theta \qquad (2.7)$$

$$I_{\perp}(\theta,\phi) = \sin^2 \theta \ \sin^2 \phi \qquad (2.8)$$

The solution will contain many fluorophores with random distribution under experimental conditions. Based on the photoselection rule, which will be discussed later, every molecule contributes to the average measured intensity. Excitation polarized along the z-axis must excite all molecules having an angle ϕ with respect to the y-axis with equal probability. This

corresponds to a symmetrical distribution of the excited fluorophores around the z-axis. Any population in an experiment will be oriented with ϕ from 0 to 2π with equal probability, and therefore the ϕ dependence in Eq. (2.8) can be eliminated. Then, the average value of $\sin^2 \phi$ is given by

$$\langle \sin^2 f \rangle = \frac{\int_0^{2p} \sin^2 f \, df}{\int_0^{2p} df} = \frac{1}{2} \tag{2.9}$$

and therefore Eq. (2.7) and (2.8) result in

$$I_{\parallel}(\theta) = \cos^2 \theta \tag{2.10}$$

$$I_{\perp}(\theta) = \tfrac{1}{2} \sin^2 \theta \tag{2.11}$$

Finally the photoselection rule says that a fluorophore aligned along the z-axis will absorb light along this axis with a probability proportional to $\cos^2 \theta$ to this axis. Here θ is the angle the absorption dipole makes with the z-axis. The result is an excited state population which is symmetrically distributed around the z-axis. Hence, the number of molecules at an angle between θ and $d\theta$ is proportional to $\sin \theta \, d\theta$. This quantity is proportional to the surface area on a sphere within the angles θ and $\theta + d\theta$. Therefore, the distribution of molecules excited by vertically polarized light is given by

$$f(\theta) \, d\theta = \cos^2 \theta \, \sin \theta \, d\theta \tag{2.12}$$

Substitution of Eq. (2.12) in Eqs. (2.10) and (2.11) results in

$$I_{\parallel} = \int_0^{p/2} f(q) \cos^2 q \, dq = k \langle \cos^2 q \rangle \tag{2.13}$$

$$I_{\perp} = \frac{1}{2}\int_0^{p/2} f(q)\sin^2 q\, dq = \frac{k}{2}\langle \sin^2 q\rangle \qquad (2.14)$$

where $f(\theta)\, d\theta$ is the probability that a fluorophore is oriented between θ and θ + dθ, and k is an instrumental constant. Using Eq. (2.8) and the relation $\sin^2\theta = 1 - \cos^2\theta$, the result is

$$r = \frac{3\langle \cos^2 q\rangle - 1}{2} \qquad (2.15)$$

This means that the anisotropy is governed by the average value of $\cos^2\theta$, where θ is the angle of the emission dipole relative to the z-axis. This is based on the fact that the observed intensities $I_{\parallel}$ and $I_{\perp}$ are proportional to the square of the projection of the individual transition moments onto the x-axis and the z-axis (see Fig. 10).

In consideration of the relationship between r and θ, the result for a single fluorophore oriented along the z-axis with collinear transitions is r = 1.0 if θ = 0°. The anisotropy is always less than 1.0, as it is impossible to have a perfectly oriented excited state population in a homogenous solution. This is due to the dependence of r and $\langle\cos^2\theta\rangle$ where for collinear absorption and emission dipoles the maximum value for $\langle\cos^2\theta\rangle$ is given by

$$\langle \cos^2 q\rangle = \frac{\int_0^{p/2} \cos^2 q\ f(q)\, dq}{\int_0^{p/2} f(q)\, dq} \qquad (2.16)$$

Substitution of Eq. (2.12) into (2.16) yields $\langle\cos^2\theta\rangle = 3/5$. Recalling Eq. (2.15), one will find $r_{max} = 0.4$. This is the value measured for a whole population in absence of any depolarizing processes. It is considerably smaller than that for a single fluorophore (r = 1.0) oriented along the z-axis. Complete loss of anisotropy is equivalent to θ = 54.7°, where 54.7° is just the average value of θ caused by $\langle\cos^2\theta\rangle = 1/3$.

A further source for the loss of anisotropy has to be taken into account on changing from theoretical considerations to real measured samples. Up to now the absorption and emission dipoles were assumed to be collinear. This is true only for a few systems. The displacement of

the absorption and emission dipole by an angle β results in a further loss of anisotropy which multiplies with the factor of 2/5 due to photoselection.

$$r_0 = \frac{2}{5}\left(\frac{(3\cos^2 \beta) - 1}{2}\right) \qquad (2.17)$$

r_0 is referred to the anisotropy observed in the absence of other depolarizing processes such as rotational diffusion or energy transfer. As mentioned above an angle β = 54.7° results in an r_0 value of zero. If β exceeds 54.7° the anisotropy becomes negative to reach its minimum at β = 90° where r = -0.20. Table 1 illustrates the values of both r_0 and P_0 for some interesting angles β.

Table 1: Relationship between angular displacement of the transition moments β and r_0 or P_0.

β [°]	r_0	P_0
0	0.40	0.50
45	0.10	0.143
54.7	0.00	0.00
90	-0.20	-0.333

The measurement of the fundamental anisotropy requires dilute solutions (to avoid depolarization due to radiative reabsorption and emission or due to resonance energy transfer) in solvents like glycerol which form clear glasses at -60 to -70 °C. At this temperature rotational diffusion is absent thus the measured r value reveals the angular displacement between absorption and emission moment. Alternatively, the diluted sample can be polymerized into a clear glassy matrix of polyacrylnitrile, wherein the molecules are enclosed tightly enough to avoid rotational motions. Then an excitation polarization spectrum is recorded as β differs for each absorption band and therefore varies in the excitation wavelength. Typically the largest r_0 values are observed for the longest-wavelength absorption band. This is due to the responsibility of the lowest-energy singlet state for both the observed fluorescence and the longest-wavelength absorption band. The dependence of the excitation

wavelength can be explained by a changing fraction of light absorbed by the molecules with a certain β value for which an electronic transition is possible. Therefore a polarization spectrum is a plot of the polarization versus the excitation wavelength of a fluorophore in diluted vitrified solution [3].

2.2 Measurement of Fluorescence Anisotropy

Two methods are commonly used for steady state measurements of fluorescence anisotropies. These are the T-format and the L-format method. The second one was used in this work. The L-format is the most commonly used method since most fluorimeters only have one emission channel. Some procedures have to be introduced to correct for the different efficiencies of the emission detection equipment.

In Fig.11 (upper drawing) a sample is excited with vertically polarized light and the emission is observed through a monochromator or an emission filter. The monochromator normally has different transmission efficiencies for vertically and horizontally polarized light. Although filters normally do not have any polarizing effect rotation of the emission polarizer can cause the focused image of the fluorescence to change position, effecting the real sensitivity. As a result there is a difference between the measured and the desired parallel and perpendicular intensities.

In the following equations the order of appearance of the subscripts corresponds to the way the light passes through the instrument, i.e. I_{VH} means vertically polarized excitation followed by horizontally polarized emission.

The different sensitivities of the emission channel S_V and S_H for vertically and horizontally polarized light have to be taken into account for an objective measurement of $I_\perp$ and $I_\parallel$ unbiased by the detection system.

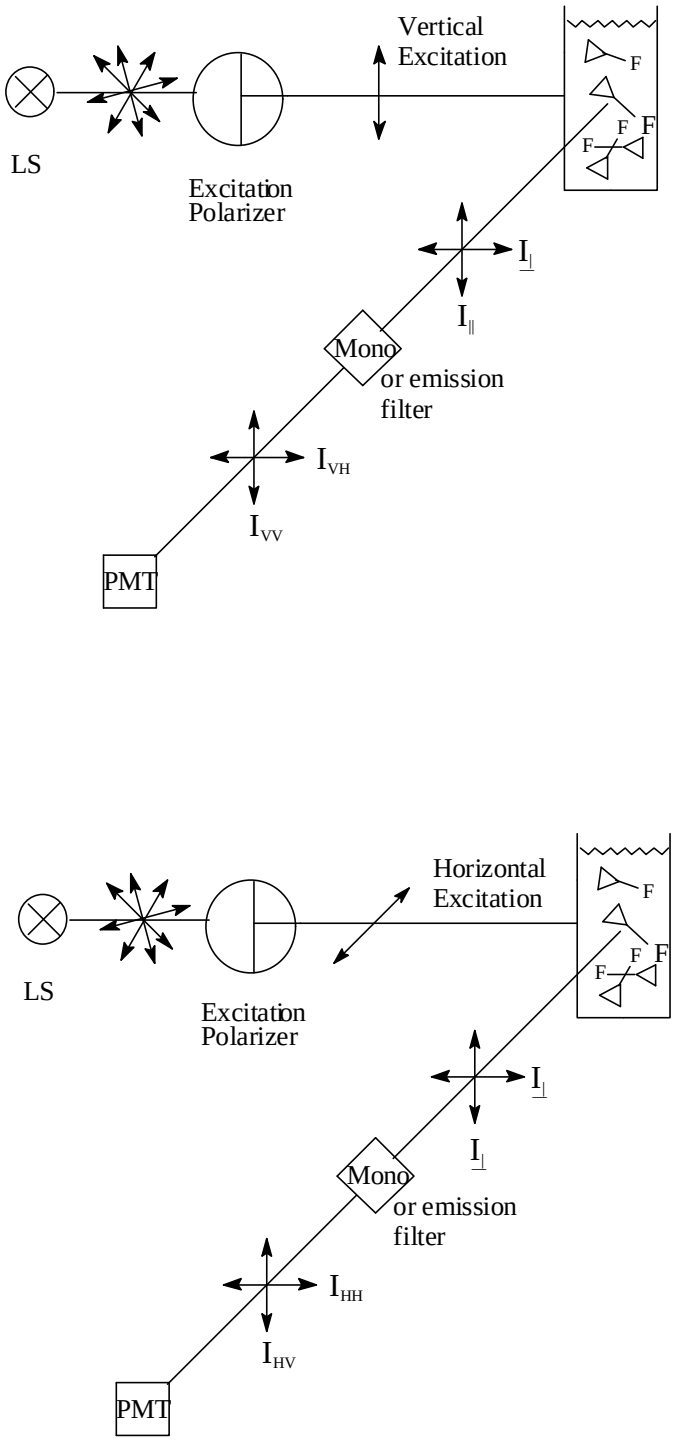

Fig. 11. Lightpath of L-format measurements of the anisotropy with vertically (upper drawing) and horizontally (lower drawing) polarized excitation light and respective orientations of the emission intensities.

Following vertically polarized excitation, the measured polarized intensities are

$$I_{VV} = k\, S_V\, I_{\|} \tag{2.18}$$

$$I_{VH} = k\, S_H\, I_{\wedge} \tag{2.19}$$

where k is a proportionality factor to account for the Q.Y. of the fluorophore and other instrumental factors.

Division of Eq. (2.18) by Eq. (2.19) results in

$$\frac{I_{VV}}{I_{VH}} = \frac{S_V\, I_{\|}}{S_H\, I_{\perp}} = G\,\frac{I_{\|}}{I_{\perp}} \tag{2.20}$$

where G is the ratio of the sensitivities of the detection system for vertically and horizontally polarized light. G is dependent upon the emission wavelength and the bandpass of the emission monochromator. G is determined with horizontally polarized excitation where both the vertical and the horizontal component of the emission light are equal and proportional to $I_{\perp}$ (see Fig. 11) because both orientations are perpendicular to the polarization of the excitation light. Therefore any measured difference in I_{HV} and I_{HH} reflects the different efficiencies of the detection system (see Fig 11, lower drawing).

$$\frac{I_{HV}}{I_{HH}} = \frac{S_V\, I_{\perp}}{S_H\, I_{\perp}} = \frac{S_V}{S_H} = G \tag{2.21}$$

Changes of the excitation intensity due to rotation of the excitation polarizer do not affect the G-factor. With a correctly determined G-factor $I_{\|}$ and $I_{\perp}$ can be calculated using Eq. (2.20) divided by G and using the definition of G in Eq. (2.21)

$$\frac{I_{VV}}{I_{VH}}\frac{1}{G} = \frac{I_{VV}}{I_{VH}}\frac{I_{HH}}{I_{HV}} = \frac{I_{\|}}{I_{\perp}} \tag{2.22}$$

The anisotropy is given by

$$r = \frac{\frac{I_{\parallel}}{I_{\perp}} - 1}{\frac{I_{\parallel}}{I_{\perp}} + 2} \quad \text{or alternatively} \quad r = \frac{I_{VV} - GI_{VH}}{I_{VV} + 2GI_{VH}} \tag{2.23}$$

In the T-format method the intensities are measured simultaneously in two separate detection systems, one for the detection of the parallel and one for the detection of the perpendicular intensity. The different sensitivities of the two detection systems have to be determined using horizontally polarized excitation because the positions of the emission polarizers are left unchanged. Except from a shorter acquisition time the T-format method nowadays no longer has significant advantages over the L-format method [4].

2.3 The Effect of Rotational Diffusion on Fluorescence Anisotropies as a Tool for Determination of Antigen Concentrations in Homogenous Immunoassays

Rotational diffusion is an important cause of depolarization of the emission light coming from a fluorescently labeled macromolecule. This depolarization is dependent from the molecular mass and therefore a fluorescently labeled macromolecule can act as an indicator for antigen-antibody interactions in immunoassays.

The time resolved decay of anisotropy r(t) for a spherical molecule is single exponential

$$r(t) = r_0 e^{-t/q} \tag{2.24}$$

where r_0 is the fundamental anisotropy of the label and θ is the rotational correlation time. The steady state anisotropy can be obtained from the average of the anisotropy decay r(t) over the intensity decay I(t)

$$r = \frac{\int_0^\infty I(t)\, r(t)\, dt}{\int_0^\infty I(t)\, dt} \qquad (2.25)$$

I(t) can be expected to decay as a single exponential for a fluorophore in a homogenous environment

$$I(t) = I_0 e^{-t/t} \qquad (2.26)$$

where τ is the fluorescence lifetime. Substitution of Eq. (2.24) and Eq. (2.26) into Eq. (2.25) gives

$$r = \frac{r_0}{1 + \frac{t}{q}} \qquad (2.27)$$

which is one of different forms of the Perrin equation. For globular proteins, the rotational correlation time is approximately related to the molecular mass M of the protein by

$$q = \frac{hV}{RT} = \frac{hM}{RT}(\bar{n} + h) \qquad (2.28)$$

where $\bar{n}$ is the specific volume and h the hydration volume of the protein, T is the temperature in Kelvin, R the universal gas constant and η is the viscosity in poise [5].

Due to the dependence of the anisotropy of the ratio (τ/θ) (see Eq. (2.27)) there is a demand for fluorophores with sufficiently long fluorescence lifetimes because τ and θ have to be in a comparable order of magnitude to detect changes in the molecular mass of an antigen due to an immunoreaction. This is demonstrated by a calculation of the anisotropy of a labeled macromolecule depending on its molecular mass and the fluorescence lifetime of the label (see Fig. 12). The calculation was performed by the author of this work.

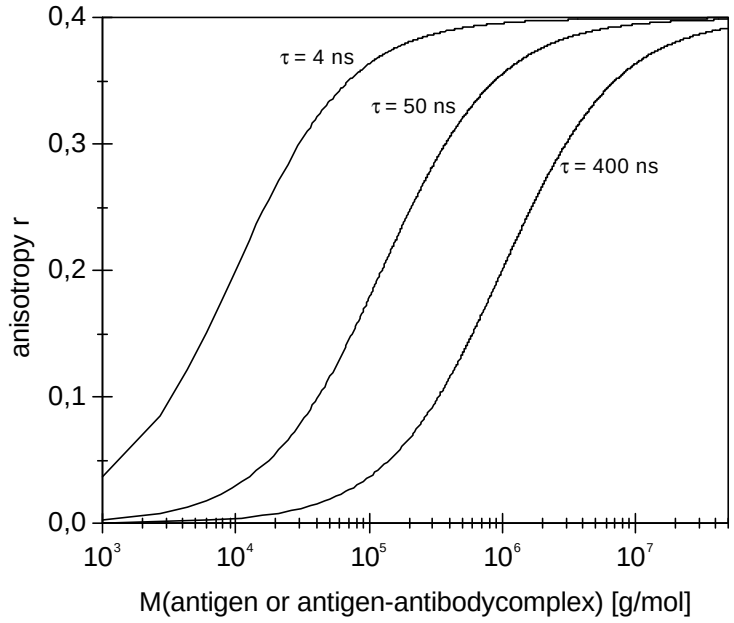

Fig. 12. Molecular mass-dependent anisotropies for different fluorescence lifetimes of the label molecules (T = 298 K, r_0 = 0.4, η = 1 cP, $\bar{n} + h$ = 2,1 mL/g).

The ruthenium metal ligand complexes synthesized previously offer lifetimes of hundreds of nanoseconds [6,7]. This makes them suitable for fluorescence polarization immunoassays with medium weight antigens. Re(I) complexes display very long lifetimes of up to 2.7 μs [8] and therefore are more suitable for very heavy-weight antigens of > 500,000 g/mol.

2.4 Literature

1. Lakowicz, J. R., 1999, *Principles of Fluorescence Spectroscopy*, 2nd Edition, Kluwer Academic/Plenum Publishers, New York, 291-292.
2. Selényi, P., 1939, Wide-angle interferences and the nature of the elementary light sources, *Phys. Rev.*, **56**, 477-479.
3. see Ref. 1, 293-296.
4. see Ref. 1, 298-300.
5. see Ref. 1, 303-304.

6. Terpetschnig, E., Szmacinski, H., Malak, H., Lakowicz, J. R., 1995, Metal-ligand complexes as a new class of long lived fluorophores for protein hydrodynamics, *Biophys. J.*, **68**, 342-350.
7. Szmacinski, H., Terpetschnig, E., Lakowicz, J. R., 1995, Synthesis and evaluation of Ru-complexes as anisotropy probes for protein hydrodynamics and immunoassays of high-molecular weight antigens, *Biophys. Chem.*, **62**, 109-120.
8. Guo, X-Q., Castellano, F. N., Li, L., Lakowicz, J. R., 1998, Use of a long-lifetime Re(I) complex in fluorescence polarization immunoassays of high-molecular weight analytes, *Anal. Chem.*, **70**, 632-637.

3. Ruthenium Complexes as Labels for Polarization Immunoassays

3.1 Syntheses

3.1.1. Synthesis of the Pyrazine Ligands

It was decided first to synthesize MLCs based on reactive bipyrazyl ligands (see Fig. 13) in order to investigate whether these ligands would shift the excitation maximum of the complex to the 488-nm line of the argon ion laser. One of the disadvantages of the probes synthesized previously was the excitation maximum at 460 nm [1,2]. A 488-nm excitation was not used in these assays because fluorescence polarization is strongly dependent on the excitation wavelength. Furthermore, the bipyrazyl-Ru-MLC should display a higher fundamental polarization P_0 due to further charge localization at the ligand. The complex was also supposed to display lifetimes in the μs range which would have made it suitable for polarization immunoassays with antigens of a molecular mass of > 200,000 g/mol.

First, 4-methylphenyl-glyoxal was prepared from 4-methyl-acetophenone by oxidation with selenium dioxide in aqueous dioxane solution [3]. The glyoxal was coupled to glycineamid hydrochloride to yield the respective 2-hydroxy-5-(4-methylphenyl)-pyrazine in basic methanol solution [4].

Unfortunately, the substitution of the OH-group at the 2-hydroxy-5-(4-methylphenyl)-pyrazine with PBr_3 failed even though many methods were attempted [5,6]. The main problem was that no main reaction product could be identified on the TLC after hydrolysis, neither in the aqueous nor in the organic layer of the hydrolyzed reaction mixture. This was tried after 15 min., 30 min., 1 h, 2 h, 6 h, 12 h and 24 h. The reaction was performed at 50 °C, 100 °C and under reflux at 140 °C. TLCs showed that the 2-hydroxy-5-(4-methylphenyl)-pyrazine was consumed during the reaction but no product was obtained that could be identified as the desired 2-bromo-5-(4-methylphenyl)-pyrazine from ^{1}H-NMR. Although a preparation of sterically more hindered 2-bromo-3,5,6-triphenylpyrazine from the respective hydroxy compound was described [6], these methods for the preparation for bromopyrazines were not successful in this case.

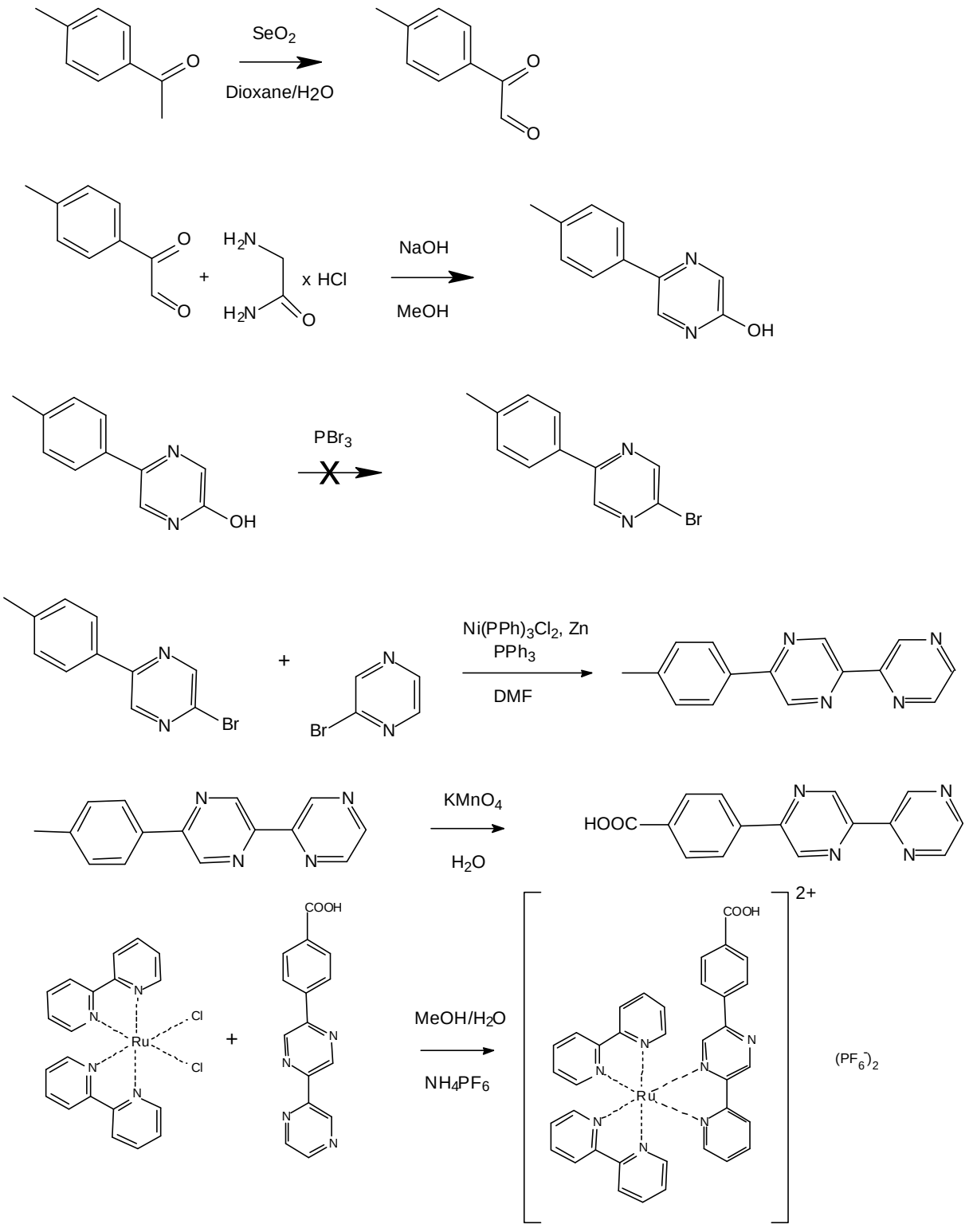

Fig. 13. Scheme for the planned synthesis of a bipyrazyl substituted Ru MLC.

3.1.2 Synthesis of the Bipyridine Ligands

It seemed worthy to try the synthesis of 5,5'-dicarboxy-2,2'-bipyridine after the attempt to obtain bipyrazines as the desired asymmetrical ligands failed. Complexes based on 4,4'-dicarboxy-2,2'-bipyridine having an excitation polarization maxima in immunoassays at 460 nm were described previously [1,2]. We hoped to receive longer wavelength absorption and polarization maxima using bipyridine ligands substituted in position five. The excitation polarization maximum is normally shifted to longer wavelengths compared to the absorption maximum [7]. From a sterical point of view a carboxy group in 5-position at the pyridine ring is only slightly more hindered against nucleophilic attacks compared to the 4-position. Thus, covalent coupling to amino groups of proteins is possible.

A well established procedure exists for the coupling of bromopyridines to the respective bipyridines [8]. The method involves the formation of $Ni(PPh_3)_4Cl_2$ from $NiCl_2$ and PPh_3 in DMF under nitrogen atmosphere. The addition of zinc dust reduces the Ni(II) salt to $\overset{0}{Ni}(PPh)_3$. This complex enables the formation of the 2,2'-bipyridines **1a** and **1b** from the respective bromopyridines (see Fig. 14).

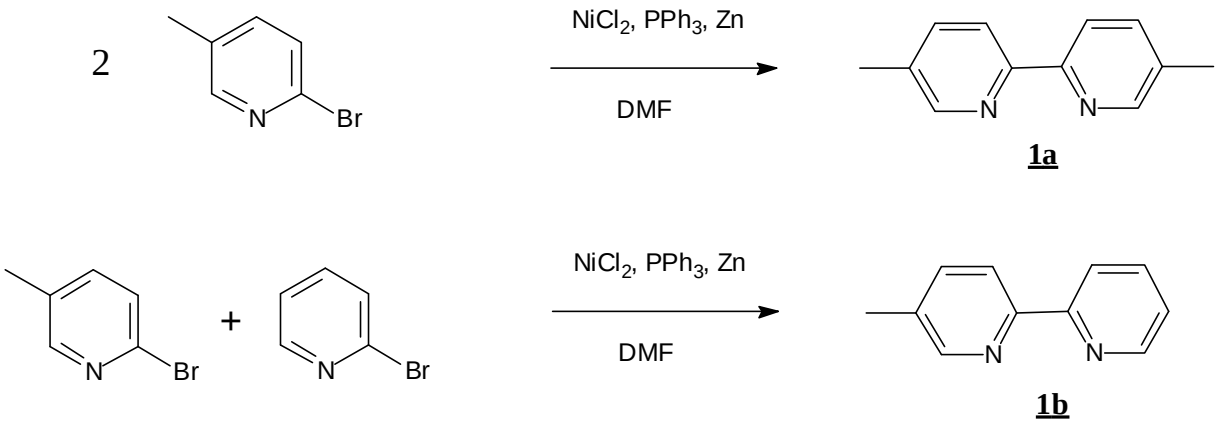

Fig.14. Synthetic route to the methyl-2,2'-bipyridines from the respective bromopyridines.

The synthesis procedure is the same for both 5-methyl-2,2'-bipyridines (**1b**) and 5,5'-dimethyl-2,2'-bipyridine (**1a**) but for purification two different methods were used. In the case of **1a** a high-vacuum sublimation was made and **1b** was purified by Kugelrohrdistillation at 10^{-1} torr.

The sublimation yields the product in very high purity and should be preferred if a vacuum of 10^{-2} torr or lower is available. The Kugelrohrdistillation allows an easier separation of the two symmetric and the asymmetric bipyridines which are obtained from the reaction work-up procedure. The yields are about 40%.

This is the only sophisticated reaction step of all syntheses to yield the respective ruthenium complexes. Here, the use of toxic $NiCl_2$ cannot be avoided, but for the other steps no more harmful chemicals are necessary. One of the most important objectives for the synthesis of our new complexes was a simple synthesis using harmless chemicals. The other important goal was to obtain MLC probes with improved spectral properties.

The oxidation of the methylbipyridines to the respective carboxybipyridines is carried out by a simple oxidation step using aqueous $KMnO_4$ (see Fig. 15) [9].

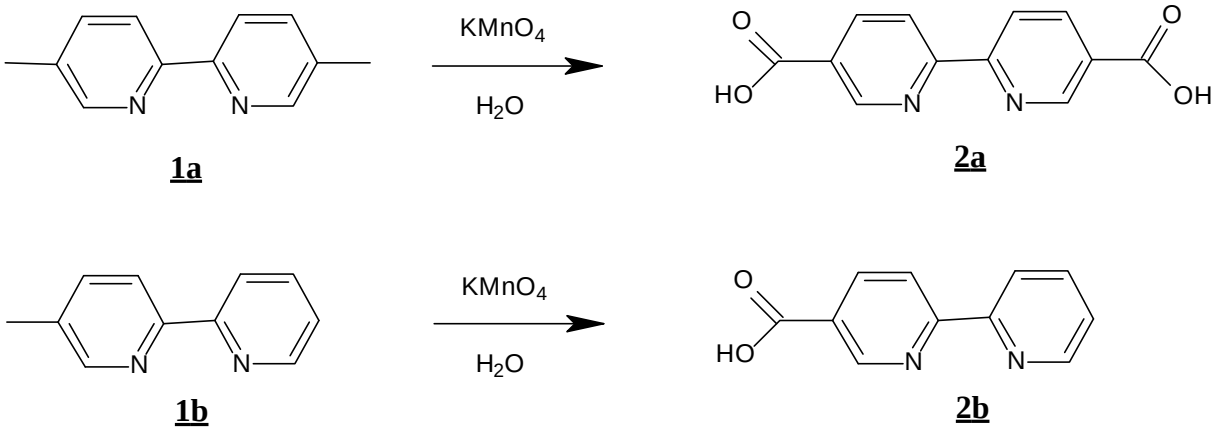

Fig. 15. Synthetic routes from the methylbipyridines to the respective carboxybipyridines.

The yields are around 50%, which is quite good for oxidations with permanganate [9]. The structure analysis of these compounds is not easy due to melting points exceeding 295 °C. Another difficulty is the insolubility in nearly all organic solvents commonly used [10]. Therefore no ^{1}H-NMR spectrum could be recorded, but EI-Mass spectra showed the products **2a** and **2b** to be very pure.

Attempts to oxidize **1a** to the corresponding monoacid using less permanganate or lower reaction temperatures remained unsuccessful.

3.1.3 Synthesis of the Ruthenium Metal Ligand Complexes

The coupling of the third ligand different from a simple 2,2'-bipyridine to $Ru(bipy)_2Cl_2 \cdot 2\ H_2O$ was performed in a methanol/water mixture (4/1) (see Fig. 16), satured with $NaHCO_3$ as described in literature [1,2]. This was the only solvent mixture **2a** and **2b** could be dissolved in upon heating to 50 °C. The reaction time had to be elongated from 8 h [1,2] to 24 h. This is probably due to an enhanced steric hindrance of the bipyridine substituted in position five when coupling to the ruthenium center atom. The yields were generally higher than 70%.

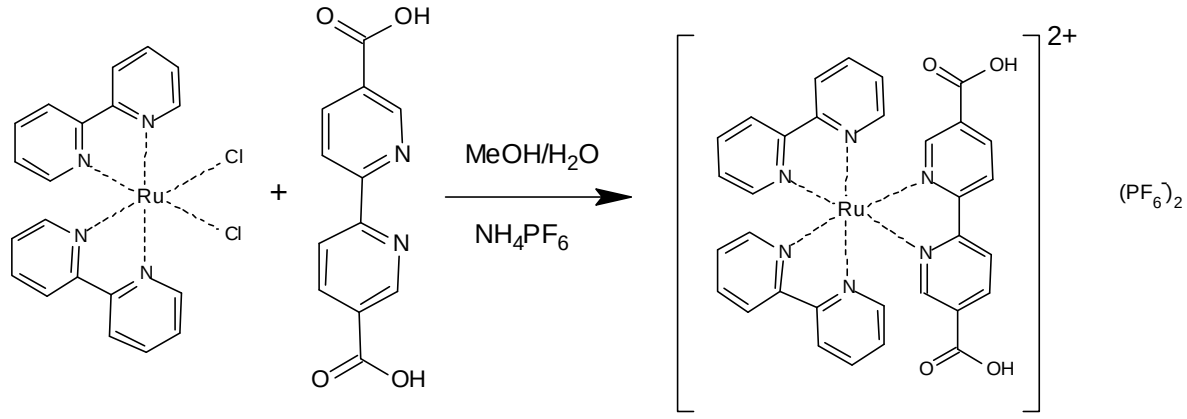

3a

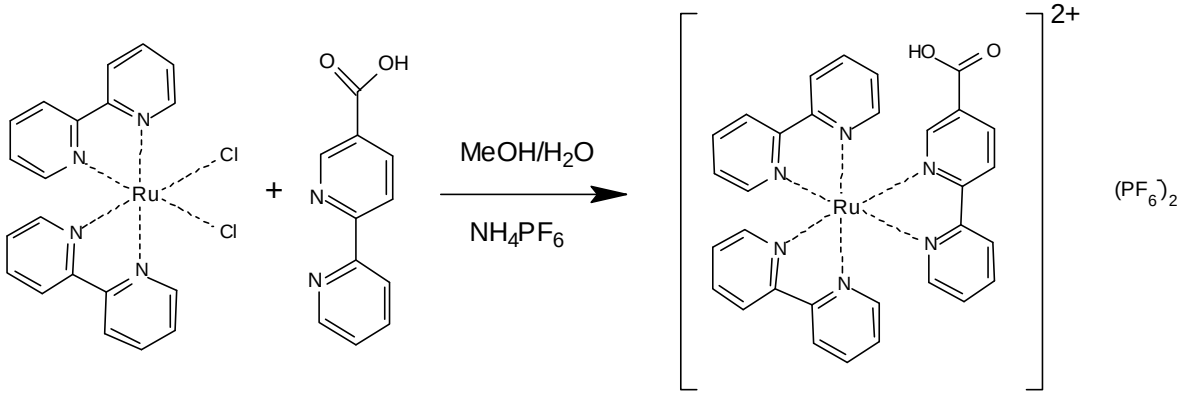

3b

Fig. 16. Coupling of the third ligand to $Ru(bipy)_2Cl_2$ to yield the Ru-tris(bipyridine) complexes.

For easier nomenclature complex **3a** will be referred to as 55DC (5,5'-Dicarboxy Complex) and **3b** will be named 5MC (5-Monocarboxy Complex).

The activation of the carboxy groups was performed via the NHS/DCC method (NHS: N-hydroxysuccinimide, DCC: Dicyclohexylcarbodiimide) to obtain the reactive NHS-esters (see Fig.17). Here no effect of higher steric hindrance influencing the reaction time was noticed. This means that the reactive NHS-esters in position five at the bipyridine will couple to a amino group of a protein with equal efficiency.

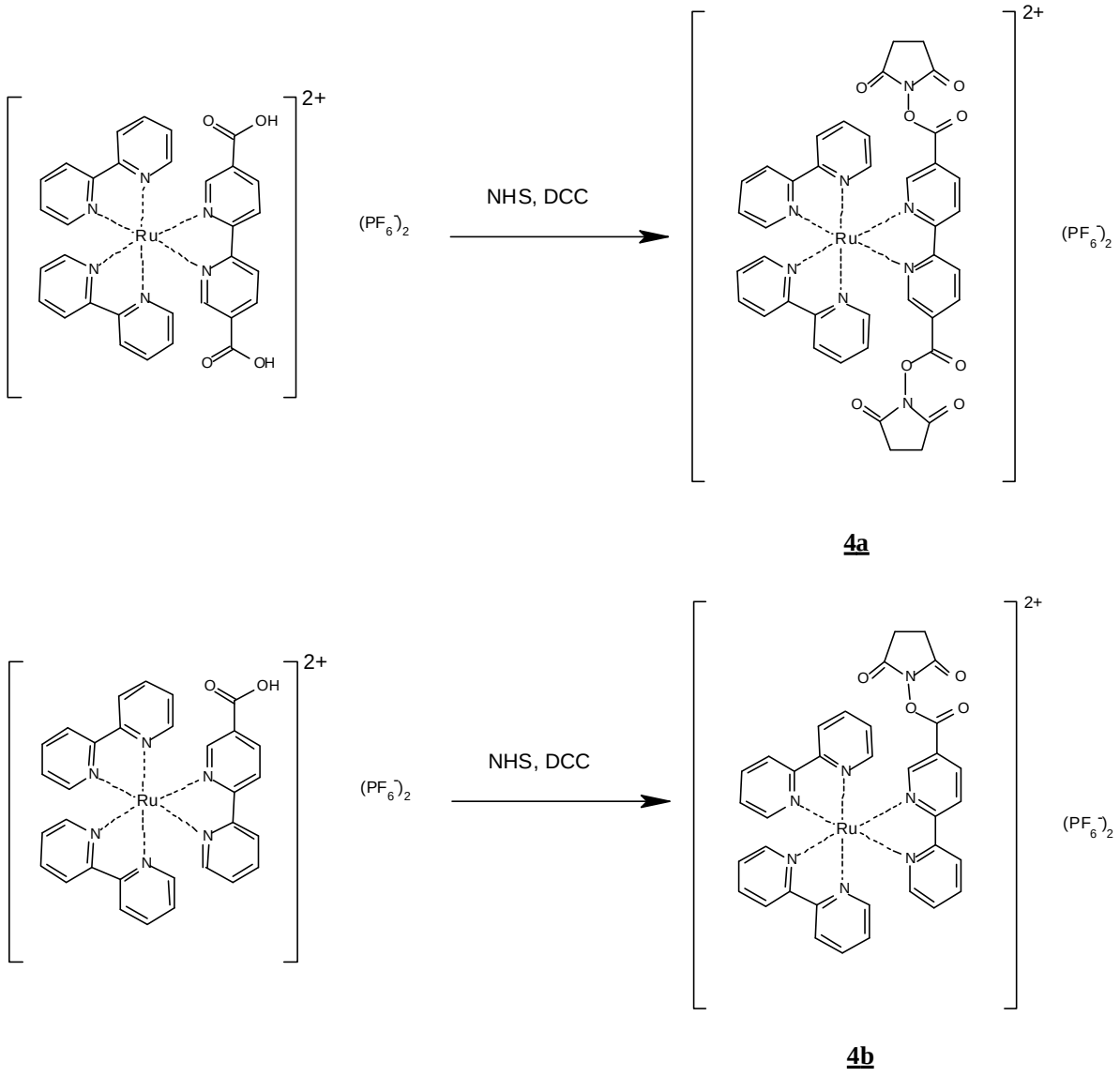

Fig. 17. Activation step to yield the reactive NHS-esters.

For easier nomenclature complex **4a** will be referred to as 55DC-DNHS (5,5'-Dicarboxy Complex DiNHS-ester) and **4b** will be named 5MC-NHS (5-Monocarboxy Complex NHS-ester).

3.2 Spectral Characterization of the Complexes and Their Protein Conjugates

Absorption and emission wavelengths are in the typical range for Ru(II)-tris(bipyridine) complexes having an absorption maximum of 453 nm for 5MC and 449 nm for 55DC, respectively. The emission maxima are at 675 nm for 5MC and 705 nm for 55DC, respectively. The absorption and emission spectra of the complexes are shown in Fig. 18. The excitation wavelength for the emission spectra was the wavelength of the respective absorption maximum. All of these measurements were performed in 22 mmol/L phosphate buffered saline (PBS) pH 7.2 at dye concentrations between 10^{-5} to 10^{-6} mol/L.

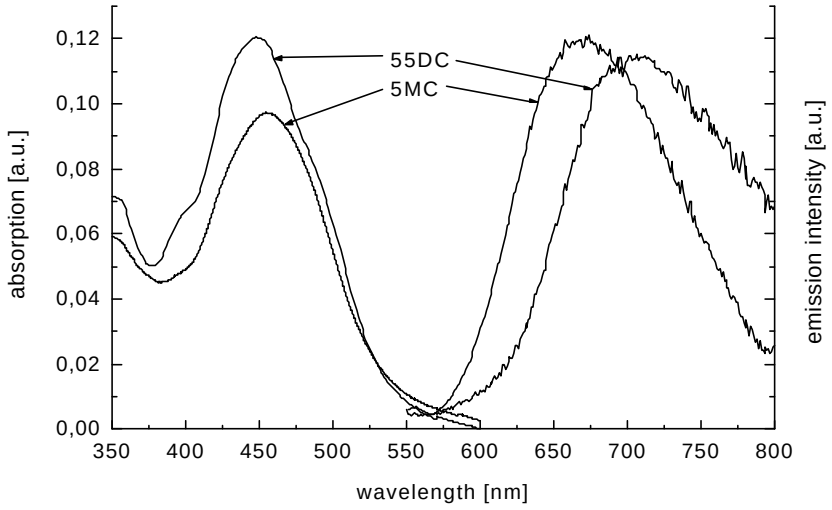

Fig. 18. Absorption and emission spectra of 5MC and 55DC in 22 mmol/L PBS pH 7.2.

The complexes were conjugated covalently to both HSA and myoglobin to perform polarization immunoassays. These proteins were used due to their molecular masses of 17,500 g/mol for myoglobin and 66,000 g/mol for HSA, respectively. They span over the very interesting area of mid and high-molecular weight globular proteins. Both complexes display a
red shift of 25-30 nm when covalently attached to HSA. The respective spectroscopic data are shown in Table 2. The red shift of the complexes attached to myoglobin is comparably smaller to that when bound to HSA. Quantum yields (QYs) were determined relative to $Ru(bipy)_3Cl_2$ having a QY of 0.042 [11]. The QY of 5MC and 55DC increases from 0.3% and 0.2%, respectively, to 1% upon binding to a protein. The complex attached to the protein is better

shielded from water molecules due to the more lipophilic protein surrounding. Therefore, there is less probability for radiationless energy transfer to the water molecules and a higher probability for energy transfer to the triplet state and thus the QY rises.

Table 2: Spectral properties and quantum yields of the complexes and their conjugates to HSA and myoglobin in 22 mmol/L PBS pH 7.2.

Ru-complex	*Abs. max. [nm]*	*Em. max. [nm]*	*ε [L/(mol · cm)]*	*QY*
5MC	453	675	10000	0.003
5MC-HSA	478	700	[a]	0.01
5MC-Myoglobin	[a]	681	[a]	[a]
55DC	449	705	19000	0.002
55DC-HSA	457	735	[a]	0.01
55DC-Myoglobin	[a]	712	[a]	[a]

[a] not determined

Both complexes display a shoulder in the main absorption band of myoglobin at 413 nm when covalently bound to myoglobin. This is demonstrated in Fig. 19 for myoglobin labeled with 55DC. The absorption spectrum of labeled myoglobin clearly shows the increase of the absorption at wavelengths > 425 nm due to the ruthenium label. The absorption spectra of myoglobin as well as that of the free complex are shown for convenience.

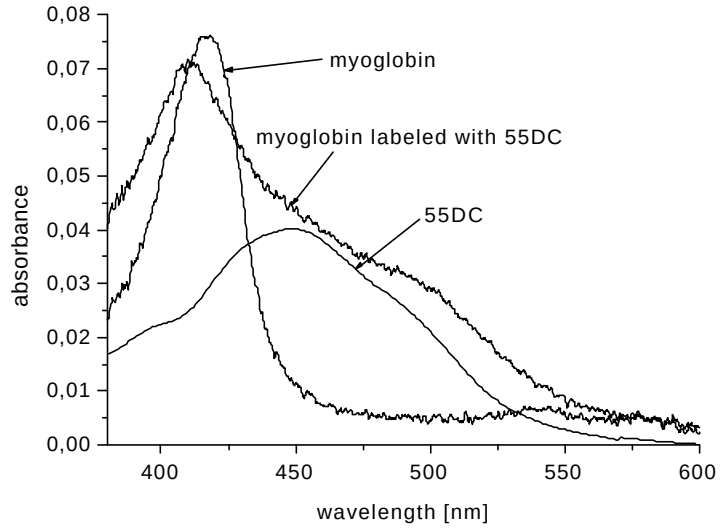

Fig. 19. Absorption spectra of 55DC-labeled myoglobin in 22 mmol/L PBS pH 7.2, free 55DC and unlabeled myoglobin.

The dye-to-protein ratio of the labeled myoglobin samples was determined by a two wavelength absorption measurement. This was performed at wavelengths of 450 and 540 nm with known molar extinction coefficients for both protein and label at these wavelengths. The additivity of the absorptions of the two compounds according to Lambert Beer's law was used to determine both complex and protein concentration. A detailed description of the procedure is given in the experimental part in chapter 5.4.2.

Concentrations of labeled HSA were obtained using the standard protocol of the BCA Protein Assay Reagent Kit from Pierce for the determination of protein concentrations based on bichinoinic acid. There is no source of error due to absorption of the complex because the molar extinction coefficient of the bichinoinic acid at 562 nm in this test is over tenfold higher as compared to that of the ruthenium complexes at 562 nm (see Fig. 18). Furthermore, the concentration of the bichinoinic acid is over threefold higher than the concentration of the ruthenium complex. The concentrations of the Ru complex in solutions of labeled HSA were determined according to Lambert-Beer's law from the absorbance of the Ru-MLC at the absorption maximum.

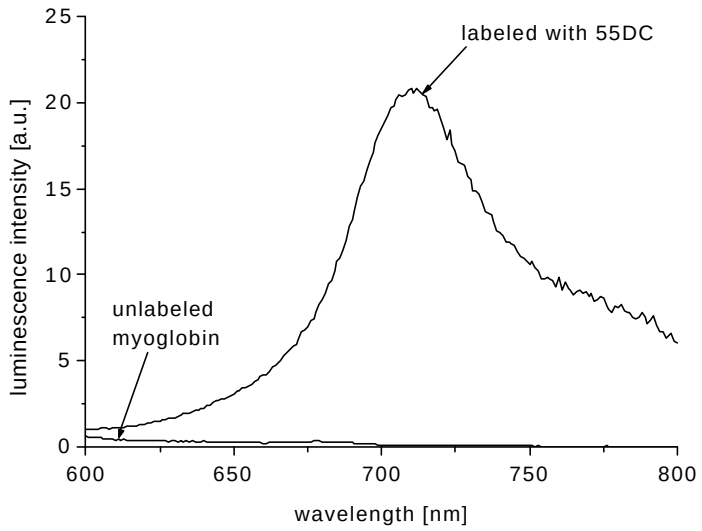

Fig. 20. Emission spectra of myoglobin and of myoglobin labeled with 55DC (in 22 mmol/L PBS of pH 7.2).

Myoglobin has a strong absorption band at 410 nm due to its heme chromophore. Thus it was necessary to find out whether emission of this chromophore would influence the emission from a label. A comparison of the emission spectra of unlabeled and 55DC-labeled myoglobin (see Fig. 20) shows that neither emission nor scattered light originating from the protein influences the luminescence from the label.

The excitation polarization spectrum and a P_0-value of 0.33 was taken from a frozen solution of 55DC in glycerol at - 80 °C. The spectrometer at the University of Jena employed for these measurements was no longer available for the determination of the P_0 value of 5MC. Therefore we enclosed this complex in a rigid polymer matrix of poly-acrylnitrile to measure the excitation polarization spectrum in absence of rotational motions. An influence due to some remaining rotational motions could be excluded by measurements at 5 °C and at 20 °C which resulted in the same fundamental polarization P_0 of 0.18 for 5MC. The higher P_0-value for 55DC corresponds well with the results of Terpetschnig et al. [1, 2, 12] who also found a higher P_0-value for the dicarboxy complex. The excitation maxima for both 5MC and 55DC at 500 nm are shifted to longer wavelengths compared to these works [1,2,12].

3.3 Homogenous Polarization Immunoassays with Labeled HSA and Myoglobin for the Determination of Antibody Concentrations

Both 5MC and 55DC were labeled to HSA and myoglobin to detect the respective polyclonal antibodies in various concentrations in a homogenous immunoassay. The concentration of the ruthenium label was adjusted to 1 nmol/2 mL for the assay. All samples were measured against a reference sample containing equal quantities of unlabeled antigen and unlabeled antibody. Labeled to HSA both complexes display a saturation curve upon titration with a rising amount of antibody (see Fig. 21). The polarization reaches 0.262 for 55DC and 0.147 for 5MC, respectively, attached to HSA at a twofold molar excess of unlabeled anti-HSA.

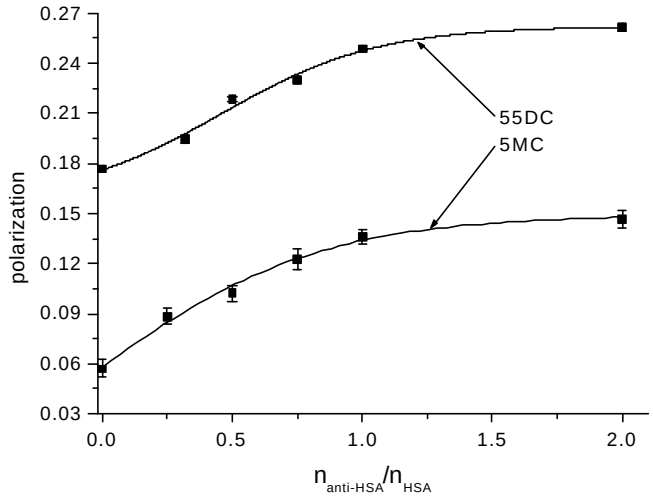

Fig. 21. Steady state polarization of 5MC and 55DC labeled to HSA in an immunoassay at various concentrations of polyclonal anti-HSA.

I also found saturation curves for labeled myoglobin when we determined anti-myoglobin (see Fig. 22). The saturation values for myoglobin labeled with 55DC and 5MC at high concentrations of unlabeled anti-myoglobin are 0.241 and 0.154, respectively. The saturation values found here and in the assay shown in Fig. 21 do not exceed the measured P_0 values. Thus interferences by scattered light can be excluded.

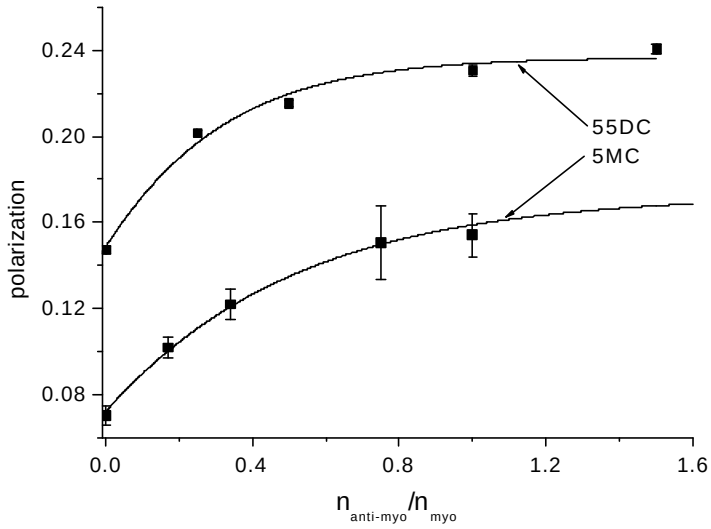

Fig. 22. Steady state polarization of 5MC and 55DC labeled to myoglobin in an immunoassay at various concentrations of polyclonal anti-myoglobin

The rising polarization upon rising amount of antibody is cased by an increased rotational correlation time of the antigen-antibody complex. This is based on the dependence of θ of a labeled makromolecule on its molecular mass M

$$q = \frac{hM}{RT}(\bar{n} + h) \qquad (3.1)$$

where η is the viscosity, $\bar{n}$ the specific volume of the biomolecule and h the hydration volume of the biomolecule. The result is a lower P in the Perrin Equation

$$\left(\frac{1}{P} - \frac{1}{3}\right) = \left(\frac{1}{P_0} - \frac{1}{3}\right)\left(1 + \frac{3t}{q}\right) \qquad (3.2)$$

where P is the polarization, P_0 the polarization in absence of rotational motions (e.g. in frozen solutions or a rigid polymer matrix) and τ the fluorescence lifetime of the fluorophore (16). Here the higher molecular mass of the antigen-antibody complex compared to the labeled antigen results of the in a higher value of the Polarization.

3.4 Competitive Polarization Immunoassays with HSA and Myoglobin for the Determination of Antigen Concentrations

In competitive immunoassays, a mixture of a fixed amount of labeled antigen and an increasing amount of unlabeled antigen compete for the binding sites of a fixed amount of antibody. We determined the change of the steady state polarization of 5MC and 55DC labeled to both HSA and myoglobin. The concentration of the ruthenium label was adjusted to 1 nmol/2 mL for the assay, again. All samples were measured against a reference sample containing equal amounts of unlabeled antigen and unlabeled antibody. In case of HSA as the antigen to be determined we found an exponential like decay of the polarization value with a rising amount of unlabeled HSA (see Fig. 23).

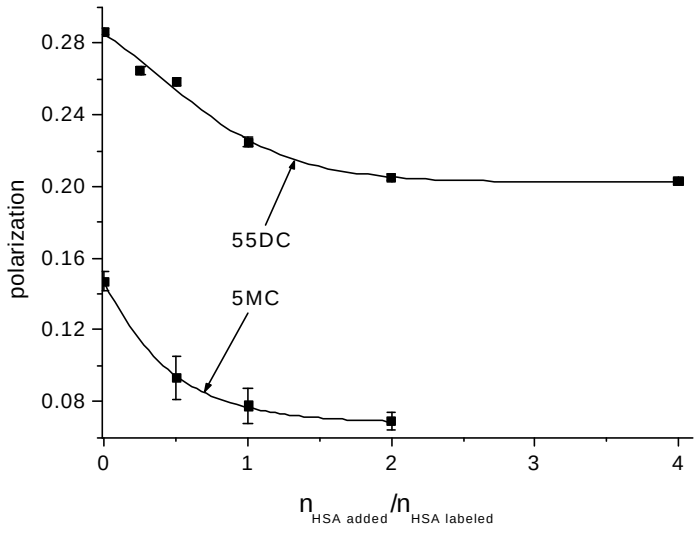

Fig. 23. Competitive polarization immunoassays of 5MC and 55DC labeled to HSA at rising concentrations of unlabeled HSA competing for polyclonal anti-HSA.

The polarization nearly decreases to the values determined in the homogenous assay for unlabeled HSA (compare Fig. 21). This is in good accordance with the situation found at the molecular level at high concentrations of unlabeled antigen. Nearly all antibody binding-sites are occupied with unlabeled HSA and most of the labeled HSA is not attached to an antibody. The result is a large fraction of fluorescently labeled molecules with a small rotational correlation time θ and a lower polarization.

This is true because θ of a labeled macromolecule is dependent on M according to Eq (3.1). A lower θ results in a lower anisotropy value according to

$$r = \frac{r_0}{1 + \frac{t}{q}} \tag{3.3}$$

where r is the measured anisotropy, r_0 the fundamental anisotropy and τ the fluorescence lifetime of the fluorophore. Using the relation

$$P = \frac{3r}{2 + r} \tag{3.4}$$

the lower r value corresponds to a lower polarization P as shown in Fig. 23 at high concentrations of unlabeled antigen. The same tendency is found, if myoglobin is the antigen to be determined (see Fig. 24). There is an exponential-like decay with rising amount of unlabeled antigen.

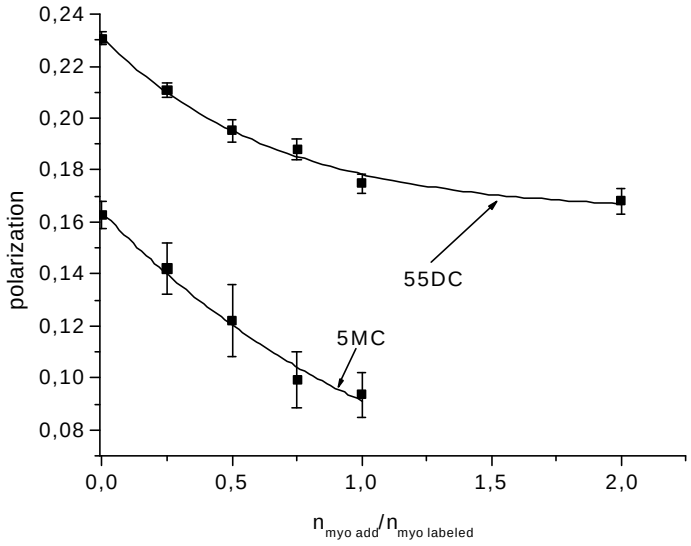

Fig. 24. Competitive polarization immunoassays of 5MC and 55DC labeled to myoglobin at increasing concentrations of unlabeled myoglobin competing for polyclonal anti-myoglobin.

Comparing the error bars of 55DC and 5MC it is obvious that the result is not satisfactory in the case of 5MC. This is due to the fact that the labeling efficiency is not as high for myoglobin compared to HSA. This means that one has to worked in more diluted solutions than 1 nmol label/2 mL. Thus here is a greater influence of the signal-to-noise ratio of the PMT on this assay compared to the other assays. Nevertheless, the values are very reasonable because they do not exceed the range of polarization values determined in the previous immunoassays (compare Fig. 22). A higher polarization at low amounts of added myoglobin would have suggested that there would have been a disturbance of the measurement due to scattered light. This is obviously not the case and therefore the assay is quite useful.

3.5 Comparison of the Competitive Polarization Immunoassay for HSA with the AlbuminBlue 580 Test

A competitive polarization assay for HSA was carried out using 55DC-labeled HSA as described above and the HSA concentration of various samples was determined. Then a calibration curve for the AlbuminBlue 580 Test was set up for the same concentration range as determined with the polarization immunoassay. Ten independent emission measurements were taken for each concentration as described in Lit. [10,11].

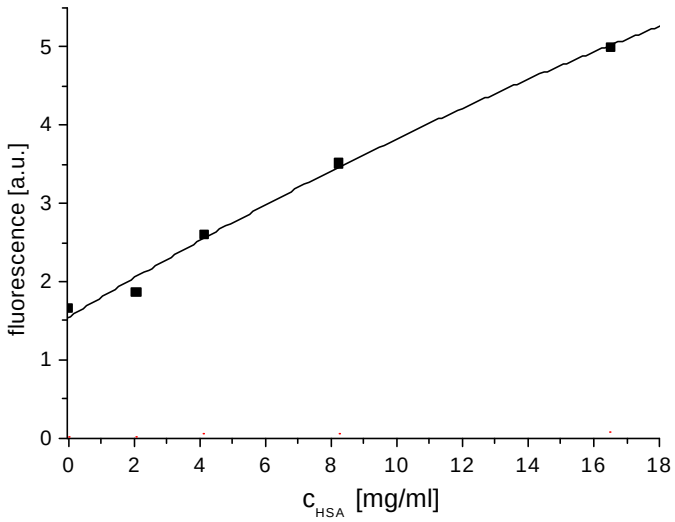

Fig. 25. Calibration curve for the AlbuminBlue 580 Test.

The concentration values obtained with the polarization immunoassay and the AlbuminBlue 580 Test are in well accordance (see Fig. 26).

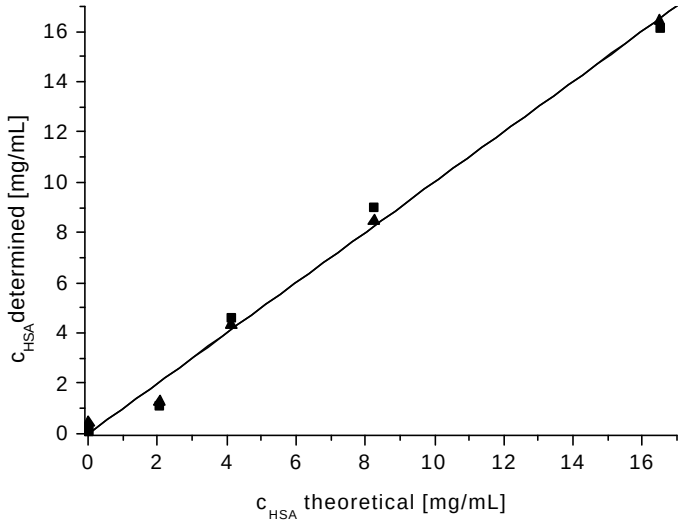

Fig. 26. Correlation of the precision of the competitive polarization immunoassay (■) and the AlbuminBlue 580 test (▲).

Regression analysis gives y = 0.999 (± 0.043) x + 0.005 (± 0.366); n = 50; r = 0.997 for the AlbuminBlue 580 Test and y = 1.000 (± 0.060) x + 0.000 (± 0.515); n = 50; r = 0.995 for the polarization immunoassay.

The data show that the values obtained with the polarization immunoassays have a lower accuracy compared to those of the AB 580 test. However, the high precision of AB 580 is only achieved with albumins. The Ru-MLCs can be bound to nearly every biomolecule that carries deprotonated amino groups to which an NHS-ester can be attached to at alkaline pH. If the antibody to the labeled antigen has to be detected, the assay is preferably carried out as a homogenous polarization immunoassay. The labeled antigen itself can be detected by performing a competitive polarization immunoassay with unlabeled antigen.

3.6 Discussion

The new ruthenium MLCs are shown to be very useful probes for performing polarization immunoassays with mid and high-molecular weight antigens. They show high fundamental polarization values of 0.33 and 0.18, respectively. The excitation maxima at 500 nm do not exactly match the 488 nm line of the argon ion laser. It will cause just a little loss of the dynamic range of the polarization if this excitation source is employed for measuring an immunoassay. Furthermore, the complexes have a Stokes' shift of over 250 nm which enables an easy separation of excitation and emission light. Therefore, simpler instrumentation can be used, e.g. cutoff filters in place of monochromators. The emission is at long wavelengths beyond 700 nm which is a red shift of 50 nm compared to $[Ru(bipy)_3]Cl_2$. Emission due to natural fluorophores is low at these wavelengths. The fact that the longer-wavelength emitting 55DC displays the higher P_0 value compared to the shorter-wavelength emitting 5DC corresponds well with the results of Lakowicz [15] with a 4-carboxy-2,2'-bipyridine and a 4,4'-Dicarboxy-2,2'-bipyridine as the respective asymmetric ligand.

The low quantum yields of the complexes (below 0.5% in the free form and of 1% when bound to proteins) are a result of the long-wavelength shifted emission. The energy gap law says that the rate of radiationless decay increases as emission is shifted to longer wavelengths [16]. The low quantum yields and the long-wavelength emission of both 5MC and 55DC require near infrared sensitive devices for the detection of the emitted photons.

A good solubility in aqueous buffered solutions at neutral pH is found for the complexes. This is a strict requirement when working with biological materials. Furthermore, MLCs do not self quench upon multiple labeling to proteins [15].

The complexes can be bound to many biomolecules because most of them carry some deprotonated amino groups to which an NHS-ester can be attached to at alkaline pH. The respective assay format is chosen depending on whether an antigen or an antibody concentration has to be determined (see Figs. 21-24).

Comparing the polarization immunoassay to the AlbuminBlue 580 Test it was found that both methods deliver nearly equal values. This agreement proves that the polarization immunoassays are reliable.

3.7 Literature

1. Terpetschnig, E., Szmacinski, H., Malak, H., Lakowicz, J. R., 1995, Metal-ligand complexes as a new class of long lived fluorophores for protein hydrodynamics, *Biophys. J.*, **68**, 342-350.
2. Szmacinski, H., Terpetschnig, E., Lakowicz, J. R., 1995, Synthesis and evaluation of Ru-complexes as anisotropy probes for protein hydrodynamics and immunoassays of high-molecular weight antigens, *Biophys. Chem.*, **62**, 109-120.
3. Peek, B. M., Ross, G. T., Edwards, S. W., Meyer, G. J., Meyer, T. J., Erickson, B. W., 1991, Synthesis of redox derivatives of lysine and related peptides containing phenothiazine or tris(2,2'-bipyridine)ruthenium(II), *Int. J. Peptide Protein Res.*, **34**, 114-123.
4. Jones, R. G., 1949, Pyrazines and related compounds I. A New Synthesis of Hydroxypyrazines, *J. Am. Chem. Soc.*, **71**, 78-81.
5. Karmas, G., Spoerri, P. E., 1952, The Preparation of Hydroxyipyrazines and Derived Chloropyrazines, *J. Am. Chem. Soc.*, **74**, 1580-1584.
6. Karmas, G., Spoerri, P. E., 1956, 2-Bromopyrazines, 2-Cyanopyrazines and their Derivatives , *J. Am. Chem. Soc.*, **78**, 2141-2144.
7. Lakowicz, J. R., 1999, *Principles of Fluorescence Spectroscopy*, 2nd Edition, Kluwer Academic/Plenum Publishers, New York, 296.
8. Tiecco, M., Testaferri, L., Tignoli, M., Chianelli, D., Montanucci, M., 1984, A Convenient Synthesis of Bipyridines by Nickel-Posphine Complex-Mediated Homo Coupling of Halopyridines, *Synthesis*, **9**, 736-738.
9. Becker, H. G., , 1996, *Organikum*, 20. Auflage, Joh. Ambrosius Barth Verlag, Heidelberg
10. Case, H., 1946, The Synthesis of Certain Substituted 2,2-Bipydidyls, *J. Am Chem. Soc*. **68**, 2574-2577.
11. Van Houten, J., Watts, R. J., 1975, *J. Am Chem. Soc.*, **97 (13),** 3843-3844.
12. see Ref. 7, 575.
13. Kessler, M. A., Meinitzer, A., Petek, W., Wolfbeis, O. S., 1997, Microalbuminuria and borderline-increased albumin excretion determined with a centrifugal analyzer and the Albumin Blue 580 fluorescence assay, *Clin. Chem.*, **43**, 6, 996-1002.

14. Kessler, M. A., Meinitzer, A., Wolfbeis, O. S., 1997, Albumin Blue 580 Fluorescence Assay for Albumin, *Anal. Biochem.*, **248**, 180-182.
15. see Ref. 7, 577.
16. see Ref. 7, 574.

4. The Europium-Tetracycline Complex as a Molecular Sensor for Hydrogen Peroxide

4.1 Properties of the Europium-Tetracycline (EuTC) System

4.1.1 Introduction and Spectral Properties of the EuTC Complexes.

The complexes of tetracycline with metal ions have been subject of extensive work [1-5]. Tetracycline is a wide range antibiotic which has been used for over 50 years. The most common tetracyclines are shown in Fig. 27 [5].

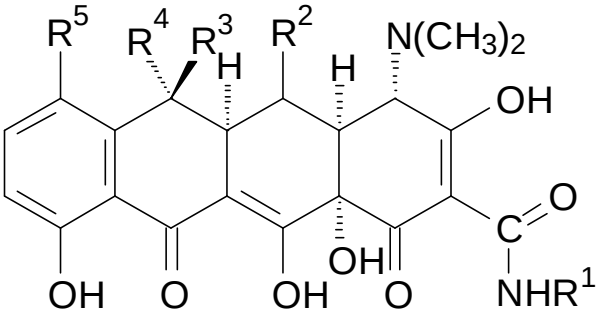

Name	R^1	R^2	R^3	R^4	R^5
Tetracycline	H	H	OH	CH_3	H
Chlortetracycline	H	H	OH	CH_3	Cl
Oxytetracycline	H	OH	OH	CH_3	H
Demethylchlortetracycline	H	H	OH	H	Cl
Doxycyclinmonohydrate	H	OH	H	CH_3	H
Minocycline	H	H	H	H	$N(CH_3)_2$
Methacycline	H	OH	$=CH_2$	-	H
Rolitetracycline	CH_2-pyrrolidino	H	OH	CH_3	H

Fig. 27. Chemical structure of tetracycline and table of commonly used tetracycline derivatives.

The stoichiometry of the complexes of europium with tetracycline have been investigated [6,7]. A luminescence enhancement of Eu^{3+} upon binding of tetracycline was mentioned. This enhancement was used to detect tetracycline by fluorescence measurements. Prototropic dissociation constants and formation constants of the complex were determined by spectrophotometric and fluorescence titrations [6,7]. A 1:1 stochiometry was deduced from these titrations, but is highly pH-dependent.

Recently, a short communication reported an up to over tenfold increase of the luminescence intensity of the $^5D_0 \rightarrow {}^7F_2$ transition of Eu^{3+}-tetracycline upon the addition of hydrogen peroxide after a 10 min. incubation time [8]. Additionally a pH dependency of this luminescence increase was presented, showing a Gaussian like curve having its pH optimum at 6.9. On careful revision of the article it was obvious that only a threefold molar excess of Eu^{3+} over tetracycline delivered the intense luminescence enhancement. If the molar excess of Eu^{3+} was reduced to give a 1:1 stoichiometry with TC the increase of the luminescence upon addition of H_2O_2 was negligible. The method of measuring the increased luminescence of Eu^{3+} was used only in order to determine lowest concentrations of tetracycline with a detection limit tenfold lower than had been described before [6,7]. The authors did not realize the potential of this method for the determination of H_2O_2 neither for the determination of hydrogen peroxide in aqueous solutions nor for the determination of enzymatically evolved H_2O_2, substrates of oxidases or products of their enzymatic reactions.

It was conceived that this enhancement could be used to determine peroxides, especially hydrogen peroxide. Thus it was tried first to reproduce the effects presented in Ref. 8. Absorption spectra of a solution containing 66 μmol/L of $EuCl_3 \cdot 6\ H_2O$ and 22 μmol/L of tetracycline hydrochloride in 13 mmol/L MOPS buffer at pH 6.9 were recorded in absence and presence of $8 \cdot 10^{-4}$ mol/L of H_2O_2 (see Fig. 28). The threefold molar excess of Eu^{3+} over TC will be referred to as Eu_3TC. The hydrogen peroxide was added as a few μL volume from a concentrated solution of H_2O_2 to a 2 mL sample to avoid dilution effects.

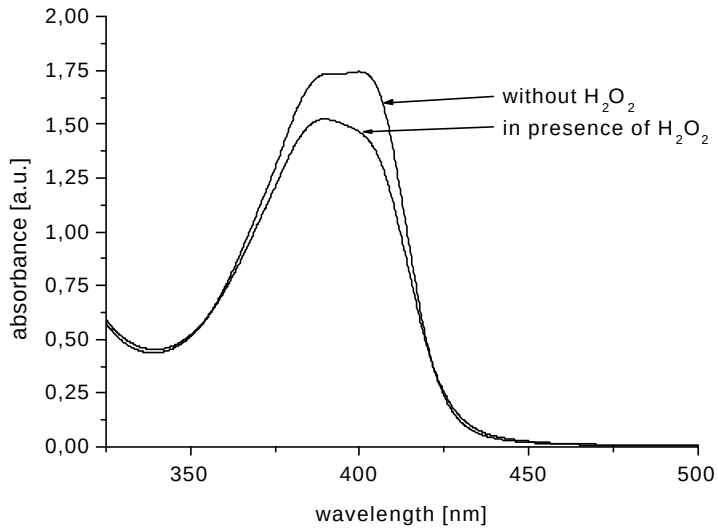

Fig: 28. Change of the absorption spectrum of Eu_3TC upon addition of $8 \cdot 10^{-4}$ mol/L H_2O_2 in 13 mmol/L MOPS buffer at pH 6.9.

The absorption maximum of Eu_3TC is at 399 nm. The whole absorption band consists of two maxima with nearly equal absorbance. In presence of hydrogen peroxide the absorption intensity decreases about 15% and the maximum is blue-shifted to 389 nm.

The lower absorption in presence of H_2O_2 was not expected because the emission intensity of the most prominent 616 nm hypersensitive $^5D_0 \rightarrow {}^7F_2$ transition rises over 13-fold (see Fig. 29). Accordingly, this line splits up into a doublet with maxima at 613 and 618 nm with nearly equal emission intensity. Upon addition of H_2O_2 the emission maximum of the other transitions shifts up to 5 nm, the emission intensity rises but none of these lines splits up. The $^5D_0 \rightarrow {}^7F_0$ transition at 579 nm increases 40-fold upon adding of peroxide. The band is a single sharp line and thus can be attributed to a homogenous population of emitting species of Eu^{3+} [9]. The hypersensitive $^5D_0 \rightarrow {}^7F_1$ transition at 590 nm is red shifted by four nm and intensifies by a factor of 16. The 654 nm $^5D_0 \rightarrow {}^7F_3$ emission is blue shifted by four nm and increases 13-fold.

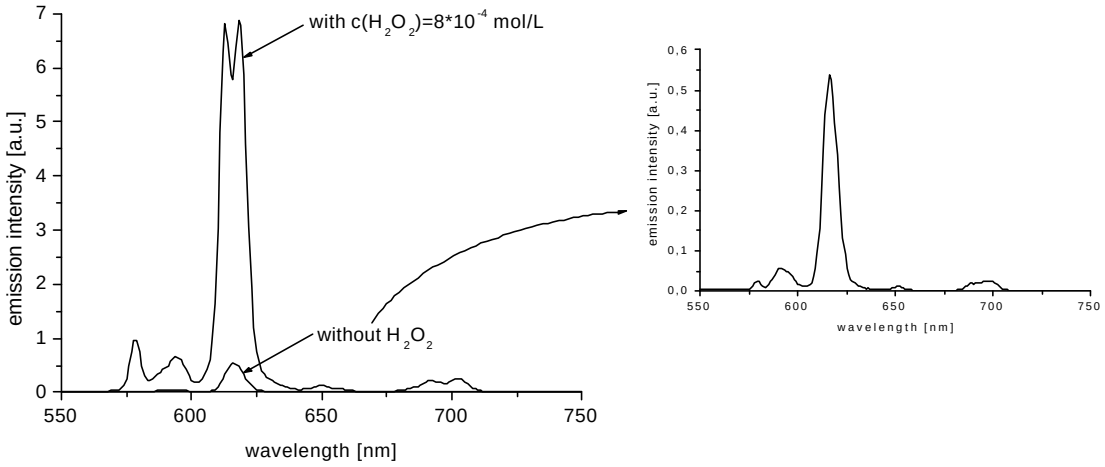

Fig. 29. Change in the emission spectrum of Eu_3TC in prescnce of $8 \cdot 10^{-4}$ mol/L of H_2O_2 in 13 mmol/L MOPS buffer at pH 6.9 and enlargement of the spectrum before peroxide addition.

Finally, the addition is accompanied by a 5 nm red shift of the two bands at 688 and 698 nm representing the $^5D_0 \rightarrow {}^7F_4$ transition increasing twelve and tenfold, respectively.

It is remarkable that apart from the $^5D_0 \rightarrow {}^7F_2$ transition the whole band pattern remains unchanged (see enlargement of Fig. 29) and each emission intensifies. The splitting of the $^5D_0 \rightarrow {}^7F_2$ transition suggests that changes in the ligand environment due to oxidation of the tetracycline may occur. This would be in accordance with a proposed mechanism for the chemiluminescence reaction of H_2O_2 and tetracyclines in presence of copper(II) and $K_2S_2O_8$ as co-oxidizer [10]. A conversion of tetracycline into its fluorescent iso or anhydro compound was suggested followed by a destruction of the tetracycline skeleton. In the case of our system emission due to chemiluminescence can be ruled out because no emission light can be detected after closing the shutter in the excitation lightpath of the fluorimeter. Nevertheless, the system displays sensitized energy transfer from the TC ligand to the Eu^{3+} ion. This is confirmed by emission spectra of separate solutions of Eu^{3+} in MOPS buffer and TC in MOPS buffer at pH 6.9 using the same adjustments of the fluorimeter as for the measurements of the spectra presented in Fig. 29 (see Fig.30). The same concentrations (66 µmol/L $EuCl_3 \cdot 6\ H_2O$ in 13 mmol/L MOPS buffer and 22 µmol/L tetracycline hydrochloride in 13 mmol/L MOPS buffer) were used as for the measurements shown Fig. 29.

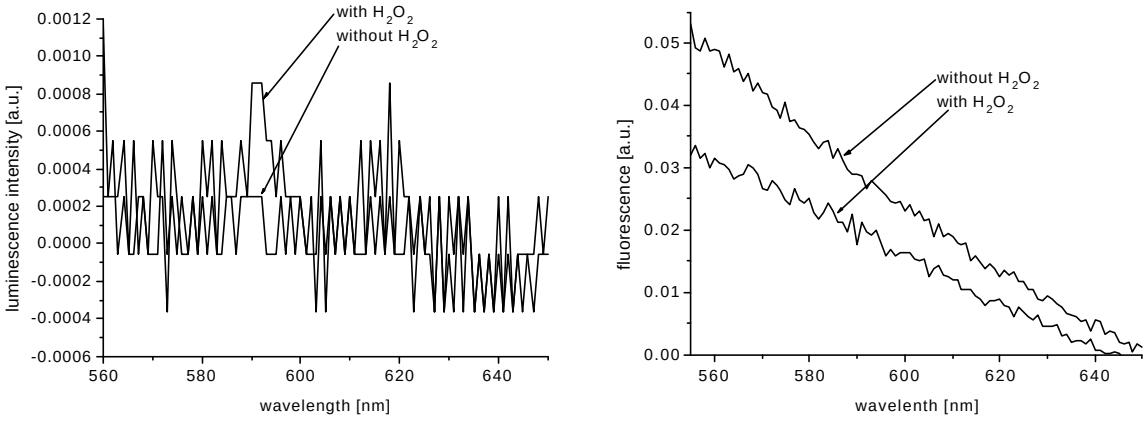

Fig. 30. Emission spectra of separate solutions of Eu^{3+} in MOPS buffer (left) and TC in MOPS buffer (right) at pH 6.9 using the same adjustments of the fluorimeter as for the measurements of the spectra presented in Fig. 28.

The $EuCl_3$ solution displays almost no emission. Only the noise of the PMT of the fluorimeter is detected (see Fig. 30, left). The TC solution without Eu^{3+} displays a very weak fluorescence which has a tenfold lower intensity compared to Eu_3TC in absence of hydrogen peroxide and a 200 fold lower intensity compared to Eu_3TC in presence of hydrogen peroxide (compare intensities of Fig. 29 and Fig. 30 right at 618 nm, the fluorimeter adjustments are the same for both spectra). The whole spectrum of TC in presence and absence of H_2O_2 will be presented in chapter 4.1.3.

It can be summarized that an emission enhancement of Eu_3TC upon adding of H_2O_2 has been detected as a result of lanthanide sensitized luminescence energy transfer [6,7].

4.1.2 Effect of the Eu^{3+}/TC Ratio on the Emission of the EuTC System

The emission enhancement of Eu^{3+} upon binding of tetracycline has been described as a result of lanthanide sensitized luminescence energy transfer [6,7]. The existence of a fluorescent oxidation product of the tetracycline ligand channeling more emission light into the $^5D_0$ state and thus reducing radiationless transitions [10] seems a reasonable explanation for the enhanced luminescence at first glance. Note that H_2O_2 is known to be a strong oxidant. Consequently a larger molar part of TC than in Eu_3TC should cause a greater enhancement of

luminescence. This does not occur. Emission measurements of solutions with a constant concentration of Eu^{3+} of 66 µmol/L were taken with molar ratios to TC of 1:0.1, 1:0.33, 1:0.5, 1:1 and 1:2. The spectra include the excitation spectra (emission detected at 616 nm) of the solutions without H_2O_2 (see Fig. 31-33). They were recorded with the same fluorimeter adjustments.

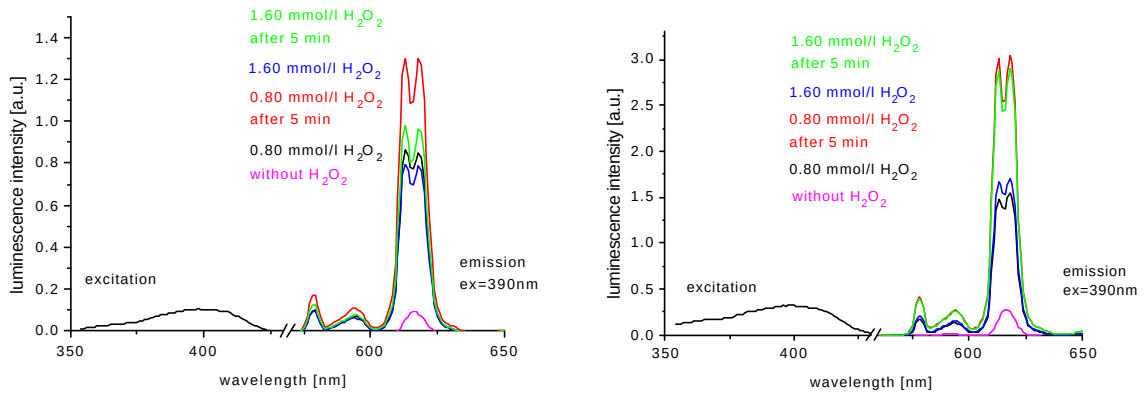

Fig. 31. Excitation and emission spectra of 1:0.1 (left) and 1:0.3 (right) Eu:TC upon addition of hydrogen peroxide in 13 mmol/L MOPS buffer pH 6.9.

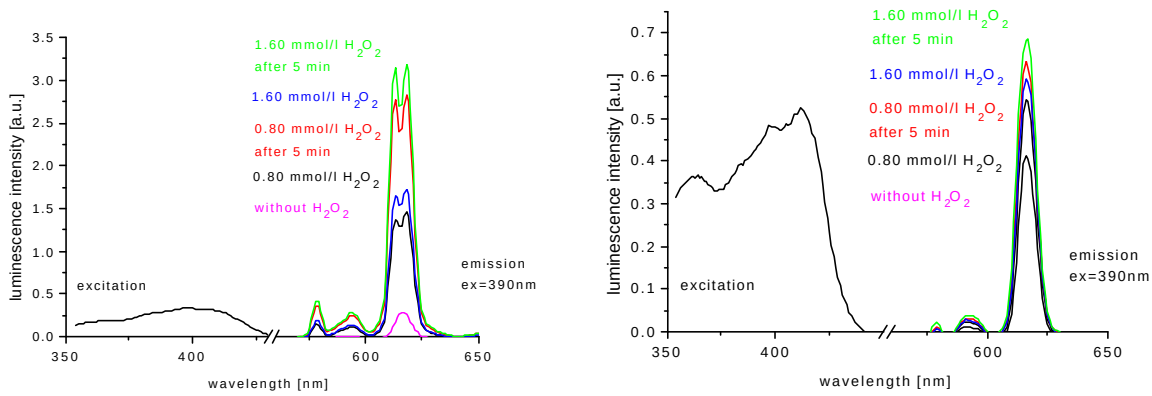

Fig. 32. Excitation and emission spectra of 1:0.5 (left) and 1:1 (right) Eu:TC upon addition of hydrogen peroxide in 13 mmol/L MOPS buffer pH 6.9.

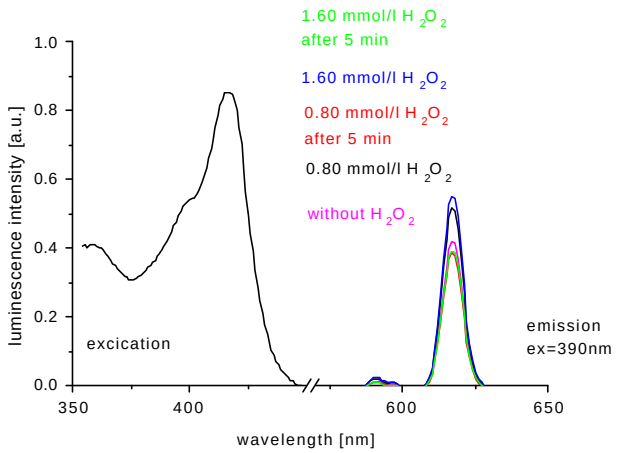

Fig. 33. Excitation and emission spectra of 1:2 Eu:TC upon addition of hydrogen peroxide in 13 mmol/L MOPS buffer pH 6.9.

In the following, the "without H_2O_2" spectra are compared with the "0.80 mmol/L" spectra. These spectra were directly taken after addition and mixing. The other spectra will be discussed in chapter 4.4. These spectra prove that upon addition of 0.8 mmol/L H_2O_2 the strongest enhancement of the 617 nm emission is obtained only if there is an over twofold excess of Eu^{3+} in solution while at 1:1 or 1:2 the intensity remains nearly unchanged. This is elucidated in Fig. 34.

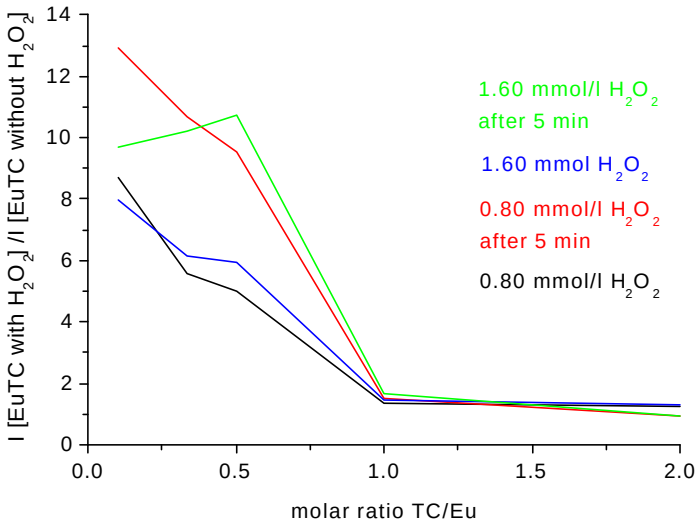

Fig. 34. Ratio of the luminescence intensities at 617 nm in presence and in absence of H_2O_2 dependent of the molar TC:Eu^{3+} ratio. Data taken from the measurements shown in Figs. 31-33.

The spectra show that the emission enhancement of the $^5D_0 \rightarrow {}^7F_2$ transition upon H_2O_2 addition is high in presence of excess Eu^{3+} and lowered with increasing amounts of TC. If the assumption of a fluorescent oxidation product [10] was true for our system, the emission enhancement of Eu_3TC would have risen with rising TC amounts. As the contrary is the case, the assumption of the formation of a fluorescent oxidation product of the tetracycline ligand channeling more emission light into the $^5D_0$ state [10] is not valid for our system.

Upon addition of 1.6 mmol/L H_2O_2 the strongest enhancement of the 617 nm emission is obtained only if there is an excess of Eu^{3+} in solution while at 1:1 or 1:2 the intensity remains nearly unchanged (see Fig.34, blue graph). A comparison of the blue and the black graph in Fig. 34 reveals that concentration dependent enhancement of the emission only occurs at 1:0.3 and 1:0.5 ratios.

4.1.3 Effect of TC on the Absorption and Emission of the EuTC System

After having excluded that an oxidation product of TC together with Eu^{3+} is responsible for the luminescence enhancement it was tested whether TC itself was responsible for the effect. The absorption spectra of a 22 µmol/L TC solution in MOPS buffer pH 6.9 in absence and presence of excess H_2O_2 were recorded (see Fig.35).

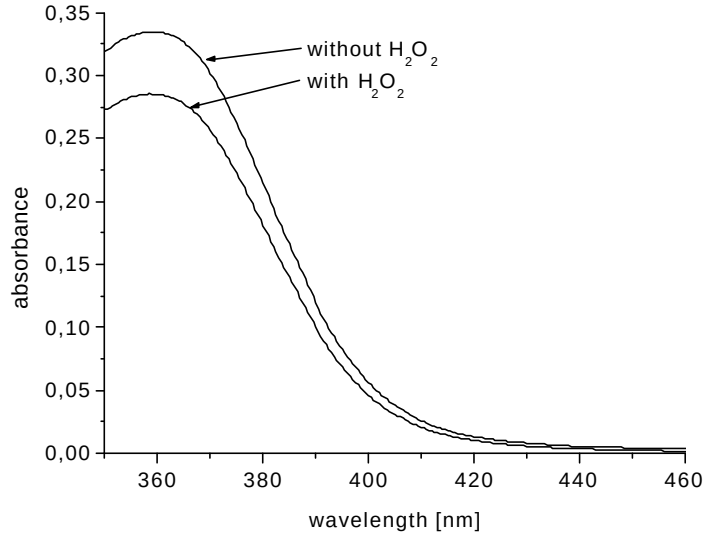

Fig. 35. Absorption spectra of 22 µmol/L TC in absence of H_2O_2 and in presence of 1 mmol/L H_2O_2 in 13 mmol/L MOPS buffer pH 6.9.

The spectra show that the absorbance of TC decreases by 15%, exactly the same amount as it was detected for Eu_3TC. Another absorption spectrum was recorded after one hour to exclude the influence of a slow oxidation of the chromophore, but no more decrease was found. It can be concluded that the lower absorption intensity of Eu_3TC in presence of H_2O_2 is due to the lower absorbance of the tetracycline ligand.

Excitation and emission spectra of 22 µmol/L tetracycline in MOPS buffer pH 6.9 in absence and presence of excess H_2O_2 were recorded (see Fig. 36).

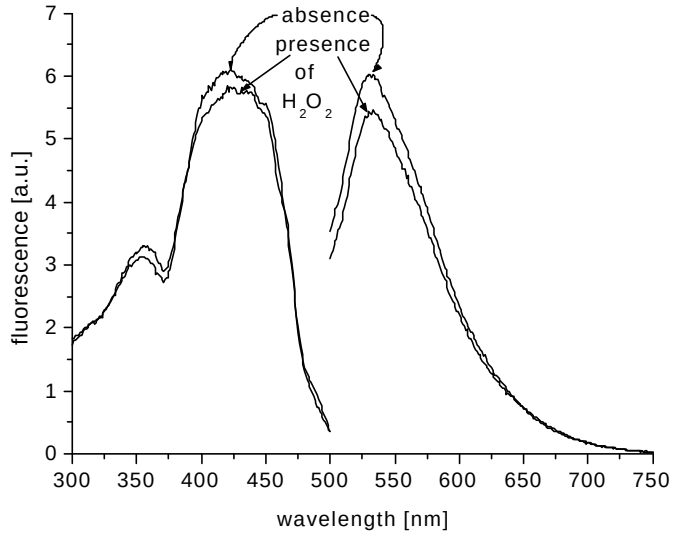

Fig. 36. Excitation (emission at 557 nm) and emission spectra (excitation at 420 nm) of 22 µmol/L tetracycline solution in absence of H_2O_2 and in presence of 1 mmol/L H_2O_2 in 13 mmol/L MOPS buffer pH 6.9.

A slight decrease of the emission intensity in both the excitation and the emission spectrum of TC on addition of H_2O_2 was detected. This is due to the decrease of the absorption of TC (see Fig. 35). After further 15 min. the emission was investigated again but no change of the emission spectrum compared to that of Eu_3TC in presence of H_2O_2 shown in Figs. 31-33 was obtained. Therefore the enhancement of the emission of the Eu_3TC complex is due to another effect but not due to the formation of an oxidation product of tetracycline.

4.1.4 Effect of Eu^{3+} on the Absorption and Emission of the EuTC System

There is a further possibility that some complexation processes caused by hydrogen peroxide may exist that may affect the coordination sphere around the Eu^{3+} ion. This could be the binding of H_2O_2, HO_2^- or O_2^{2-} as a ligand as it is found in the blue $CrO(O_2)_2$. As a result, water molecules would be displaced in the inner coordination sphere around Eu^{3+} which reduces the probability for radiationless decay to the ground state. Therefore, absorption spectra of 66 µmol/L $EuCl_3 \cdot 6\ H_2O$ were recorded in absence and presence of an excess of H_2O_2, again (see Fig. 37).

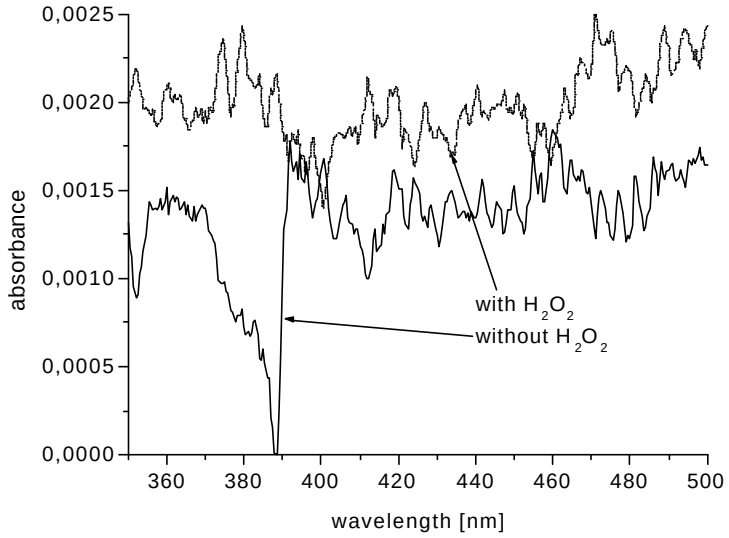

Fig. 37. Absorption spectra of 66 µmol/L $EuCl_3 \cdot 6\ H_2O$ in absence and presence of an excess of H_2O_2.

The change of the absorption found was too small to suspect an effect of hydrogen peroxide on the absorption, neither the one of $EuCl_3 \cdot 6\ H_2O$ nor the one of Eu_3TC. The change of the emission spectrum is too small to be presented. Therefore an influence on the inner coordination sphere around Eu^{3+} due to coordination of H_2O_2 can be excluded.

4.1.5 Effect of Oxygen in the Sample on the Emission of the Eu_3TC System

The emission of many MLCs is quenched by molecular oxygen in the sample. Although the

lanthanide MLCs are known not to be very sensitive to oxygen quenching the influence of oxygen on the Eu_3TC system was tested. The luminescence intensity of a 66 µmol/L solution of Eu_3TC in MOPS buffer pH 6.9 was measured in air satured solution and after 45 min. bubbling N_2 through the solution. The N_2 satured sample was sealed and the emission was recorded again (see Fig. 38).

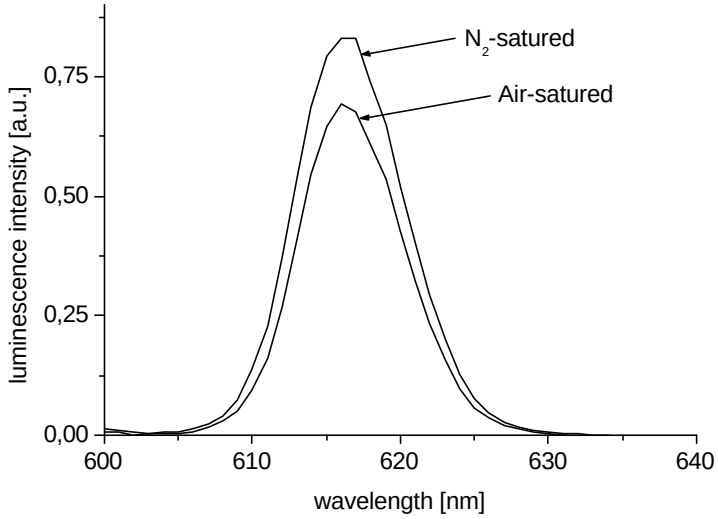

Fig. 38. Change of the luminescence intensity of a 66 µmol/L solution of Eu_3TC in MOPS buffer pH 6.9 in air satured solution and after 45 min. bubbling N_2 through the solution.

Fig. 38 shows that the effect of molecular oxygen on the emission intensity is comparatively low. The intensity increases by less than 20% upon saturating the solution with nitrogen. This is negligible compared to the 13-fold increase of the emission intensity upon adding hydrogen peroxide to Eu_3TC.

4.2 Effect of H_2O_2 on the Luminescence of other Ln^{3+} Tetracycline Complexes

4.2.1 Ln_3TC Complexes

Other lanthanide ions are known to display fluorescence in aqueous solutions [11,12].

Therefore, other lanthanide ions were complexed with tetracycline. It was investigated whether they display a similar enhancement of the luminescence intensity upon addition of H_2O_2 as it was found for Eu^{3+}. Pr^{3+}, Ho^{3+}, Sm^{3+} and Dy^{3+} were chosen because they all display comparatively strong absorption bands in the 350 to 550 nm region and all are known to fluoresce in aqueous solutions [11,12]. This is important because the molar extinction coefficients of trivalent lanthanide ions in aqueous solutions are generally below 100 L/(mol · cm) mostly between 0.1 and 3 L/(mol · cm). A high ε value is advantageous as it will be possible for the Ln^{3+} ion to be either self excited or to receive excitation energy by radiationless energy transfer from the excited triplet state of tetracycline. Additionally they are known to have hypersensitive emission bands. Therefore excitation spectra were recorded of 66 µmol/L solutions of Pr^{3+}, Sm^{3+} and Dy^{3+}, each of them with a 22 µmol/L tetracycline concentration (see Fig 39). The emission wavelength was at 560 nm. A comparison of Fig. 39 and Fig. 36 shows that these spectra basically reflect the excitation spectrum of TC with different luminescence intensities. On comparing Fig. 39 to the excitation spectrum in Fig. 31 (right) this was also true for the Eu_3TC system.

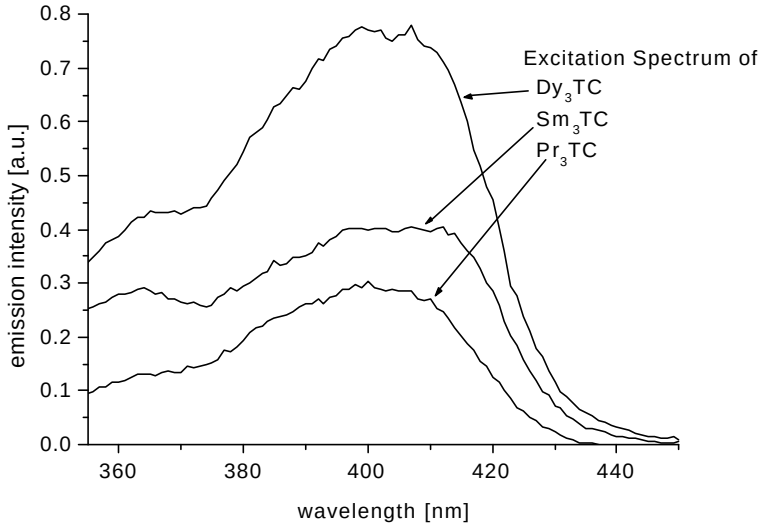

Fig. 39. Excitation spectra (emission at 560 nm) from 66 µmol/L solutions of Pr^{3+}, Sm^{3+} and Dy^{3+} each of them with a 22 µmol/L tetracycline concentration.

The emission spectra of 66 µmol/L solutions of Pr^{3+}, Sm^{3+} and Dy^{3+} in MOPS buffer pH 6.9 with a 22 µmol/L tetracycline concentration before and after addition of an excess of H_2O_2 are

shown in Figs. 40-42. The excitation wavelength was in the excitation maximum shown in Fig. 39.

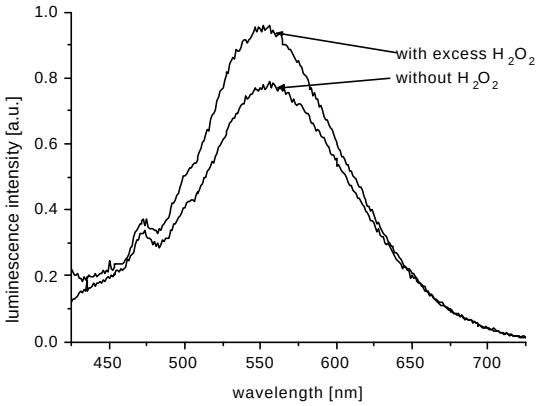

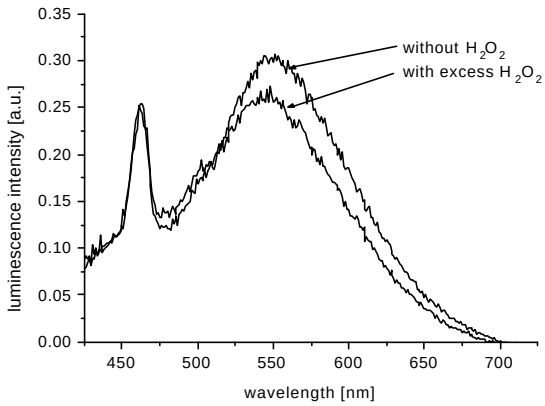

Fig. 40 (left). Change of the emission spectrum of Dy_3TC upon addition of excess H_2O_2.

Fig. 41 (right). Change of the emission spectrum of Pr_3TC upon addition of excess H_2O_2.

Figs. 40 and 41 show that no uniform effect of the addition of H_2O_2 on the emission can be stated because in the case of Dy_3TC the intensity increases but in the case of Pr_3TC the intensity decreases. Apart from the changes of the intensity both spectra basically reflect the emission spectrum of TC (compare to Fig. 36) with a Raman band at 470 nm. The emission lines of the respective Ln^{3+} ions are not visible.

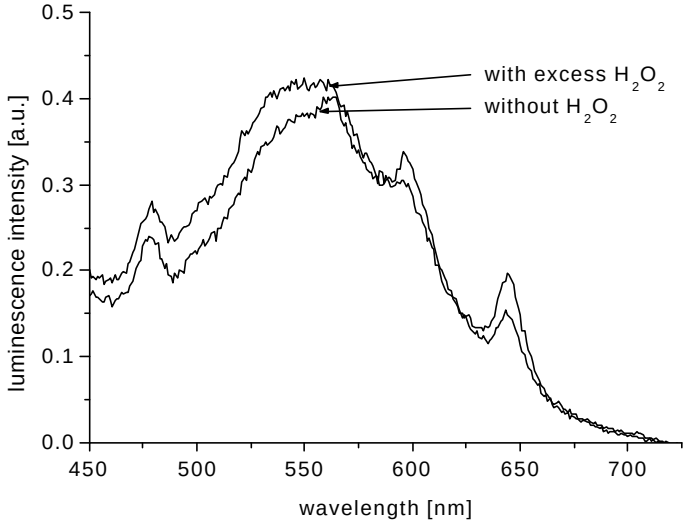

Fig. 42. Change of the emission spectrum of Sm_3TC upon addition of excess H_2O_2.

This changes gradually in Fig 42. Apart from the 470 nm Raman line, the TC emission spectrum is overlapped by some sharp peaks. Variations of the excitation wavelengths did not change the wavelength of the maxima of these peaks. They are due to emission from excited states of the Sm^{3+} metal. Their luminescence intensity increases upon addition of H_2O_2. Here, energy transfer seems to take place to some extent.

4.2.2 LnTC Complexes and Ln_{10}TC complexes

It can be seen from the measurements shown in Figs. 31-34 that the stoichiometry of Eu^{3+}:TC directly influences the increase of luminescence upon addition of hydrogen peroxide. Measurements of the emission of Ln^{3+}:TC in 1:1 and 10:1 molar ratios upon adding H_2O_2 were performed to exclude explorations that the energy transfer found for Eu_3TC only takes place either if an excess of Ln^{3+} or an equal molar quantity of Ln^{3+} is present. First, the data for the 1:1 molar ratio (c_{LnTC} = 66 µmol/L in MOPS buffer pH 6.9) are presented each containing the excitation spectrum in absence of H_2O_2 (see Fig. 43-46). Both DyTC and HoTC display an increase of the emission intensity between 30% (DyTC) and 15% (HoTC), respectively, but the shape of the whole spectrum is just the emission spectrum of tetracycline, again (see Figs. 43 and 44).

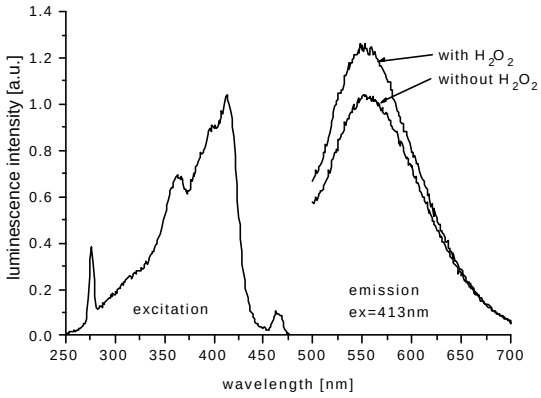

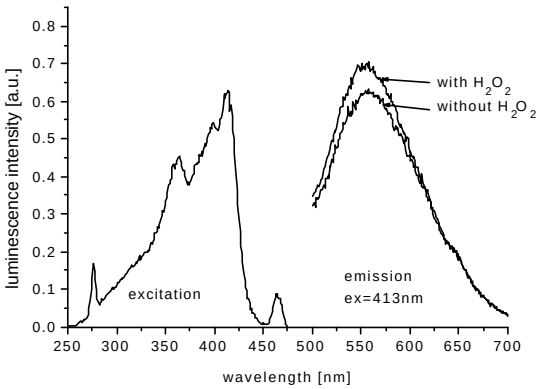

Fig. 43 (left). Change of the emission spectrum of DyTC upon addition of excess H_2O_2.

Fig. 44 (right). Change of the emission spectrum of HoTC upon addition of excess H_2O_2.

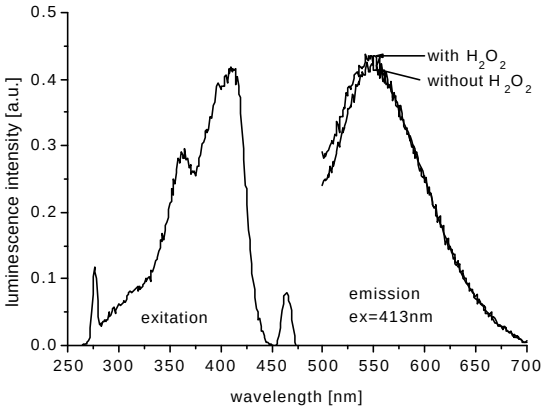

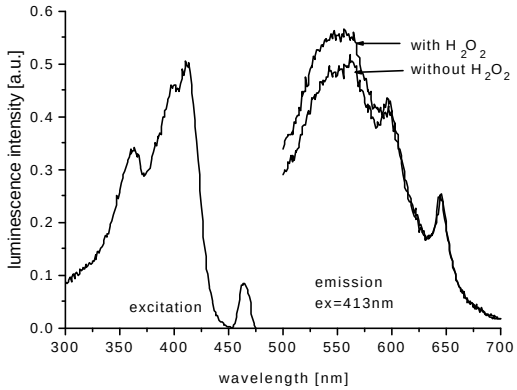

Fig. 45 (left). Change of the emission spectrum of PrTC upon addition of excess H_2O_2.

Fig. 46 (right). Change of the emission spectrum of SmTC upon addition of excess H_2O_2.

The fact that most emission emanates from tetracycline is also valid for PrTC with a spectrum being almost unchanged upon the addition of H_2O_2 (see Fig. 45). SmTC displays the TC-emission with a line pattern due to emission from excited states of the metal (see Fig. 46). Unlike Sm_3TC (see Fig. 42), the intensity of these lines remains unchanged upon adding H_2O_2. The intensity of the 550 nm emission rises about 15%.

Excitation and emission spectra were taken for the 10:1 molar ratios of Ln^{3+} for Dy^{3+}, Ho^{3+}, Pr^{3+} and Sm^{3+} ($c_{Ln^{3+}}$ = 66 µmol/L in MOPS buffer pH 6.9) but all of them solely show the emission from tetracycline. They remain unaffected upon the addition of excess of hydrogen peroxide and therefore are not presented.

It can be concluded that the enhancement of the emission intensity of complexes of Dy^{3+}, Ho^{3+}, Pr^{3+} and Sm^{3+} with tetracycline in molar ratios between 10:1 and 1:1 is only between 0 and 30% upon addition of excess H_2O_2. The emission mainly originates from tetracycline but the enhancement is against the behavior of TC to show a lowered intensity in presence of hydrogen peroxide (see Fig. 36). Therefore some sensitized luminescence as it was found for the EuTC system is present in some cases but for the ions and molar ratios to tetracycline discussed in this chapter the effects on the emission intensity are some orders of magnitude lower.

4.3 Effect of H_2O_2 on the Luminescence of Cu^{2+} and Ni^{2+} Tetracycline Complexes

It is known that energy transfer from ligands to center ions of MLCs is possible not only for lanthanides but also for transition metal ions. It would be advantageous (with regard to applications for a determination method for peroxides) if a complex of TC with an ion of these metals showed an enhanced luminescence intensity upon adding hydrogen peroxide. Copper and nickel ions display low-lying excited states to which energy may be transferred to from the tetracycline (TC) ligand. Therefore, solutions of Cu^{2+} and Ni^{2+} were examined in absence and presence of excess H_2O_2.

Solutions of 66 µmol/L CuTC and NiTC in 13 mmol/L MOPS buffer pH 6.9 were examined. Emission spectra were taken in absence and in presence of excess H_2O_2 (see Figs. 47 and 48). The excitation spectra were also taken but are not shown.

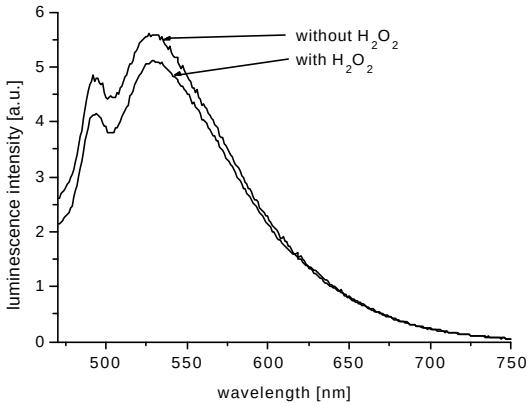

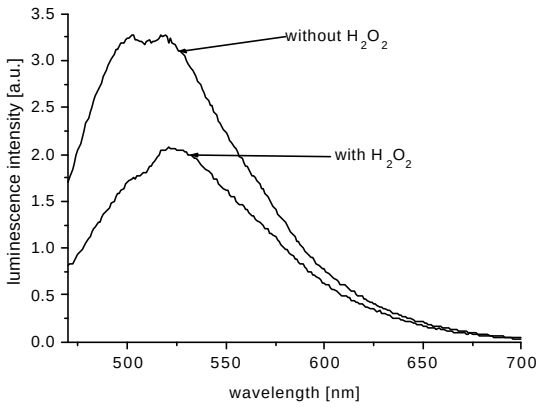

Fig. 47 (left). Change of the emission spectrum of CuTC upon addition of excess H_2O_2 (λ_{ex} = 432 nm).

Fig. 48 (right). Change of the emission spectrum of NiTC upon addition of excess H_2O_2 (λ_{ex} = 452 nm).

Fig. 47 shows a 10% increase of the emission intensity for the CuTC solution after addition of H_2O_2. This result is similar to the increase found for most of the LnTC solutions (see Figs. 43-46). Apart from a Raman band at 500 nm and the TC emission centered at 540 nm no additional emission band of the metal is found. A decrease of the emission intensity of 40%

was found for the NiTC solution. This is the strongest change apart from the EuTC system which therefore is preferable.

4.4 Effect of H_2O_2 on the Luminescence of Eu^{3+} Complexes with Other En-dione Ligands

The fact that a fluorescent ligand carrying an en-dione system like in tetracycline is able to cause a more than tenfold increase of the luminescence intensity of Eu^{3+} inspired me to use some other common dyes as sensitizer for Eu^{3+}. It was found that a Ln^{3+}: ligand ratio of 3:1 worked best in the case of the Eu_3TC system. Therefore, concentrations of 66 µmol/L Eu^{3+} and 22 µmol/L of the ligand dye in 13 mmol/L MOPS buffer pH 6.9 were employed for all measurements in chapter 4.4.

4.4.1 Sodium Alizarinesulfonate and Sodium Alizarine-3-methylamino-N,N-diacetic Acid as Ligands

Absorption (see Fig. 49) and emission spectra of Eu-alizarinesulfonate were recorded in absence and presence of excess hydrogen peroxide. The spectra show only a slight decrease of the absorption in presence of H_2O_2. The emission spectra were taken at two different excitation wavelengths. The 332 nm of the shoulder of the short-wavelength absorption of alizarine and 528 nm were used as excitation wavelengths. The emission remains almost unchanged close to zero. Therefore an excitation wavelength of 528 nm obviously carries too little energy to cause an energy transfer to the Eu^{3+} ion. The energetic difference of a $^7F \rightarrow {}^5D_0$ excitation is probably greater. This is in accordance to the results of Richardson [9]. If the 332 nm excitation is employed only the sharp emission line of stray light of second order is visible. The same result is found if sodium alizarine-3-methylamino-N,N-diacetic acid is the ligand attached to Eu^{3+}. Its absorbance decreases slightly and an emission is nearly undetectable.

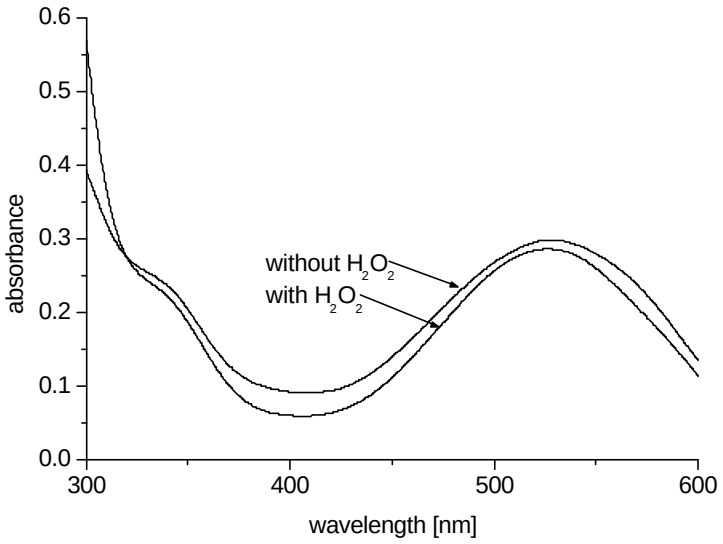

Fig. 49. Changes in the absorption spectrum of Eu_3alizarinsulfonate upon adding excess H_2O_2.

4.4.2 Salicylic Acid as Ligand

Salicylic acid is known to display fluorescence and also bears an en-dione moiety. Therefore we hoped to find an effect on the emission intensity of Eu^{3+} comparable to that of Eu_3TC when salicylic acid was bound to the europium ion. Yet, the absorption spectrum (see Fig. 50) is unaffected by the addition of excess hydrogen peroxide. The emission intensity of the salicylic acid band decreases by 20% but none of the Eu^{3+} lines are visible. This means that no additional excitation energy is not transferred to the europium ion.

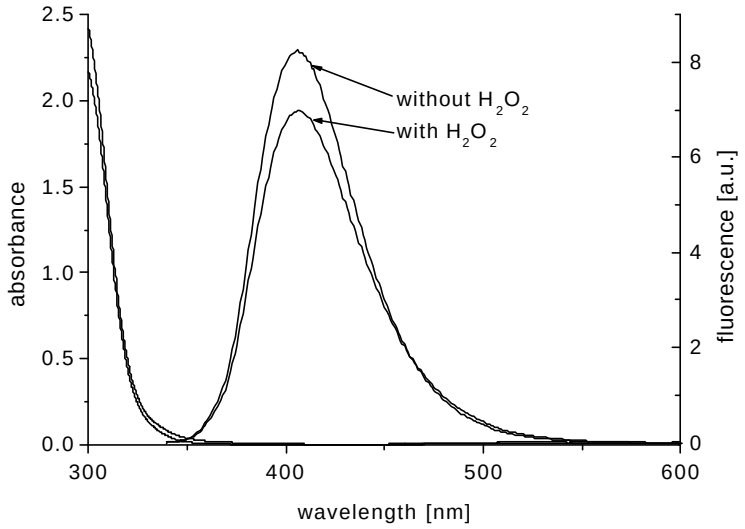

Fig. 50. Change in the absorption (left) and emission spectrum (right) of Eu_3salicylic acid upon adding excess H_2O_2.

4.4.3 Gallocyanine as Ligand

Different results were obtained when gallocyanine was employed as ligand for Eu^{3+} in presence of hydrogen peroxide. The absorption maximum is strongly red shifted from 546 to 619 nm and the long-wavelength absorbance increases (see Fig. 51, left). The red shift of the absorption is independent of time but the emission intensity rises threefold after a little decrease (see Fig. 51, right).

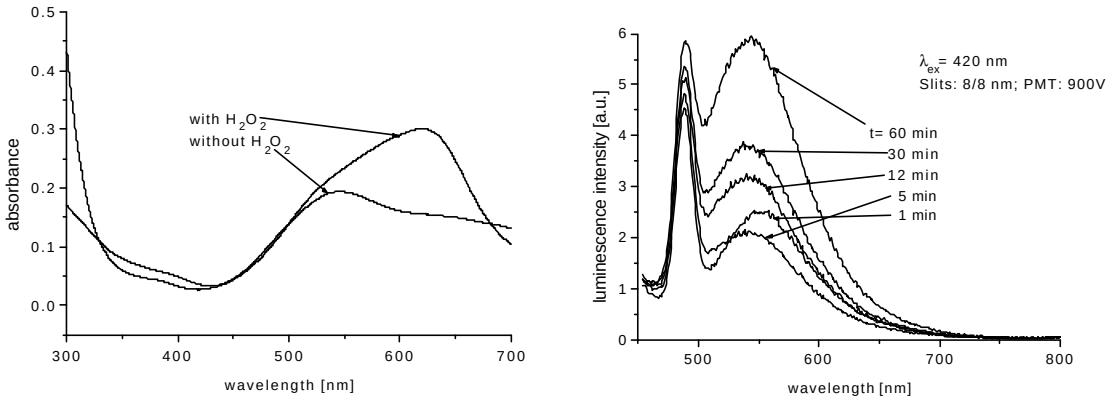

Fig. 51. Change of the absorption (left diagram) and emission spectrum (right diagram) of Eu_3gallocyanine upon adding excess H_2O_2.

Note that an excitation wavelength of 420 nm, large slitwidths and a high amplification of the emission signal was necessary. Upon excitation at 546 nm almost no fluorescence was detected. This corresponds with the fact that gallocyanine is known as an absorption dye but not as a fluorescent dye. Due to large slitwidths and the high amplification used for detection the formation of low concentrations of certain fluorescent oxidation products of gallocyanine can be supposed. It is also possible that the increase of the long-wavelength absorbance and a shorter-wavelength emission is due to the formation of a highly fluorescent oxidation product of an impurity of gallocyanine. The complete absence of line like emission bands allow the interpretation that no energy transfer to the europium ion occurs.

4.4.4 Anhydrotetracycline as Ligand

Anhydrotetracycline was synthesized according to a commonly used procedure [13] and a solution with 66 µmol/L Eu^{3+} and 22 µmol/L of Anhydrotetracycline in 13 mmol/L MOPS buffer pH 6.9 were prepared. Only a slight blue shift in the absorption spectrum is visible (see Fig. 52). This is accompanied by a 25% decrease in the absorbance at 465 nm.

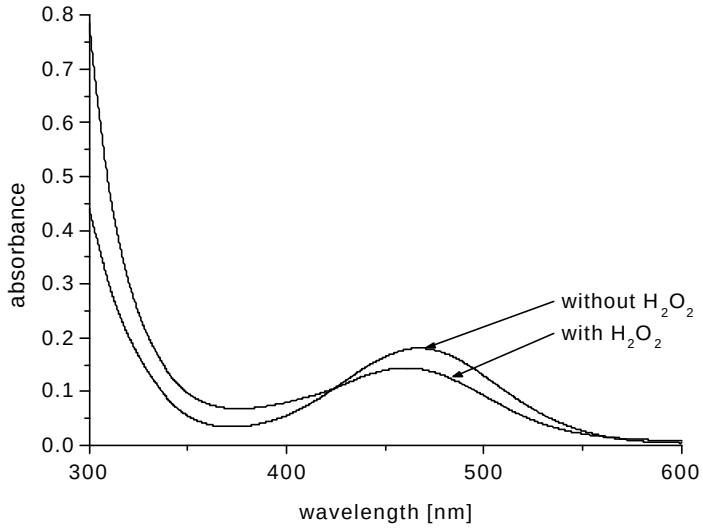

Fig. 52. Change in the absorption spectrum of Eu_3anhydrotetracycline upon adding excess H_2O_2.

No emission was found when using 320, 400 or longer-wavelength excitation. This is on the

contrary to the literature [10] where the formation of anhydrotetracycline upon oxidation of TC due to H_2O_2 was stated to be the reason for enhanced chemiluminescence of the EuTC complex. This means that the enhanced luminescence found for the Eu_3TC system cannot be deduced from the oxidation of tetracycline into its anhydro derivative. It can also be concluded that neither for an other center cation nor for an other ligand an enhancement of luminescence was found comparable to that of Eu_3TC. Therefore, the Eu_3TC is obviously a unique system where photonic energy is ideally directed to the Eu^{3+} ion.

4.5 Setup and Discussion of the New Sensing Scheme for H_2O_2

In chapter 4.1.2 different ratios of Eu^{3+}:TC were presented to show a fluorescence enhancement in presence of hydrogen peroxide. Emission spectra were taken for two different concentrations of the analyte and 5 min. after the addition (see Figs. 31-33). In an experiment using a longer detection time after the addition of H_2O_2 it was found that there was a time dependent enhancement of the luminescence at 617 nm of the samples which reached an almost constant value after 30 min (see Fig. 53).

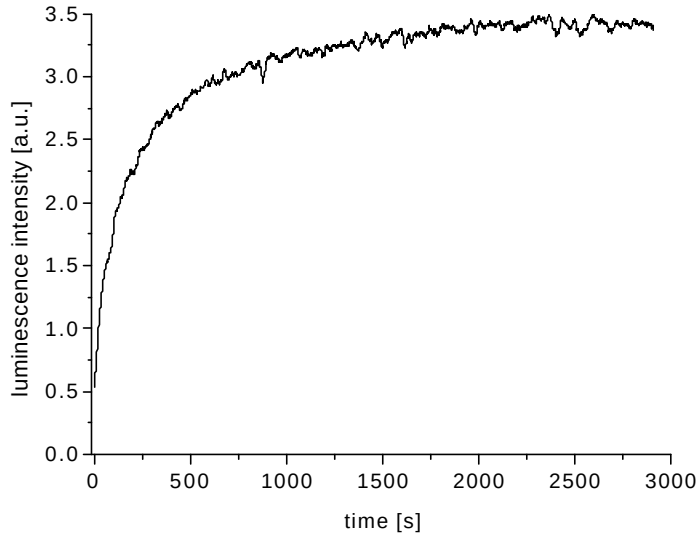

Fig. 53. Time dependent enhancement of the luminescence intensity at 617 nm of a 66 µmol/L solution of Eu_3TC in MOPS buffer pH 6.9 upon addition of 1 mmol/L H_2O_2.

Reliable values are found after 10 minutes because then the enhancement of the fluorescence intensity is complete by more than 90% compared to the value at t = 0. Fig. 34 (black and blue graph) shows that only in the case of Eu_3TC and Eu_2TC the enhancement of the intensity is proportional to an increasing peroxide concentration. Therefore a calibration curve was set up using the following procedure. The Eu_3TC solution contained 66 µmol/L Eu^{3+} and 22 µmol/L tetracycline · HCl solution in 13 mmol/L MOPS buffer pH 6.9. The analyte solution contained hydrogen peroxide at various concentrations in 13 mmol/L MOPS buffer pH 6.9. 1.00 mL of the detection solution and 1.00 mL of the analyte solution were mixed and incubated for 10 min. at 20 °C with stirring. Then the luminescence intensity was measured immediately at 616 nm with an excitation wavelength at 393 nm. The result is a sigmoidal calibration curve with linear range between 10-500 µmol/L H_2O_2 (see Fig. 54).

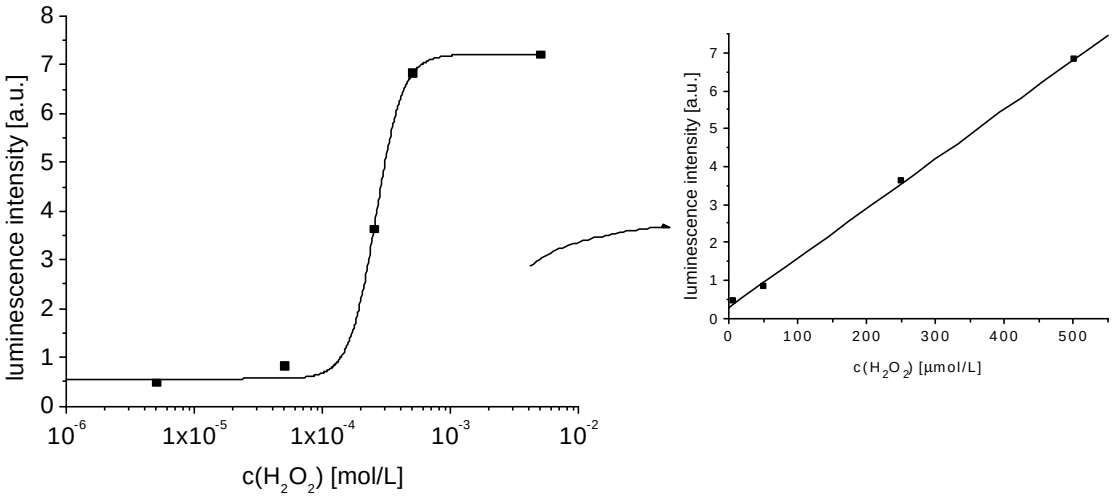

Fig. 54. Calibration curve for the H_2O_2 assay: Luminescence intensity at 616 nm after 10 min. incubation at 20 °C as a function of the log of the hydrogen peroxide concentration (left) and enlargement of the range (right) where the luminescence intensity is a linear function of the hydrogen peroxide concentration.

This test has advantages compared to those commonly available. First, it can be performed very quickly. A whole set of calibration concentrations and samples can be easily determined within 15 minutes. A standard fluorimeter can be used for this determination because the emission light is very intense and a strong photomultiplier amplification is not necessary.

Therefore, this test may be carried out in instruments with less expensive detectors like PIN-photodiodes. Even simpler instrumentation can be employed due to the large Stokes' shift of Eu_3TC. Note that the emission maximum is red-shifted over 200 nm. Such a large shift allows an easy separation of the emission light from the excitation light. Therefore, this test may be performed with instruments equipped with excitation and emission filters only, wherein the spectral bandwidth of the excitation light is naturally larger than in a device equipped with monochromators.

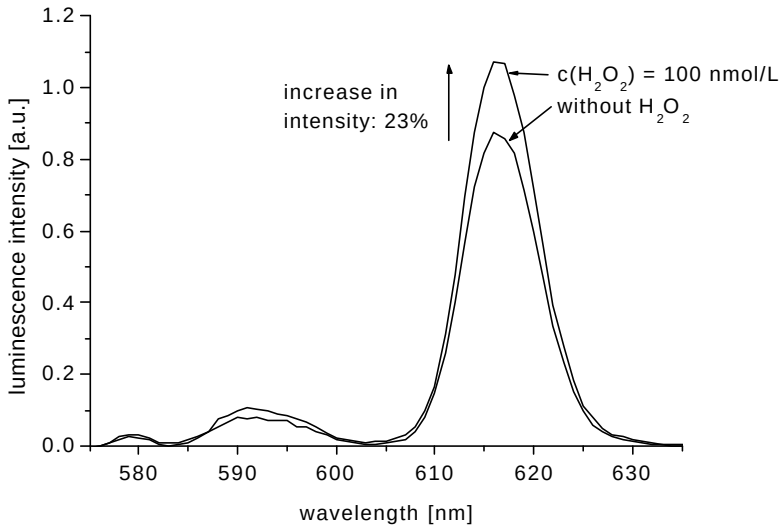

Fig. 55. Determination of the detection limit for H_2O_2 using the Eu_3TC test under standard conditions (10 min reaction time at 20 °C).

Sample handling and the time needed for this assay are similar to the photometric H_2O_2 test commercially available from Tokyo Kasei Organic Chemicals (TCI) [14]. The detection limit of 100 nmol/L is equal for both, the TCI and the Eu_3TC test. At the detection limit, the Eu_3TC test gives a reliable enhancement of the fluorescence intensity at 616 nm of 23% (see Fig. 55). The TCI test spectrophotometrically detects the decrease of the absorbance of a Ti(IV)-porphyrine complex at 432 nm. The lower the concentration of H_2O_2 the lower is the change of the absorbance. Consequently a very sensitive spectrophotometer is required for the determination of low analyte concentrations using the TCI test.

Additionally, a correction is required if other species are present in the sample which display distinct absorption in the 400-475 nm region. This is true for many biological samples

containing natural fluorophores like heme groups or porphyrines (i.e. see absorption spectrum of myoglobin, Fig. 19). The luminescence based test is nearly unaffected by these disturbances because the emission wavelength is in the optical window for biological material. A disturbance due to reabsorption of emission light or due to other emitting fluorophores may occur but only if absorbers are present with λ_{max} at 600 nm of higher.

Furthermore a detection of hydrogen peroxide via fluorescence lifetime measurements in the 1-20 µs domain seems to be possible. The pH dependence of the lifetime of the EuTC complex has already been described [7]. A test using a 370 nm LED as the excitation source in presence of 1 mmol/L H_2O_2 delivered a change of the lifetime from 13.0 µs to 9.6 µs at a modulation frequency of 20 kHz. Further work will be done to determine whether a fluorescence lifetime measurement can be used. This would enable the determination of hydrogen peroxide independent of other natural fluorophores. The lifetimes of these fluorophores are in the nanosecond range and can easily be excluded by off-gating the lifetime measurement for 100 ns. Another advantage of lifetime based measurements is their independence from disturbances like fluctuations of the intensity of the excitation source and photobleaching. This always affects intensity-based measurements.

The test works best at a neutral pH of 6.9 in a 13 mmol/L buffered solution. An influence on the luminescence intensity due to pH changes resulting from dissociated protons from the acid H_2O_2 is negligible because its pK_a value of 11.8 is too high. An aqueous solution of neutral pH often is a prerequisite for measurements in samples containing proteins, enzymes, DNA or other biological material. This is of special importance if compared to common methods [15,16] where an enzyme converts H_2O_2 and a phenol to the respective biphenol at pH 9.5. This is followed by the complexation with Tb(III)-EDTA at pH 13 in presence of CsCl. Measurements of biological processes at such a high pH are often impossible.

The TCI spectrophotometric test works best at the highly acidic pH of 0.3 in presence of $HClO_4$ [14]. This is too acidic for biological processes and the method using Tb(III) just works at too basic conditions. Furthermore $HClO_4$ is a strong oxidant at these concentrations [17]. This can cause serious damages to biological material.

The Eu_3TC solution is stable at room temperature for over three months in the dark and therefore it should be stable at least for one year if stored at 4 °C. Finally, the Eu_3TC

method allows the tuning of the concentration range to be determined by variation of the incubation time of the samples. Fig. 53 shows that even after 10 min. the increase in intensity is not finished. An incubation time of ten minutes was chosen for reasons of reliability and time consumption.

Larger increases of the luminescence intensity can be expected if a longer incubation time is used. This may improve the limits of detection for H_2O_2. Alternatively, lower or higher Eu_3TC concentrations will be subject of further investigations to enlarge the possibilities of the application of the Eu_3TC system.

4.6 Determination of Glucose

4.6.1 Test of Applicability and Optimization of GOx Concentration

The optical measurement of glucose is an evergreen in analytical chemistry. A new method based on a decreased luminescence intensity and other common methods have been described in previous works [18,19]. The determination of hydrogen peroxide with Eu_3TC theoretically allows the indirect measurement of all reaction products or educts of enzymatic reactions of oxidases. This is due to the fact that all oxidases produce H_2O_2 within the enzymatic reaction. Glucose oxidase is a typical example. It converts glucose according to the following scheme:

$$\beta\text{-D-Glucose} + H_2O + O_2 \xrightarrow{GOx} \text{Gluconolactone} + H_2O_2 \qquad (4.1)$$

In view of the promising properties of Eu_3TC to sense H_2O_2 it was decided to design a method for determination of glucose at human physiological blood levels, i.e. between 2.5 and 7.5 mmol/L. In this scheme, the H_2O_2 formed by Eq. (4.1) is followed by a second reaction (4.2) during which Eu_3TC is converted into its strongly luminescent H_2O_2 complex:

$$\underset{\text{low luminescence}}{Eu_3TC(H_2O)_n} + H_2O_2 \longrightarrow \underset{\text{high luminescence}}{Eu_3TC(H_2O_2)(H_2O)_{n-1}} + H_2O \qquad (4.2)$$

First attempts were made with a relatively high concentration of GOx in the Eu_3TC solution. Glucose solutions of various concentrations were added and the luminescence enhancement was monitored at 616 nm (see Fig. 56).

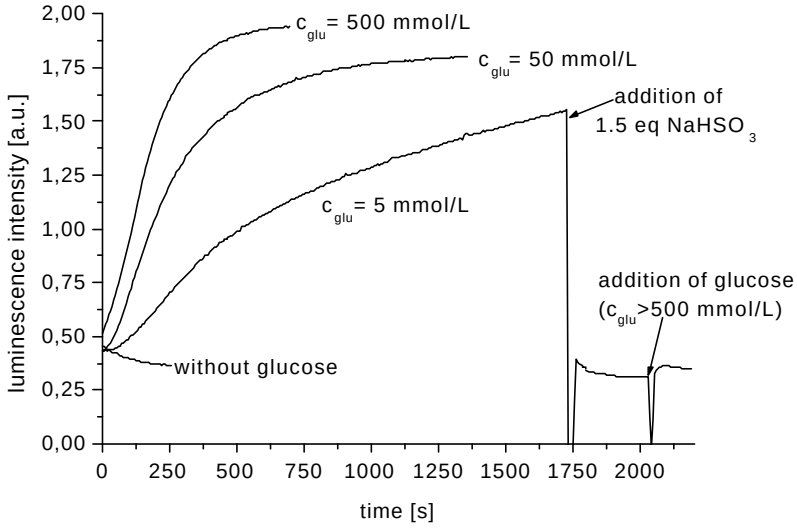

Fig. 56. Time dependent change in the luminescence intensity of Eu_3TC at 616 nm as a result of H_2O_2 produced by GOx at various concentrations of glucose and upon adding an inhibitor.

Fig. 56 shows that the luminescence intensity increases over time due to evolved hydrogen peroxide depending on the concentration of glucose. The enzyme activity can be stopped by addition of $NaHSO_3$, as it is known for oxidases [20]. As a result the luminescence intensity decreases to a level that is lower than the starting value. The graph labeled "without glucose" shows that the loss of signal intensity due to photobleaching is low compared to the 3.5-fold enhancement due to formation of H_2O_2 (see curve named c_{glu}= 5 mmol/L).

The concentration of the enzyme was optimized with respect to the determination of glucose at physiological levels. GOx concentrations of 6.5, 8.5, 10, 10.5 and 15 µg/mL in the Eu_3TC solutions were measured at concentrations of 2.5, 4.5 and 7.5 mmol/L glucose, respectively, for 10 min each (see Figs. 57-59). The optimum concentration of enzyme between saturation with excess enzyme (see Fig. 57) and saturation with excess substrate at any glucose concentration (concentration of enzyme too low, see Fig. 59) was determined to be 10 µg/mL.

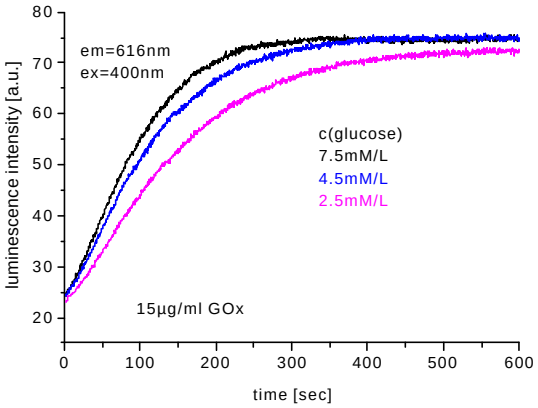

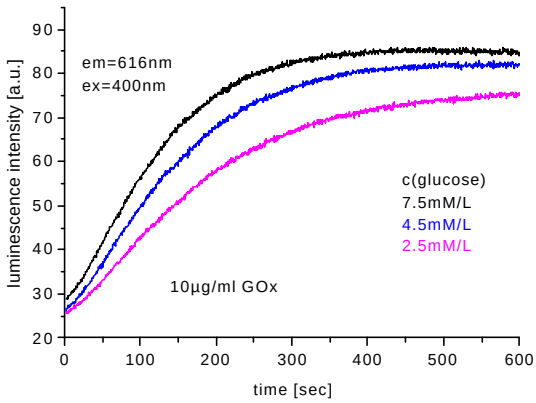

Fig. 57 (left). Time dependent increase of the luminescence of Eu_3TC at 616nm at 15 µg/mL GOx at physiological concentrations of glucose.

Fig. 58 (right). Time dependent increase of the luminescence of Eu_3TC at 616nm at 10 µg/mL GOx at physiological concentrations of glucose.

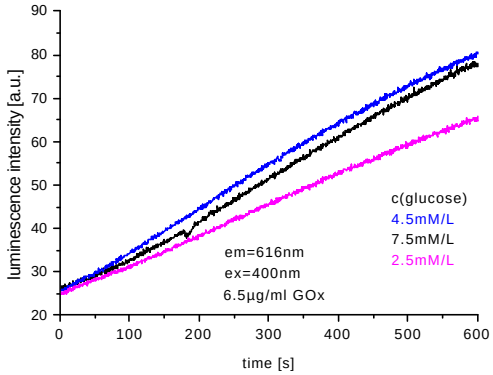

Fig. 59. Time dependent increase of the luminescence of Eu_3TC at 616 nm at 6.5 µg/mL GOx at physiological concentrations of glucose.

Fig. 58 shows the curves for the 10 µg/mL GOx concentration which was employed for the following measurements of glucose. Here, the concentrations can be distinguished very well via differences in the slope. Nevertheless, the system can be optimized to work at lower or higher concentration ranges of glucose by using other concentrations of the enzyme. Once this was known, a procedure for the glucose determination in 1 mmol/L steps in the human physiological range was set up.

4.6.2 Determination of Glucose

A Eu_3TC stock solution (Solution A) containing 264 µmol/L (96 mg/L) Eu(III) and 88 µmol/L (40 mg/L) TC and a 30 mmol/L (5.95 g/L) glucose stock solution (Solution B) are mixed in the ratios given in the mixing table in chapter 5.6.2 to receive glucose solutions of concentrations ranging from 2.5 to 7.5 mmol/L after mixing with the enzyme solution (Solution C). A solution of 20 µmol/L GOx (Solution C) is also prepared and both solutions are kept at 20 °C. 1.00 mL of the GOx solution is pipetted into a cuvette equipped with a stirrer bar and placed in the cuvette holder of a fluorimeter and thermostated to 20 °C. Then, 1.00 mL of the respective glucose solution is added. After 10 s mixing time the enhancement of the luminescence intensity of Eu_3TC at 616 nm is monitored for ten minutes. The result is shown in Fig. 60.

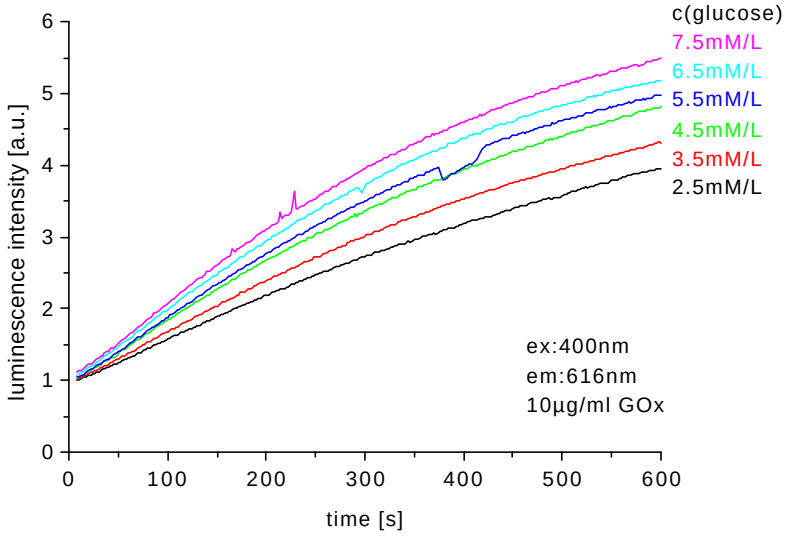

Fig. 60. Time dependent enhancement of the luminescence intensity of Eu_3TC at 616 nm as a result of the formation of H_2O_2 by GOx during oxidation of glucose.

Fig. 60 shows curves which display the kinetics of the increase of the hydrogen peroxide concentration produced by the conversion of glucose due to the GOx. The slight fluctuations of the emission intensity in the curve taken with 5.5 mmol/L glucose are variations of enzyme activity and may be caused by catalase impurities in the GOx. This may be avoided using the more expensive “catalase free GOx” which was not used in our experiments.

Finally, it had to be found out at what time to measure the luminescence intensity. Therefore, a procedure described in the experimental part in chapter 5.6.2 was used to calculate the slope of each curve as a function of time (see Figs. 61 and 62).

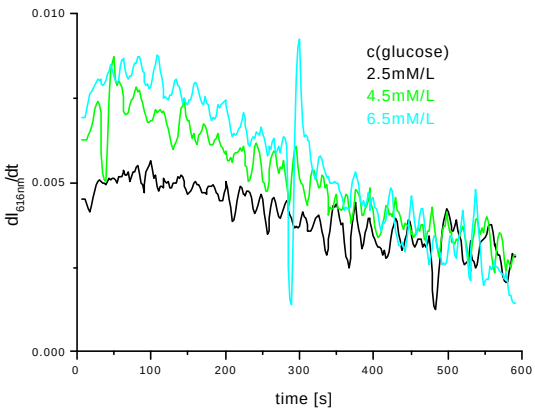

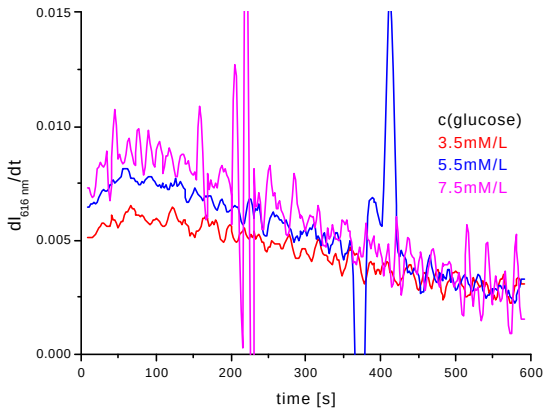

Fig. 61 (left). Time dependent change of the slope of three concentration of glucose from Fig. 60.

Fig. 62 (right). Time dependent change of the slope of three concentration of glucose from Fig. 60.

For reasons of better comprehension, only three graphs were placed into each figure. Figs. 61 and 62 show that each curve rises within the first 50-100 seconds to reach a maximum and clearly decreases after 200 s. The highest absolute y-values are obtained within these 200 s. This means that during these 200 s each curve rises most steeply. Therefore, reliable results can be obtained just after three minutes. From 400 s until 600 s the average value of the three curves becomes approximately equal at 0,003. With respect to Fig. 60 this means that the difference of the luminescence intensities between the curves approaches zero. The separation of the emission signals in Fig. 60 does not increase from here any more.

The fluctuations of the emission intensity mentioned above appear in a more drastic way in these representations because the change of signal intensity per time unit is much stronger. Figs. 60, 61, and 62 show that whenever there is a fluctuation the average $dI_{616\ nm}/dt$ values deviate strongly (i.e. see Figs. 60 and 61, purple curve, t = 280 s; Figs. 60 and 62, dark blue curve, t = 360 and 410 s; Figs. 60 and 62, bright blue curve, t = 215 and 235 s). Nevertheless, if the kinetics of the reaction is known this determination of the slope can be used as a control to ensure that the value of the emission intensity is not affected by a fluctuation of the

enzyme. By taking ten values each five seconds and calculating the slope in the given manner will deliver a correct result is obtained. After calibration of the fluorimeter the glucose concentration can be derived from the data after 3 min. A comparison of the slope of the calibration plots during the respective 50 s time with the slope of the measured sample displays whether the result was disturbed by a fluctuation or not. Related to Figs 61 and 62 this means that $dI_{616\,nm}/dt$ has to be within 0.025 and 0.01.

It can be concluded that the enhancement of the luminescence intensity of the Eu_3TC system can be used to measure hydrogen peroxide and glucose, respectively. A variation of the enzyme concentration allows the adaptation of the system to measurement of either glucose or H_2O_2 in different concentration ranges. Obviously, the determination of glucose in the human physiological concentration range works very well. This has to be stressed because most of the systems described or commonly used [18] are too sensitive (by 2-5 orders of magnitude).

The determination of glucose can be performed rather quickly. A whole set of calibration concentrations and samples can be easily determined within 2 hours. Once the fluorimeter is calibrated the assay takes less than 5 minutes. Moreover, standard instruments can be used for this method because the emission light is very intense and no high photomultiplier amplification is necessary. Therefore, simpler instrumentation with detectors like PIN-photodiodes or devices equipped with excitation and emission filters may be used to perform this test. This is due to the large Stokes' shift of Eu_3TC which allows an easy separation of the emission from the excitation light because the emission maximum is red shifted over 200 nm away from the excitation maximum.

The emission light of the glucose assay is within the optical window of biological matter. Therefore it may remain almost unaffected by disturbances due to reabsorption. This is because the emission appears at wavelengths > 600 nm where absorption and particularly emission due to natural fluorophores is very low.

4.7 Literature

1. Colaizzi, J. L., Knevel, A. M., Martin, A.N., 1965, Biophysical Study of the Mode of Action of the Tetracycline Antibiotics, *J. Pharm. Sci.*, **54**, 1425-1436.

2. Hahn, H. (Hrsg.), 1979, *Antibiotics*, Bd. 5, Springer Verlag, Berlin, 304-328.
3. Menachery, M. D., Cava, M. P., 1984, Amino derivatives of Anhydrotetracycline, *Can. J. Chem.*, **62**, 2583-2585.
4. Dürckheimer, W., 1975, Tetracycline: Chemie, Biochemie und Struktur-Wirkungs-Beziehungen, *Angew. Chemie*, **87**, 751-784.
5. 1995, *CD Römpp Chemie Lexikon*, Version 1.0, Georg Thieme Verlag, Stuttgart/New York.
6. Hirschy, L. M., Dose, E. V., Winefordner, J. D., 1983, Lanthanide-Sensitized Luminescence for the Detection of Tetracyclines, *Anal. Chim. Acta*, **147**, 311-316.
7. Hirschy, L. M., Van Geel, T. F., Winefordner, J. D., Kelly, R. N., Schulman, S. G.,1984, Characteristics of the Binding of Europium(III) to Tetracycline, *Anal. Chim. Acta*, **166**, 207-219.
8. Rakicioglu, Y., Perrin, J. H., Schulman, S. G., 1999, Increased luminescence of the tetracycline-europium(III) system following oxidation by hydrogen peroxide, *J. Pharm. Biomed. Anal.*, **20**, 397-399.
9. Richardson, F. S., 1982, Terbium(III) and Europium(III) Ions as luminescent Probes and Stains for Biomolecular Systems, *Chem. Rev.*, **82**, 541-552.
10. Zhang, X. R., Baeyens, R. G., Van den Borre, A., Van der Weken, G., Calokerinos, A. C., Schulman, S. G., 1995, Chemiluminescence Determination of Tetracyclines Based on Their Reaction With Hydrogen Peroxide Catalyzed by the Copper Ion, *Analyst*, **120**, 463-466.
11. Petersheim. M., 1981, Luminescent Trivalent Lanthanides in Studies of Cation Binding Sites, *Modern Fluorescence Spectroscopy, Vol. 2*, Wehry, E. L. (Ed.), Plenum Press, New York/London, 43-71.
12. Carnall, W. T., 1979, The Absorption and Fluorescence Spectra of Rare Earth Ions in Solution, *Handbook on the Physics and Chemistry of Rare Earths*, Gschneider K. A. jr. and Eyring, L. (Eds.), North Holland Publishing Company, Vol. 3, 171-207.
13. Green, A., Wilkinson, R. G., Boothe. J. H., 1960, Chemistry of the Tetracycline Antibiotics. II. Bromination of Dedimethylaminotetracyclines, *J. Am. Chem. Soc.*, **82**, 39046-39050.
14. Matsubara, C., Kawamoto, N., Takamura, K., 1992, Oxo[5,10,15,20-tetra(4-pyridyl) porphyrinato]titanium(IV): An Ultra-high Sensitivity Spectrophotometric Reagent for Hydrogen Peroxide, *Analyst*, **117**, 1781-1784.

15. Meyer, J., Karst, U., 1999, Zeitverzögerte Fluoreszenzspektroskopie mit Lanthanoid-komplexen - Prinzipien und Anwendungen, *NChTL.*, **47**, 1116-1119.
16. Meyer, J., Karst, U., 1998, Verfahren zur Bestimmung von Peroxiden, *DE 198 13 247.6.*
17. Gutmann, V., Hengge, E., 1975, *Allgemeine und Anorganische Chemie*, 2. neubearbeitete und erweiterte Auflage, Verlag Chemie, Weinheim.
18. Dürkop, A., 1998, Synthesis and Characterization of a Glucose-Binding Ruthenium Metal-Ligand Complex, *Diploma Thesis*, University of Regensburg.
19. Wolfbeis, O. S., Klimant, I., Werner, T., Huber, C., Kosch, U., Krause, C., Neurauter, G., Dürkop, A., 1998, A set of luminescence decay time based chemical sensors for clinical applications, *Sens. Actuators B*, **51**, 17-24.
20. Sigma, 2000, *Biochemicals and Reagents*, 464.

5. Experimental Part

5.1 General Remarks

5.1.1 Chemicals, Solvents and Proteins

All chemicals and solvents used were purchased from Aldrich (Steinhein, Germany), Fluka (Buchs, Switzerland), Roth (Karlsruhe, Germany) or Merck (Darmstadt, Germany). They were of analytical grade and used without further purification. Proteins, antibodies, Sephadex G25 and GOx (50,000 Units) were obtained from Sigma (Steinhein, Germany). The AlbuminBlue 580 was a gift from M. Kessler (Norske Skog, Graz, Austria). Tetracycline (pharm.) was from Serva (Heidelberg, Germany) and $EuCl_3 \cdot 6\ H_2O$ was from Alfa. Water was doubly distilled.

5.1.2 Buffer Solutions and pH Measurements

Phosphate buffer pH 7.2 (22 mmol/L): 25.79 g of $Na_2HPO_4 \cdot 12\ H_2O$, 4.37 g of $NaH_2PO_4 \cdot 2\ H_2O$ and 50 mg of NaN_3 were dissolved in 1 L of doubly distilled water to give a 100 mmol/L stock solution of pH 7.2 which was diluted to 22 mmol/L. The pH was adjusted using 1 mol/L HCl.

Carbonate buffer pH 9.0 (0.1 mol/L) and carbonate buffer pH 10.2 (0.1 mol/L): 0.1 mol/L solutions of $NaHCO_3$ (8.40 g/L) and Na_2CO_3 (10.60 g/L) were mixed in a volume ratio of 95 : 5 to give the buffer with pH 9.0 and in a ratio of 40 : 60 to result in a pH 10.2 buffer, respectively [1].

13 mmol/L MOPS buffer of pH 6.91 was obtained by dissolving 1.48 g of MOPS Na-salt in 500 mL of doubly distilled water. Some drops of $HClO_4$ (70%- 72% weight) were added until a pH of 6.91 was reached.

The pH measurements were performed with a WTW pH 196 pH meter with temperature compensation.

5.1.3 Thin Layer Chromatography and Gel Permeation Chromatography

Analytical thin layer chromatography was carried out on plates from Merck (Silica Gel 60 F_{254} or RP-18 F_{254a}, thickness 0.2 mm each). Mixtures of solutions for the mobile phase are given

in the ratio of their volumes. Gel permeation chromatography was performed on Sephadex G 25 (medium) as the stationary phase in a 20 x 1 cm glass column.

5.1.4 Determination of Melting Points

Melting points were measured using a melting point apparatus “Dr. Tottoli” from Büchi. They were determined in open capillary tubes and are not corrected.

5.1.5 Spectra

The ^{1}H-NMR spectra were acquired at the Zentrale Analytik of the University of Regensburg on a 250 MHz PFT-NMR Spectrometer AC 250 (Bruker). Tetramethylsilane (TMS) was used as the internal standard.

EI mass spectra were recorded on a Finnigan MAT 311 A, ESI mass spectra on a Thermoquest TSQ 7000 and FAB mass spectra on a Finnigan MAT 95 at the University of Regensburg.

Absorption spectra were acquired with a UV/VIS spectrophotometer U-3000 from Hitachi. Luminescence spectra were recorded with a luminescence spectrometer (Aminco Bowman, Series 2, from SLM) with a 150-W xenon lamp as the excitation source.

Excitation polarization spectra of 55DC were recorded on an Edinburgh Instruments CD-900 fluorimeter equipped with a xenon lamp, polarizers and a sample compartment with liquid nitrogen cooling at the University of Jena.

The excitation polarization spectrum of 5MC was measured on luminescence spectrometer (Aminco Bowman, Series 2 from SLM). 5MC was polymerized into polyacrylnitrile, a 3 x 1 x 1 cm^3 piece was cut out and the surfaces were polished. The excitation polarization was taken in the four polarizer adjustments and the polarization was calculated according to Eqs. (2.23) and (2.5).

Steady state polarization spectra were acquired on a multifrequency luminescence spectrometer K2 from ISS in L-format using a RG 630 cutoff filter from Schott (Mainz, Germany). Excitation was performed with a 300-W xenon lamp from ILC using 19 A strength of the lamp current. Excitation wavelength was 500 nm for both labeled 5MC and labeled 55DC. All samples were measured against a reference sample containing the same amount of unlabeled antigen and antibody to exclude disturbances of the measurements due to scattered light. Each measurement included the tenfold determination of the emission intensity in the

four positions of the polarizers during a 10 s integration time. The calculation of both the G-factor and the polarization value was carried out using the ISS spectra acquisition software. All polarization measurements were performed at (20 ± 1) °C .

5.1.6 Determination of Molar Absorbance

Three stock solutions of the substances to determine were diluted to give an extinction of ~0.1 or lower at the absorption maximum. Absorbances were determined and the extinction coefficients calculated according to Lambert-Beer's law and averaged.

5.2 Synthesis of the Bipyridine Ligands

5.2.1 General Procedure for the Coupling of Bromopyridines to the Respective Bipyridines [2]

In a 250 mL round bottom flask 2.36 g of $NiCl_2 \cdot 6\ H_2O$ (10 mmol) and 10.4 g of triphenyl-phosphine (40 mmol) are dissolved in 75 mL of DMF at 50 °C under N_2, whereupon the solution turns blue. After 30 min. 0.64 g of Zn dust (10 mmol) is added. After stirring for another hour at 50 °C the color turns to dark brown, whereupon 1.73 g of 2-bromo-5-methylpyridine (10 mmol) in the case of 5,5'-dimethyl-2,2'-bipyridine, or 0.83 g of 2-bromo-5-methylpyridine (5 mmol) and 0.5 mL of 2-bromopyridine (5 mmol) in the case of 5-methyl-2,2'-bipyridine are added and the solution is stirred for 5 h at 50 °C. After cooling to 20 °C the reaction mixture is poured into 200 mL of 12.5% aqueous ammonia solution under vigorous stirring. The mixture first turns to light brown at first due to the precipitation of excess PPh_3, then to black. After 10 min. the mixture is filtered and the filtrate is extracted three times with 100 mL of $CHCl_3$. During this process the color of the aqueous phase changes from violet to blue. The combined organic phases are extracted three times with 100 mL of H_2O, dried over Na_2SO_4 and evaporated to dryness.

5.2.1.1 Preparation of 5-Methyl-2,2'-bipyridine

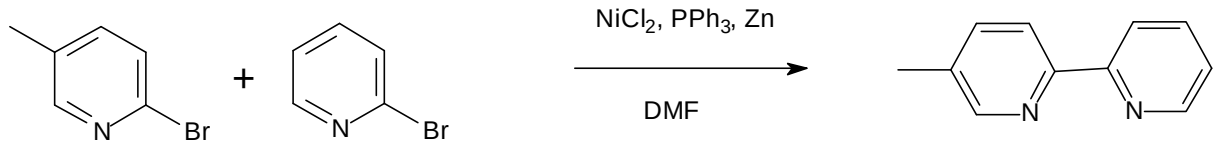

C_6H_6BrN 172.02 | C_6H_5Br 157.01 | $C_{11}H_{10}N_2$ 170.21

Following the protocol given in 5.2.1 the crude product is purified by Kugelrohrdistillation at 10^{-1} torr. After separation of a first byproduct at 80-90 °C, the second fraction containing the desired product is collected at 115-120 °C as a colorless liquid. The product was used without further characterization.

Yield: 319.5 mg (1.9 mmol, 38%) of $C_{11}H_{10}N_2$ (M = 170.21 g/mol), colorless liquid.

TLC: R_f = 0.91 (Silica gel, $CHCl_3$: MeOH = 20/1).

5.2.1.2 Preparation of 5,5'-Dimethyl-2,2'-bipyridine

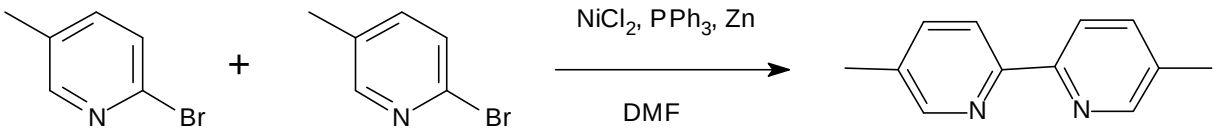

C_6H_6BrN 172.02 | C_6H_6BrN 172.02 | $C_{12}H_{12}N_2$ 184.24

Crude 5,5'-dimethyl-2,2'-bipyridine (**1b**) (see 5.2.1) is purified by sublimation at 84-94 °C at 10^{-2} torr to give a white powder.

Yield: 368 mg (2 mmol, 40%) of $C_{12}H_{12}N_2$ (M = 184.24 g/mol), white powder.

TLC: R_f = 0.95 (Silica gel, $CHCl_3$: MeOH = 20/1).

M.p.: 114-114.5 °C (Lit. 114-115 °C) [3].

EI-MS: $M^{+\cdot}$: m/z = 184.1, (calculated: 184.2).

5.2.2 General Procedure for the Oxidation of the Methylbipyridines to the Respective Carboxybipyridines [4]

350 mg (1.9 mmol) of 5,5'-dimethyl-2,2'-bipyridine is dissolved in 15 mL of water by heating to 90 °C. 2 g (12.5 mmol; 3.3 Mol-equiv. per CH_3-unit) of $KMnO_4$, dissolved in 20 mL of water, is added in three portions each time the color of the $KMnO_4$ has disappeared. The reaction mixture is refluxed for 4 h, filtered hot and the residue is washed with 5 x 20 mL of boiling water. An aqueous solution of 5 g/100 mL $NaHSO_3$ is added dropwise in order to decolorize the filtrate containing MnO_2. The solution is concentrated to 15 mL and pH 3 is adjusted using concentrated HCl whereupon the product precipitates as a white solid. The product is allowed to crystallize overnight at 4 °C, filtered and dried over P_2O_5.

5.2.2.1 Preparation of 5-Carboxy-2,2'-bipyridine

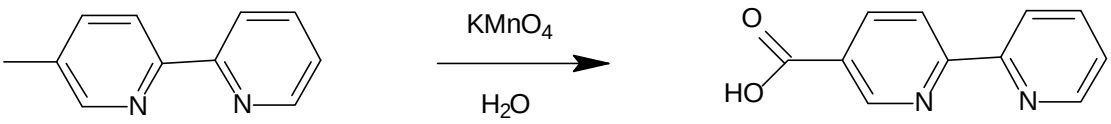

$C_{11}H_{10}N_2$
170.21

$C_{11}H_8N_2O_2$
200.20

Yield: 60 mg (0.3 mmol, 15%) of $C_{11}H_8N_2O_2$ (M = 200.20 g/mol), white powder.

TLC: R_f = 0.89 (RP-18, NEt_3 : MeOH = 1/3).

M.p.: >295 °C.

EI-MS: $M^{+\cdot}$: m/z = 200.1, (calculated: 200.2), M^{-}-CO_2: m/z = 155.0 (calculated: 156.1).

No NMR possible because 5-carboxy-2,2'-bipyridine is insoluble in all organic solvents [3].

5.2.2.2 Preparation of 5,5'-Dicarboxy-2,2'-bipyridine

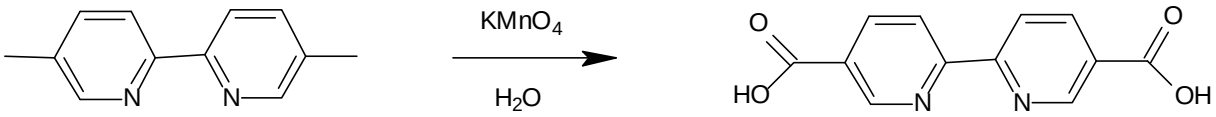

$C_{12}H_{12}N_2$
184.24

$C_{12}H_8N_2O_4$
244.21

Yield: 210 mg (0.86 mmol, 45%) of $C_{12}H_8N_2O_4$ (M = 244.21 g/mol), white powder.

TLC: R_f = 0.94 (RP-18, NEt_3 : MeOH = 1/3).

M.p.: >330 °C.

EI-MS: $M^{+\cdot}$: m/z = 244.1, (calculated: 244.2), M^{-}-CO_2: m/z = 199.1 (calculated: 200.1).

No NMR possible because 5,5'-dicarboxy-2,2'-bipyridine is insoluble in all organic solvents [3].

5.3 Synthesis of the Activated Ruthenium Trisbipyridine Complexes

5.3.1 General Procedure for the Addition of a Third Bipyridine Ligand to $Ru(bipy)_2Cl_2$ [5]

To a solution of 32 mL of methanol and 8 mL of a satured aqueous solution of $NaHCO_3$, 24.4 mg (0.1 mmol) of 5,5'-dicarboxy-2,2'-bipyridine is added and heated to 50 °C until the solution is clear. Then 48.4 mg (0.1 mmol) of $Ru(bipy)_2Cl_2 \cdot 2\ H_2O$ are added and the mixture is refluxed for 24 h. After cooling in an ice bath for 1 h conc. H_2SO_4 is added dropwise to adjust the solution to pH 3. Then the mixture is filtered. After concentration to 10 mL, 5 mL of an aqueous solution of 2 g of NH_4PF_6 is added and the product is allowed to crystallize overnight at 4 °C. The purple crystals are sucked off, dissolved in 0.5 mL of acetone, and precipitated with 10 mL of ether, sucked off and dried in vacuo.

5.3.1.1 Preparation of [Ru(2,2'-bipyridine)$_2$(5-carboxy-2,2'-bipyridine)](PF$_6$)$_2$

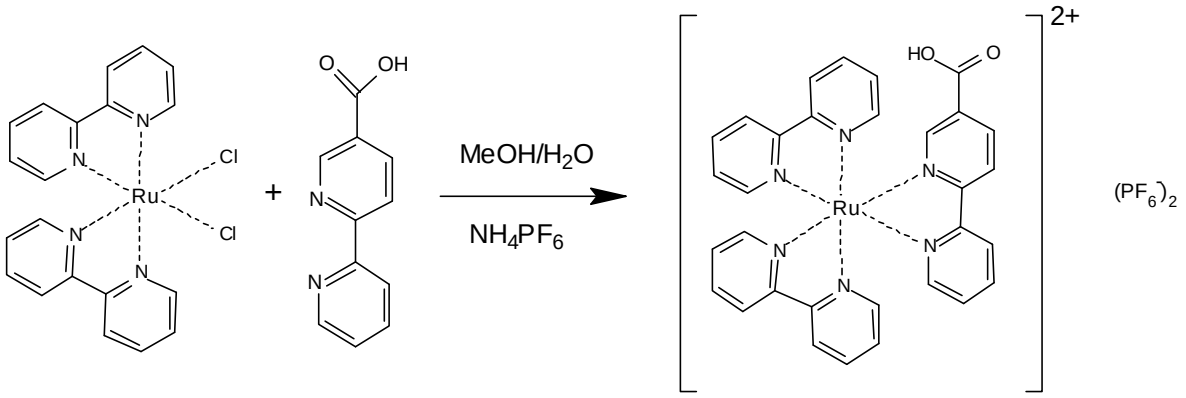

$C_{20}H_{16}Cl_2N_4Ru$	$C_{11}H_8N_2O_2$	$C_{31}H_{24}F_{12}N_6O_2P_2Ru$
484.35	200.20	903.57

Yield: 66 mg (73 µmol, 73%) of $C_{31}H_{24}N_6O_2P_2F_{12}Ru$ (M = 903.57 g/mol), fine purple crystals.

M.p.: >330 °C.

FAB-MS: M(PF$_6$)$^+$: m/z = 759.5, (calculated: 759.0), M^{2+}: m/z = 614.5 (calculated: 613.6).

5.3.1.2 Preparation of [Ru(2,2'-bipyridine)$_2$(5,5'-dicarboxy-2,2'-bipyridine)](PF$_6$)$_2$

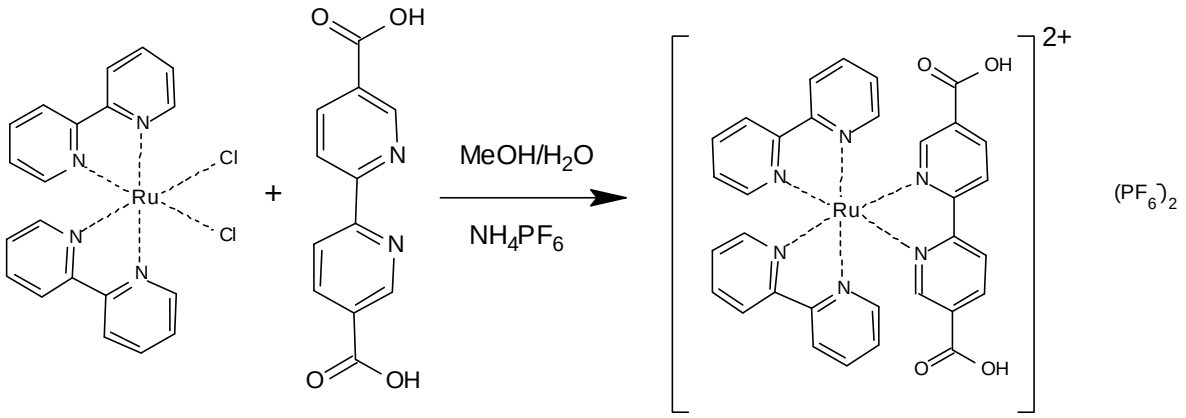

$C_{20}H_{16}Cl_2N_4Ru$	$C_{12}H_8N_2O_4$	$C_{32}H_{24}F_{12}N_6O_4P_2Ru$
484.35	244.21	947.58

Yield: 81.5 mg (86 µmol, 86%) of $C_{32}H_{24}N_6O_4P_2F_{12}Ru$ (M = 947.58 g/mol), fine purple crystals.

M.p.: >330 °C.

FAB-MS: M^{2+}: m/z = 658.4 (calculated: 657.7), M^{2+}-CO_2: m/z = 613.5 (calculated: 613.6).

5.3.2 General Procedure for the Conversion of the Ruthenium Trisbipyridine Complexes to the Corresponding NHS-Esters

5 mg (5 µmol) of [Ru(2,2'-bipyridine)$_2$(5,5'-dicarboxy-2,2'-bipyridine)]$(PF_6)_2$ is dissolved in 600 µL of dry acetonitrile and 1.2 mg (10 µmol) of NHS and 3.1 mg (15 µmol) of DCC are added. The mixture is stirred at room temperature overnight in the dark. The precipitate (mostly dicyclohexylurea) is removed using a 0.2 µm syringe filter and the solvent is removed on a rotary evaporator. The crude product is dissolved in a few drops of acetone and precipitated by the addition of 5 mL of ether. The ether is decanted and the product is washed twice with 5 mL of ether and dried in vacuo.

5.3.2.1 Preparation of [Ru(2,2'-bipyridine)$_2$(5-carboxy-(N-succimidyl)-2,2'-bipyridine)]$(PF_6)_2$

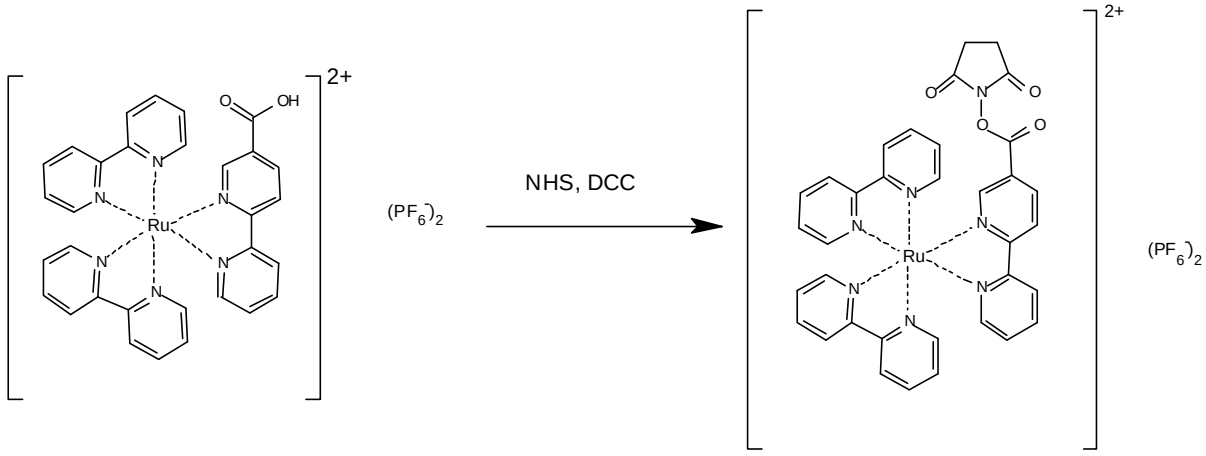

$C_{31}H_{24}F_{12}N_6O_2P_2Ru$
903.57

$C_{35}H_{27}F_{12}N_7O_4P_2Ru$
1000.64

Yield: 4.9 mg (4.9 µmol, almost quantitative) of $C_{35}H_{27}N_7O_4P_2F_{12}Ru$ (M = 1000.64 g/mol), fine purple crystals.

M.p.: >330 °C.

ESI-MS: M^{2+}: m/z = 851.4 (calculated: 851.8), M^{2+}-NHS: m/z = 754.4 (calculated: 753.7).

5.3.2.2 Preparation of [Ru(2,2'-bipyridine)$_2$(5,5'-dicarboxy-bis-(N-succimidyl)-2,2'-bipyridine)]$(PF_6)_2$

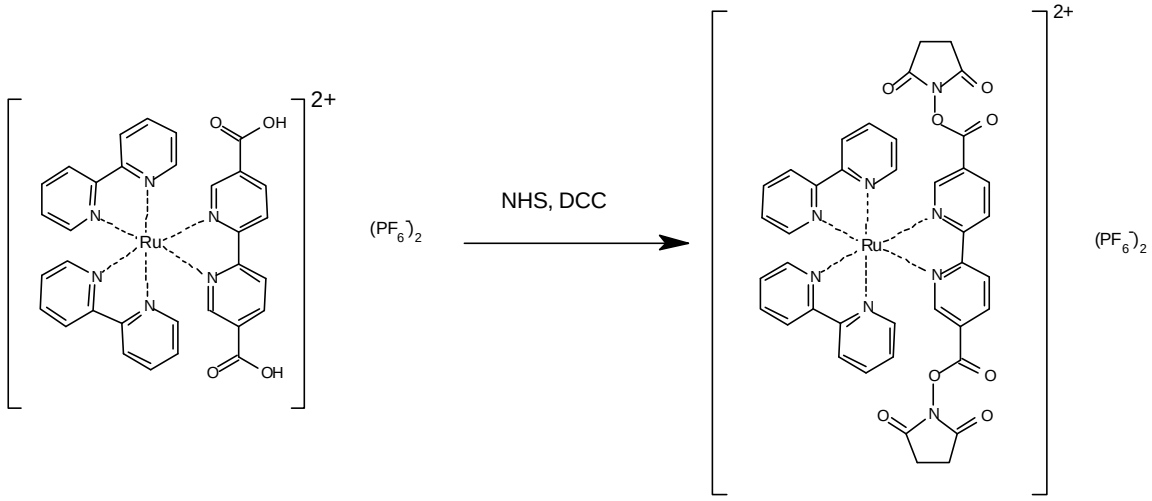

$C_{32}H_{24}F_{12}N_6O_4P_2Ru$
947.58

$C_{40}H_{30}F_{12}N_8O_8P_2Ru$
1141.73

Yield: 4.9 mg (4.3 mmol, 86%) of $C_{40}H_{30}N_8O_8P_2F_{12}Ru$ (M = 1141.73 g/mol), fine purple crystals.

M.p.: >330 °C.

ESI-MS: M^{2+}: m/z = 992.2 (calculated: 992.9),

5.4 Labeling Procedures, Determination of Dye-to-Protein Ratios and Quantum Yields

5.4.1 General Protein Labeling Procedures

Protein labeling was carried out using 100 mmol/L carbonate buffer of pH 9.0 for HSA and 100 mmol/L carbonate buffer pH 10.2 for myoglobin, respectively . A solution of 2 mg of NHS ester of the respective Ru-MLC in 50 µL DMF was added to 1 mg of the protein dissolved in 1 mL of the corresponding buffer. The solutions were stirred for 6-8 h (myoglobin) or 24 h (HSA) in the dark. Unconjugated Ru-complex was separated from the labeled proteins by gel permeation chromatography using a 22 mmol/L phosphate buffer of

pH 7.2 as the eluent. As usual, the first colored band contained the Ru-MLC-protein conjugate and was collected. The band with a much longer retention time contained the unconjugated Ru-MLC [6].

5.4.2 Determination of Dye-to-Protein Ratios

The HSA concentrations were determined using the BCA Protein Assay Reagent Kit from Pierce (Rockford, IL). Dye concentrations in solutions of labeled HSA were determined according to Lambert-Beer's law from the absorbance of the Ru-MLC at the absorption maximum.

Dye and myoglobin concentrations in solutions of labeled myoglobin were calculated from the absorbance of the labeled protein at 450 nm and 540 nm, respectively, considering the additivity of the absorptions of the protein (ε_{myo}^{450} = 24,000 L/(mol · cm) , ε_{myo}^{540} =13,500 L/(mol · cm)) [7] and the Ru-MLC at the respective wavelengths. This results in two equations with two unknown variables. The solution of the two equations yields concentrations of dye and myoglobin, respectively. For all the absorption measurements it is assumed that the bound and the unbound Ru-MLC have equal molar absorbances. Dye-to-protein ratios (DPRs) of up to 8 were achieved. The typical range is from 3 to 4. The DPR statistically expresses the number of label molecules covalently bound to one protein molecule.

5.4.3 Determination of Quantum Yields

Quantum yields (QYs) were determined relative to $Ru(bipy)_3Cl_2$ as reference fluorophore with a QY of Φ = 0.042 in water [8]. The formula

$$\Phi_S = \Phi_{Ref} \cdot (E_{Ref}/E_S) \cdot (A_S/A_{Ref}) \cdot (n_S^2 / n_{Ref}^2) \qquad (5.1)$$

was used, where

Φ_S is the quantum yield of the substance to determine,

Φ_{Ref} is the quantum yield of the reference substance,

E_{Ref} is the absorbance at the excitation wavelength of the reference substance,

E_S is the absorbance at the excitation wavelength of the substance to determine,

A_S is the integrated area under the corrected emission spectrum of the substance to determine,

A_{Ref} is the integrated area under the corrected emission spectrum of the reference substance,

n_S^2 is the square of the refractive index of the solvent of the substance to determine,

n_{Ref}^2 is the square of the refractive index of the solvent of the reference substance.

The term containing the refractive indices cancels out because the same solvents were used for sample and reference for all determinations.

The absorbance of the solutions was kept below 0.1 to avoid disturbances due to inner filter effects. The “corrected emission spectra” feature and the “integration mode” feature of the Aminco Bowman AB2 software version 4.0 were applied.

5.5 Immunoassays

5.5.1 Homogenous Immunoassay for the Determination of Antibody Concentrations

The solutions containing a known quantity of labeled proteins and antibody were mixed in the corresponding antigen : antibody ratios and the solutions stirred for 15 min. The solutions were calculated to reach a final concentration of the label of about 1 nmol in 2 mL after all additions. The DPRs of the labeled antigen were between 3 and 4. Then the fluorescence polarization was measured as described in chapter 5.1.5.

5.5.2 Competitive Immunoassay for Antigen Determination

A fixed amount of labeled and various amounts of unlabeled protein were mixed in PBS pH 7.2 and a fixed amount of antibody was added. The molar amounts of labeled antigen and of antibody are equal. The solutions were calculated to reach a final concentration of the label of 1 nmol in 2 mL after all additions. The DPRs of the labeled antigen were between 3 and 4. The solution was stirred for 15 min at room temperature. Then the fluorescence polarization was measured as described in chapter 5.1.5.

5.5.3 Comparison of the Competitive Polarization Immunoassay for HSA with the Albumin Blue 580 Test

A competitive polarization assay for HSA was carried out using 55DC-labeled HSA as described above. Then a calibration curve for the AlbuminBlue 580 Test was set up for the same concentration range as determined with the polarization immunoassay. Ten independent emission measurements were taken for each concentration as described in Lit. [10,11].

5.6 Measurements with EuTC

5.6.1 Reagent Solutions and Analytical Procedure for the Determination of Hydrogen Peroxide

MOPS-Buffer (Solution A)

1.48 g of MOPS Na salt is dissolved in 490 mL of bidistilled water, adjusted to pH 6.91 with 72% $HClO_4$ (p.A.) and filled up to 500 mL.

EuTC Stock Solution (Solution B)

4.0 mg of tetracyclin (pharm.) and 9.6 mg of $EuCl_3 \cdot 6\ H_2O$ (99,9%) are dissolved in Solution A and filled to 200 mL.

Calibration Plot

Mix 1.00 mL of Solution B and 1.00 mL of solutions containing $1 \cdot 10^{-6}$, $1 \cdot 10^{-5}$, $1 \cdot 10^{-4}$, $5 \cdot 10^{-3}$, $1 \cdot 10^{-3}$ and $1 \cdot 10^{-2}$ mol/L H_2O_2 in Solution A and incubate for 10 min. at room temperature. Then measure the emission intensity of the sample at 616 nm using an excitation wavelength of 393 nm.

Assay Protocol

Mix 1.00 mL of the Solution B and 1.00 mL of the sample containing between 10-500 µmol/L H_2O_2 in Solution A and incubate for 10 min. at room temperature. Then measure the emission intensity of the sample at 616 nm using an excitation wavelength of 393 nm and calculate the concentration of peroxide from the calibration plot.

5.6.2 Reagent Solutions and Analytical Procedure for the Determination of Glucose

Buffer Solution (Solution A)

1.48 g of MOPS Na salt is dissolved in 490 mL of bidistilled water, adjusted to pH 6.91 with 72% $HClO_4$ (p.A.) and filled up to 500 mL.

EuTC Stock Solution (Solution B)

4.0 mg of tetracyclin (pharm.) and 9.6 mg of $EuCl_3 \cdot 6\ H_2O$ (99.9%) are dissolved in Solution A and filled to 100 mL.

Glucose Stock Solution (Solution C)

594.5 mg of glucose is dissolved in Solution A and filled to 100 mL.

GOx Stock Solution (Solution D)

2.0 mg of GOx (50,000 units) are dissolved in 10 mL of Solution A.

Calibration solutions for glucose measurements were prepared according to the table below.

$c_{Glucose}$ in calibration solution after addition of Solution D. [mmol/L]	$V_{Solution\ B}$ [mL]	$V_{Solution\ C}$ [mL]	$V_{Solution\ A}$ [mL]
7.5	5.00	5.00	-
6.5	5.00	4.33	0.66
5.5	5.00	3.66	1.33
4.5	5.00	3.00	2.00
3.5	5.00	2.33	2.66
2.5	5.00	1.66	3.33

Calibration Graph

1.00 mL of calibration solution is pipetted into a 1 cm cuvette equipped with a stirrer bar. The cuvette is placed in the luminescence spectrometer. The cuvette holder is thermostatized to (20±1) °C. 1.00 ml of Solution D is added under stirring and after ten seconds mixing time the change of the emission intensity at 616 nm is monitored using 400 nm as the excitation wavelength.

Glucose Assay

1.0 mL of the sample containing 2.5-7.5 mmol/L glucose in Solution A is pipetted into a 1 cm cuvette equipped with a stirrer bar. The cuvette is placed in the luminescence spectrometer. The cuvette holder is thermostatized to (20±1) °C. 1.00 ml of Solution D is added under stirring and after ten seconds mixing time the change of the emission intensity at 616 nm is monitored using 400 nm as the excitation wavelength.

Calculation of the Slopes

This procedure was carried out using with Microsoft Excel 7.0 and Microcal Origin 6.0. The values of the emission intensity from the measurement were taken in 5 second intervals. The value from ten seconds earlier was subtracted from each of these intensities and the result was divided by 10. This delivers the $dI_{616\ nm}/dt$ value. The $dI_{616\ nm}/dt$ values are smoothed by a second order Savitzky Golay polynom from Microcal Origin. The smoothing reduces the noise and enables an easier visualization of the slope. Extreme changes like at fluctuations of the enzyme remain unaffected, however.

5.7 References

1. Perrin, D. D., Dempsey, B.,1974, *Buffers for pH Metal Ion Control*, Chapman and Hall, London.
2. Tiecco, M., Testaferri, L., Tignoli, M., Chianelli, D., Montanucci, M., 1984, A Convenient Synthesis of Bipyridines by Nickel-Posphine Complex-Mediated Homo Coupling of Halopyridines, *Synthesis*, **9**, 736-738.
3. Case, H., 1946, The Synthesis of Certain Substituted 2,2-Bipydidyls, *J. Am Chem. Soc.*, **68**, 2574-2577.
4. Becker, H. G., 1996, *Organikum*, 20. Auflage, Joh. Ambrosius Barth Verlag, Heidelberg.
5. Terpetschnig, E., Szmacinski, H., Malak, H., Lakowicz, J., R., 1995, Metal-Ligand Complexes as a New Class of Long-lived Fluorophores for Protein Hydrodynamics, *Biopys. J.*, **68**, 342-350.
6. Brinkley, M., 1992, A brief survey of methods for preparing protein conjugates with dyes, haptens, and cross-linking reagents, *Bioconjugate Chem.3*, 2-13.

7. Abraham, J., 1939, *Biochem. J.*, **33**, 622.
8. Van Houten, J., Watts, R. J., 1975, *J. Am Chem. Soc.*, **97,** 3843-3844.
9. Demas, J. N., Crosby, G. A., 1971, The measurement of photoluminescence quantum yields. A Review., *J. Phys. Chem.*, **75**, 991-1024.
10. Kessler, M. A., Meinitzer, A., Petek, W., Wolfbeis, O. S., 1997, Microalbuminuria and borderline-increased albumin excretion determined with a centrifugal analyzer and the Albumin Blue 580 fluorescence assay, *Clin. Chem.*, **43**, 996-1002.
11. Kessler, M. A., Meinitzer, A., Wolfbeis, O. S., 1997, Albumin Blue 580 Fluorescence Assay for Albumin, *Anal. Biochem.*, **248**, 180-182.

6. Abbreviations Used

5MC	[Ru(2,2'-bipyridine)$_2$(5-carboxy-2,2'-bipyridine)]$(PF_6)_2$
55DC	[Ru(2,2'-bipyridine)$_2$(5,5'-dicarboxy-2,2'-bipyridine)]$(PF_6)_2$
5MC-NHS	[Ru(2,2'-bipyridine)$_2$(5-carboxy-(N-succimidyl)-2,2'-bipyridine)]$(PF_6)_2$
55DC-DNHS	[Ru(2,2'-bipyridine)$_2$(5,5'-dicarboxy-bis-(N-succimidyl)-2,2'-bipyridine)]$(PF_6)_2$
BCPDA	4,7-Bis(chlorosulfophenyl)-1,10-phenanthroline-2,9-dicarboxylic acid
bipy	2,2'-Bipyridine
conc.	concentrated
DCC	Dicyclohexylcarbodiimide
DMF	Dimethylformamide
DPH	1,6-Diphenyl-1,3,5-hexatriene
dppz	Dipyrido-[3,2a:2',3'-c] phenazine
EB	Ethidium bromide
Eq.	Equation
GOx	Glucose oxidase
HPTS	1-Hydroxypyrene-3,6,8-trisulfonate
HSA	Human serum albumin
LC	Ligand centered
LED	Light emitting diode
Lit.	Literature
MeOH	Methanol
MLC	Metal-ligand complex
MLCT	Metal to ligand charge transfer
M.p.	Melting point
Mono	Monochromator
MOPS	N-Morpholinopropane sulfonic acid
NEt_3	Triethylamine
NHS	N-Hydoxysuccinimide
NMR	Nuclear magnetic resonance
PBS	Phosphate buffered saline

PMT	Photomultiplier
PPh_3	Triphenylphosphine
QY	Quantum Yield
R_f	Ratio of fronts (on thin layer chromatograms)
Ref.	Reference
RT	Room temperature
SNAFL	Seminaphthofluorescein
SNARF	Seminaphthorhodamine
TC	Tetracycline
TLC	Thin-layer chromatography
TMS	Tetramethylsilane
UV	Ultra-violet

7. Summary

7.1 In English

The aim of this work was to synthesize and characterize new ruthenium based MLCs which can be covalently attached to biomolecules to show changes of their fluorescence polarization in various formats of homogenous immunoassays.

Two complexes were synthesized containing 5-carboxy-2,2'-bipyridine and 5,5'-dicarboxy-2,2'-bipyridine as the asymmetric ligand. The absorption maxima were found to be around 450 nm and the emission maxima are 675 nm and 705 nm, respectively. The emission maxima show a red shift of up to 30 nm if the complex is covalently conjugated to a protein. The emission is in a range beyond 600 nm suitable for biological applications. The fundamental polarization values were 0.33 for [Ru(2,2'-bipyridine)$_2$(5,5'-dicarboxy-2,2'-bipyridine)](PF$_6$)$_2$ and 0.18 for [Ru(2,2'-bipyridine)$_2$(5-carboxy-2,2'-bipyridine)](PF$_6$)$_2$, respectively, at 500 nm excitation wavelength.

The complexes were activated to the respective NHS esters, attached covalently to HSA and myoglobin, respectively. Homogenous polarization immunoassays were performed in normal and competitive format. A comparison of a competitive polarization immunoassay using one of the MLCs with the common AlbuminBlue 580 Test was made. Both methods delivered equal results which shows the value of the new polarization labels.

Furthermore, a determination method for hydrogen peroxide using an up to 13-fold enhancement of the luminescence intensity of a europium tetracycline complex upon binding of H_2O_2 was established. This method works at neutral pH and the luminescence is detected at 616 nm after a 10 min. incubation time of the samples. Linear calibration plots were obtained in the range of 10-500 µmol/L H_2O_2 and the detection range can be shifted to higher or lower concentrations.

Finally a glucose sensing method, based on an up to 5 fold enhancement of the luminescence intensity of a europium tetracycline complex due to enzymatically generated H_2O_2 at physiological glucose concentrations was developed. The method works at neutral pH and uses 616 nm emission as the detection wavelength. A determination of the concentrations of glucose using fluorescence lifetime seems to be possible.

7.2 In German

Ziel dieser Arbeit war, neue Ruthenium Metall-Liganden Komplexe zu synthetisieren und zu charakterisieren, die man kovalent an Biomoleküle binden kann. Diese Komplexe können dann in verschiedenen Immunoassayformaten mit Fluoreszenzpolarisationsdetektion eingesetzt werden.

Es wurden zwei Komplexe synthetisiert, die entweder 5-carboxy-2,2'-bipyridin oder 5,5'-dicarboxy-2,2'-bipyridin als asymmetrischen Liganden enthalten. Die Absorptionsmaxima sind um 450 nm und die Emissionsmaxima sind bei 675 nm und 705 nm. Die Emissionsmaxima werden bis zu 30 nm rotverschoben, wenn der Komplex kovalent an ein Protein gebunden ist. Die Emission liegt in einem Bereich, der für bioanalytische Anwendungen sehr geeignet ist, weil biologische Materialien bei >600 nm Wellenlänge kaum noch Eigenfluoreszenz zeigen. Die Fundamentalpolarisation wurde bei einer Anregungswellenlänge von 500 nm bestimmt. Der Wert beträgt 0,33 für [Ru(2,2'-bipyridin)$_2$(5,5'-dicarboxy-2,2'-bipyridin)](PF$_6$)$_2$ und 0,18 für [Ru(2,2'-bipyridin)$_2$(5-carboxy-2,2'-bipyridin)](PF$_6$)$_2$.

Die Komplexe wurden nach Aktivierung zum NHS-Ester kovalent an humanes Serumalbumin und Myoglobin gebunden. Es wurden homogene einfache und kompetitive Polarisationsimmunoassays durchgeführt. Der kompetitive Assay wurde mit dem AlbuminBlue 580 Test validiert. Beide Bestimmungsmethoden ergaben identische Ergebnisse, was den Wert der neuen Polarisationsmarker und dieser Bestimmungsmethode untermauert.

Weiterhin wurde eine Methode zur Bestimmung von mikromolaren Konzentrationen von Wasserstoffperoxid entwickelt. Sie beruht auf einer bis zu dreizehnfachen Zunahme der Lumineszenzintensität eines Komplexes aus Europiumionen und Tetracyclin bei einer Wellenlänge von 616 nm. Die Bestimmung wird bei neutralem pH-Wert durchgeführt und ergibt im Bereich von 10-500 µmol/L H_2O_2 lineare Eichgeraden. Der Meßbereich kann auch zu höheren oder niedrigeren Konzentrationen bis zu 100 nmol/L hin verschoben werden.

Schließlich wurde noch eine Methode zur Bestimmung von Glucose im physiologischen Konzentrationsbereich bei neutralem pH-Wert entwickelt. Diese Methode ermöglicht die optische Bestimmung von Glucose und beruht auf einer bis zu fünffachen Zunahme der Lumineszenzintensität eines Komplexes aus Europiumionen und Tetracyclin durch

enzymatisch gebildetes Wasserstoffperoxid. Auch hier wird wieder im langwelligen Bereich bei 616 nm Emissionsionswellenlänge gemessen. Eine Glucosebestimmung mittels Änderungen der Fluoreszenzlebenszeit scheint möglich zu sein.

8. Curriculum Vitae

Personal Data

Surname	Dürkop
Given Names	Axel
Date of Birth	12. 02. 1973
Place of Birth	Landshut (Bavaria)
Nationality	German

Education

09/1979 - 07/1983	Primary School Bodenmais (Landkreis Regen)
09/1983 - 06/1992	Gymnasium Zwiesel (Landkreis Regen)
06/1992	Abitur

Studies

11/1992 - 03/1997	Studies of Chemistry at the University of Regensburg (Diploma)
05/1997 -02/1998	Experimental Diploma Work at the Institute of Analytical Chemistry, Chemo- and Biosensors (Prof. Wolfbeis)
03/1998	Diploma
04/1998 - 03/2001	Ph.D. Work at the Institute of Analytical Chemistry, Chemo- and Biosensors (Prof. Wolfbeis)

Practical Work

06/1992 - 10/1992	Work at Deutsche Post and Schott Zwiesel Glaswerke AG
08/1996 - 09/1996	Work at the Research Laboratory for Chemical Reactors of the Deggendorfer Werft und Eisenbau GmbH
since 05/1997	Tutor for Dentistry Students Attending Chemistry Courses
since 05/1999	Tutor for Chemistry Students Attending Courses in Bioanalytical Chemistry

Further Skills

Languages	English (good), Latin (good), Italian (moderate)
Data Processing	Microsoft Office, SAP R/3 (Modules CO and FI), Maple, Turbo Pascal, Internet, Corel Draw, Beilstein
Other Skills	Controlling, Accounting, German Patent Law

Hobbies

Photography, Wine-Tasting, Cooking (Italian and Greek), Traveling (Through Italy and Other Wine-Growing Counties)

9. List of Papers, Patents, Posters and Presentations

9.1 Papers

Wolfbeis, O. S., Klimant, I., Werner, T., Huber, C., Kosch, U., Krause, C., Neurauter, G., Dürkop, A., 1998, A set of luminescence decay time based chemical sensors for clinical applications, *Sens. Actuators B*, **51**, 17-24.

Dürkop, A., Lehmann, F., Wolfbeis, O. S., 2001, Ruthenium Metal Ligand Complexes as Labels for Proteins in Polarization Immunoassays, *Anal. Biochem.*, to be submitted in April.

9.2 Patent

Appl. Nr. *101 11 392.7,* Bio-analytisches Messverfahren unter Verwendung von Oxidasen, (of 09.03.2001).

9.3 Poster

Dürkop, A., Lehmann, F., Wolfbeis, O. S., 1999, Metal Ligand Complexes as Luminescent Probes for Proteins, *Third Conference on Fluorescence Microscopy and Fluorescent Probes*, 20.6.-23.6., Prague, Czech Republic.

9.3 Oral Presentations

Dürkop, A., Lehmann, F., Wolfbeis, O. S., 1999, A New Metal Ligand Complex as Label for Biomolecules in Polarization Immunoassays, *ASCOS Advanced Study Course on Optical Chemical Sensors*, 27.9-29.9, Neusiedl am See, Austria.

Dürkop, A., Lehmann, F., Wolfbeis, O. S., 2000, New Ruthenium Metal Ligand Complexes as Labels for Polarization Immunoassays, *Euroanalysis XI*, 3.9.-9.9., Lisbon, Portugal.